MODELLING, SIMULATION AND DAMPING OF FLEXIBLE MANIPULATORS

By

Ankur Gupta

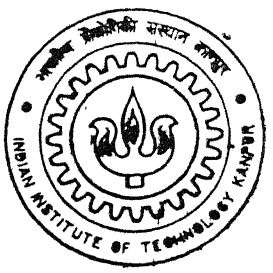

DEPARTMENT OF MECHANICAL ENGINEERING

Indian Institute of Technology Kanpur

APRIL, 2002

MODELLING, SIMULATION AND DAMPING OF FLEXIBLE MANIPULATORS

A Thesis Submitted
In Partial Fulfilment of the Requirements
for the Degree of
Master of Technology

by

ANKUR GUPTA

to the

DEPARTMENT OF MECHANICAL ENGINEERING
INDIAN INSTITUTE OF TECHNOLOGY KANPUR
INDIA

April, 2002

CERTIFICATE

It is certified that the work contained in the thesis entitled "***Modelling, Simulation and Damping of Flexible Manipulators***", by ***Mr. Ankur Gupta*** , has been carried out under our supervision and that this work has not been submitted elsewhere for a degree.

Dr. Bishakh Bhattacharya
Asst.Professor
Dept. of Mechanical Engineering
I.I.T Kanpur

Dr. Bhaskar Dasgupta
Asst. Professor
Dept. of Mechanical Engineering
I.I.T. Kanpur

April, 2002

Acknowledgements

I would like to express my deep sense of gratitude towards my thesis supervisors Dr. B. Bhattacharya and Dr. B. Dasgupta for their excellent guidance, invaluable suggestions and generous help at all stages of my research work. Their interest and confidence in me was the main reason for all the success I have made.

I am greatly indebted to all my teachers for their endeavour to make me learn as much as possible. In particular I would like to thank Dr. P. M. Dixit for his guidance in solving the system of non-linear equations.

I am thankful to Dr. Amitabha Mukharjee for extending me the facilities of Centre for Robotics for the completion of this work. It was pleasure to be associated with the Centre for Robotics and I would like to thank staff at Centre for Robotics for making it a place to work in.

I am extremely grateful to my Robotics Lab mates Shamik, Kaushik, Pavan and Gaurav for all the encouragement and support I have received from them at all times.

And lastly, I thank all my friends for making my stay at I.I.T. Kanpur enjoyable and memorable one.

Ankur Gupta

Dedicated to My Parents and Teachers

Abstract

A flexible robot is characterized by its lightweight and highly flexible joints and links. Therefore it responds to the gross motion of links in the form of undesirable vibration. In this thesis an effort has been made to counter this problem by modelling and damping of single-link and two-link planer robots with rotary joints. In this work bending and axial deformation of the flexible links are considered using Euler Bernoulli beam theory. To model a flexible robot link, which is essentially a continuous system, it is discretized by using finite element method. Compared to other methods, like assumed mode method, this method is of particular advantage as boundary conditions and physical properties may be imposed in the traceable and natural manner while deriving the equations of the motion. After finding the expression for displacement at any point using finite element method, the dynamic equations of motion are derived using Lagrangian formulation. For complex dynamic systems, like the flexible link manipulator system where mass and elasticity are distributed over the finite regions, it is easier to derive the equations of motion by using Lagrange's method. In the case of two-link manipulator, the effect of flexibility of first link on the generalized position of any point on second link is considered by incorporating the tip-deflection of first link in the transformation matrix between the two links and after getting the sets of dynamic equations for two links, they are solved simultaneously to get the solutions. Time response results are obtained for undamped and viscous damped systems. Finally each of the link is modeled as a typical laminated composite beam made up of number of layers of passive damping coating and a magnetostrictive material. A combined passive and active damping strategy in hybrid mode using combination of layers of ferromagnetic (passive) and smart (active) magnetostrictive (Terfenol-D) materials is proposed.

Contents

List of Figures

List of Tables

Chapter 1

Introduction

1.1 Introduction

The studies on the robot systems till recent years were confined to rigid robots. Here the term rigid robot refers to the robots, which can be modeled using rigid body dynamics. This assumption is fairly acceptable for typical industrial robots having slow movement with heavy and bulky arm structural design. Consequently they are limited to low load carrying capacity (typically 5 to 10 percent of their own weight) by the requirements of their rigidity. Rigid robots, with all these features exhibit good repeatability and accuracy with ease in design (Fraser and Anthony 1991).

With the advancement in actuator technology coupled with new designs, such as direct-drive arms, have led to rapid increase in the speed and load carrying capacity of the robots. Also, with the extension of robot applications to newer fields like in space, medical surgery etc., light weight and high flexibility of robot arms have become important factors in the design and put additional constraints on the rigid robots.

All these have led to the greater need of considering flexibility of nominally rigid links of a robot. However, as the assumption of rigid links is relaxed, the rigid body dynamics no longer remains applicable which consequently opens a completely new area of research, called flexible robots.

1.2 Advantages of Flexible Robots

Apart from the factors which requires the use of flexible links and light weight of robots there are several other features of flexible robots viewed as the potential advantages for industry and other applications.

1. Lower energy consumption - lighter links and in turn lighter joints have lower inertia which leads to less power consumption to produce same acceleration for a constant payload capacity.

2. Smaller actuators - to move lighter arms and joints smaller and cheaper actuators can be used.

3. Less bulky design - trimmer arm design leads to a more compact and lightweight robot.

4. Compliant structure - mechanical compliance can be achieved by the use of flexible arms and joints. This is particularly useful in delicate operations like surgical robots, some assembly operation etc where arms themselves act as the force/torque-sensing device.

5. Faster in operation and better maneuverability - with high speed they are particularly helpful in increasing the productivity in an industry. Due to their lighter weight flexible robots are easy to maneuver without exerting much load on joints and actuators.

6. Safer operation - due to compact design and lightness in structure they cause lesser damage in case of any accident.

1.3 Problems Associated with Flexible Robots

Unfortunately, if the flexibility of a manipulator link is considered the modelling of the system as well as equations describing the dynamics become more complex. In addition to gross motion of the arms, the deformation behavior of the individual links has to be taken into account. The deformation behavior is exhibited in the form of undesirable vibrations at the tip of the links. The two effects interact with each other further complicating the system dynamics. Some other problems faced by flexible manipulators are as follows:

1.3.1 Phase lag

As observed the propagation speed of the elastic deformation waves in a flexible link is finite and this normally gives rise to a phase lag between control input and sensor output when an actuator and sensor are non-collocated (Spector and Flashner 1990). Further this phase lag is observed to be frequency dependent. In case of a single flexible link, if the sensor and actuator are collocated there is no phase lag. Nonetheless, in a multi-link case the phase problems are much more complex. Even when an actuator and sensor are collocated, there may be phase lag, because of phase delayed disturbances due to the motion of other links.

1.3.2 Spillover

In a flexible manipulator each link is a continuous system and is defined by infinite degrees of freedoms, however for control purpose usually the system is considered as a combination

of finite number of lumped masses making the controller a finite dimensional system. In order to discretize the continuous system using independent modal space control, the high frequency terms are usually truncated. As a result the neglected higher frequency mode terms interact with the feedback control loop, causing the system instability. This is referred as the Spillover problem (Balas 1982).

1.3.3 Effect of Payload and Nonlinear Terms

As mentioned earlier, flexible manipulators have high payload to robot weight ratio which signifies that the payload weight becomes considerable as compared, to the robot weight and can no longer be neglected as in case of rigid robots. However with the inclusion of the payload dynamics into manipulator model the inertia of the link gets considerably changed and with that also changes the flexible modes of vibration. Another feature of flexible manipulators is that they typically have high-speed motions unlike the slow movements of rigid robots. Due to its high speed the velocity dependent nonlinear terms like centrifugal and coriolis force terms, becomes considerably large and neglecting them in the system model causes the error in the dynamics and leads to numerical instability in system simulation (Rex 1995).

1.3.4 Flexible-Link with Prismatic Joints

In the case of flexible manipulators with prismatic joints the effective length of flexible arm changes with time and spatial domain no longer remains fixed. It has been observed that extending and contracting motions of arms have destabilizing and stabilizing effect on the vibratory motions respectively (Wang and Wie 1987). Flexible beams with payload gives rise to a moving boundary value problem with time varying boundary conditions which leads to time dependent modal functions and modal frequencies of flexible links, further complicating the system.

1.4 Literature Survey

In a flexible manipulator, the flexibility is due to both link and joint elasticity. However the effect of each is mainly dependent on the manipulator geometry. It has been observed that for manipulator with long, thin and lightweight links, flexure of manipulator link plays considerable role, therefore in present thesis only the effect due to link flexibility has been considered. Related work done by various researchers is reviewed and has been presented in the following sections.

1.4.1 Modelling of the System

A flexible manipulator being a continuous dynamics system has infinite degrees of freedom and is governed by the coupled-nonlinear-partial differential equations. Finding the solution of such a system is extremely difficult, particularly as we move onto multi-link cases. Besides this other practical constraints like finite dimensional actuators and sensors make it necessary to discretize the system while finding the system dynamics equations.

In past mainly two types of discretization methods have been employed by the researchers namely assumed mode method and finite element method. In assumed mode method the flexible displacements of each link are expressed as summation of finite number of assumed mode terms. Each mode term is product of mode shape function, which is purely a function of displacement along link and time dependent modal amplitude. Assumed mode method greatly improves the efficiency of the final algorithm (Fraser and Anthony 1991). Further it has been found that with increase of mode number the inertia matrix tends to become ill posed (Yan, Meng and Wang 1999).

In finite element method, unlike assumed mode method, each of the flexible links is considered as an assemblage of finite number of elements, where each element satisfies the required continuity and convergency condition (Zienkiewicz 1986). Further a joint-beam element for revolute joint manipulators can be proposed for planer (Yue, Yu and Bai 1997) as well as for spatial flexible manipulator (Zhang and Yu 1999). Since the displacement at a junction point (Node) of any two elements is same for both the elements the internal forces are balanced so that after assembly we get the model of complete link. Similar to assumed mode method the flexible displacement at any point is expressed as summation of terms containing the product of polynomial shape functions (different for different continuity requirements) and time dependent nodal displacements. Owing to simplicity of the shape functions, which are local in nature, less number of mathematical operations are required for inertia matrix computation as compared to that in case of assumed mode method (Rex 1995). However main advantage of this method lies in the traceable and natural manner in which the boundary conditions and physical properties may be imposed while deriving the equations of the motion (Badoor and Almusallam 1999). All these factors have encouraged the wide use of this method in modelling of the flexible manipulator (Usoro, Ndira and Mahil 1986; Petric 1995; Gamarra and Yuhara 1999).

After finding the expression for displacement at any point using any of the discretization method the equations of motion are derived using either of Lagrangian formulation or Newton-Euler formulation. In case of the Lagrangian formulation, firstly the total kinetic and potential energies are found for each link in terms of flexible degrees of freedom and joint variables. Subsequently the standard Lagrange's equation is applied to get the dynamic equations (Meirovitch 1967). It has been observed that in complex dynamic systems, particularly the flexible links manipulator system where mass and elasticity are distributed

over the finite regions. It is easier to derive the equations of motion by using Lagrange's method (Rex 1995). Therefore in this thesis Lagrangian formulation has been used to derive the dynamic equations of motion.

Another approach for finding the dynamic equations is by application of Newton-Euler model. In the case of rigid manipulator, Newton-Euler model have given the best results to solve the simulation and control problems, as far as time consumption and programming simplicity are concerned. This fact has encouraged many researchers to extend this method for flexible manipulators. The basic approach in Newton-Euler/finite element method is to divide the arm into number of elements and carry out a dynamic balance on each element. However, for a large number of elements clearly it is a tedious process (Fraser and Daniel 1991). Generalized Newton-Euler model based on the principle of virtual power and formalism of description of motion has been found to provide a fast recursive simulation algorithm (Boyer and Coiffet 1996).

Damping is another important aspect, which requires to be considered in the modelling of a flexible system. Every elastic system inherently exhibits some amount of natural damping which has seldom been considered by the researchers. Although the appropriate damping can only be modelled by experiments (Book 1993), Rayleigh Damping has been found to give good results with experimentally determined damping coefficients (Petric 1995).

1.4.2 Control of Flexible Manipulators

The purpose of control is to maintain the dynamic response of the system in accordance with given performance criterion. The main problem in the control of a rigid manipulator is that the manipulator dynamics is highly nonlinear and complex (Fu, Gonzalez and Lee 1987). In the case of flexible manipulator, design of controller becomes extremely difficult as flexible arms respond to gross link motion in the form of undesirable vibrations. Now the controller has to do an additional task of suppressing the flexible arm vibration along with joint position control. Various passive damping and active damping schemes have been proposed in the past research. Passive Damping of structures, especially using layers of soft viscoelastic or hard ceremics having high damping characteristics, has attracted extensive attention. Some ceremics and ferromagnetic coatings yield significant structural damping which depends on the strain induced in the material (Bhattacharya, Vidyashankar and Tomlinson 2000). Smart materials like piezoelectric materials have been used successfully for controlling the single link (Dong and Mills 1999) and two-link planer manipulators (Ho and Seung 2001). Other smart materials like Terfenol-D have shown good potential for active damping. A combined passive and active damping using combination of layers of ferromagnetic (passive) and smart (active) magnetostrictive material in hybrid mode has been proposed to control vibration (Bhattacharya, Vidyashankar and Tomlinson 2000).

1.5 Motivation

As discussed in Section 1.2 flexible manipulators possess several features, which make the modelling of the manipulator quite difficult, and give rise to system defined by extremely complex dynamic equations. In addition to this, formulating a satisfactory control strategy has emerged as another big challenge. Thus, inspite of great advantages (discussed in Section 1.1) the application of flexible manipulator has been quite limited. All these factors have interested many researchers to solve the problem of modelling and control of flexible manipulators in a systematic manner. This is also the motivation for current thesis.

1.6 Thesis Objectives and Contributions

The main objectives of this thesis are as follows:

- Firstly, to model a flexible single link manipulator having revolute joint, considering the link flexibility and then to derive the dynamic equations of motion for this model.
- Secondly, to incorporate the appropriate damping to reduce the vibrations and thereby to minimize the error at the end effector.
- Thirdly, to extend the work of modelling, derivation of system dynamic equations and damping to a two-link planer flexible manipulator having revolute joints only.

With this in mind the main contributions of the thesis can be summarized in the following:

1. To model a flexible single link manipulator, which is essentially a continuous system, it is discretized by using finite element method. Then Lagrangian formulation is employed to derive the dynamic equations.
2. Damping of link vibration is assumed to be viscous damping and included in the system model. Results have shown it to suppress the link vibrations effectively.
3. In addition a combined passive and active damping strategy using combination of layers of ferromagnetic (passive) and smart (active) magnetostrictive (Terfenol-D) materials is proposed in hybrid mode.
4. A two link flexible manipulator is modelled by considering the effect of flexibility of first (shoulder) link on the dynamics of second (elbow) link by modifying the transformation matrix between the two links. In this case also, while deriving the system dynamics equations, damping is considered.

1.7 Thesis Organization

In Chapter 2, a general scheme based on Lagrangian formulation is presented to derive the equations of motion of a multi-link planer flexible as well as rigid manipulator with rotary joints. In case of flexible links finite element method is used to discretize the continuous system. With this proportional and hybrid damping are discussed. In Chapter 3, dynamic equations of motion are derived for a single link rigid and flexible manipulators on the basis of formulation discusses in Chapter 2. After that time response results are discussed for undamped and damped cases. In Chapter 4, the work is extended to two-link rigid and flexible manipulators cases. After deriving the equations time response results are discussed for undamped and damped cases. Finally in Chapter 5, we summarize the work and give suggestions for future work.

Chapter 2

Robot Arm Dynamics

In this chapter, firstly a general scheme, based on the Lagrangian formulation is presented to derive the dynamic equations of motion for a multi-link planer robot having rigid joints and links. In Section 2.2, Lagrange's equation in conjunction with finite element method is used to develop the equations of motion for a multi-link robot having flexible links. Finally proportional and hybrid damping schemes are discussed and are incorporated into the model.

2.1 Dynamics of Rigid Robot Arm

To start with, we consider the dynamics of a multi-link planer robot, assuming the joints and arms to be rigid. The general equations of motion are found through the direct application of the Lagrangian formulation to a non-conservative system (Fu, Gonzalez and Lee 1987). The Lagrange's equation is given as:

$$\frac{d}{dt}\left(\frac{\partial \mathcal{L}}{\partial \dot{\mathbf{q}}}\right) - \frac{\partial \mathcal{L}}{\partial \mathbf{q}} = \mathbf{Q} \tag{2.1}$$

where $\mathcal{L}$= Lagrangian function = Kinetic Energy (T) - Potential Energy (V)

$\mathbf{q}$ = Generalized coordinates of the robot arms

$\dot{\mathbf{q}}$ = Time derivative of generalized coordinates, $\mathbf{q}$

$\mathbf{Q}$= Generalized force (or torque) applied to the system

Dynamic formulation of a rigid robot is presented in the following section.

2.1.1 Planer Manipulator Kinematics

As suggested by Equation 2.1, Lagrangian formulation requires the knowledge of kinetic energy of the manipulator, which in turn requires the knowledge of the velocity of each link. In this section, the velocity at a point on link j is derived. Figure 2.1 shows the schematic of a multi-link planer manipulator.

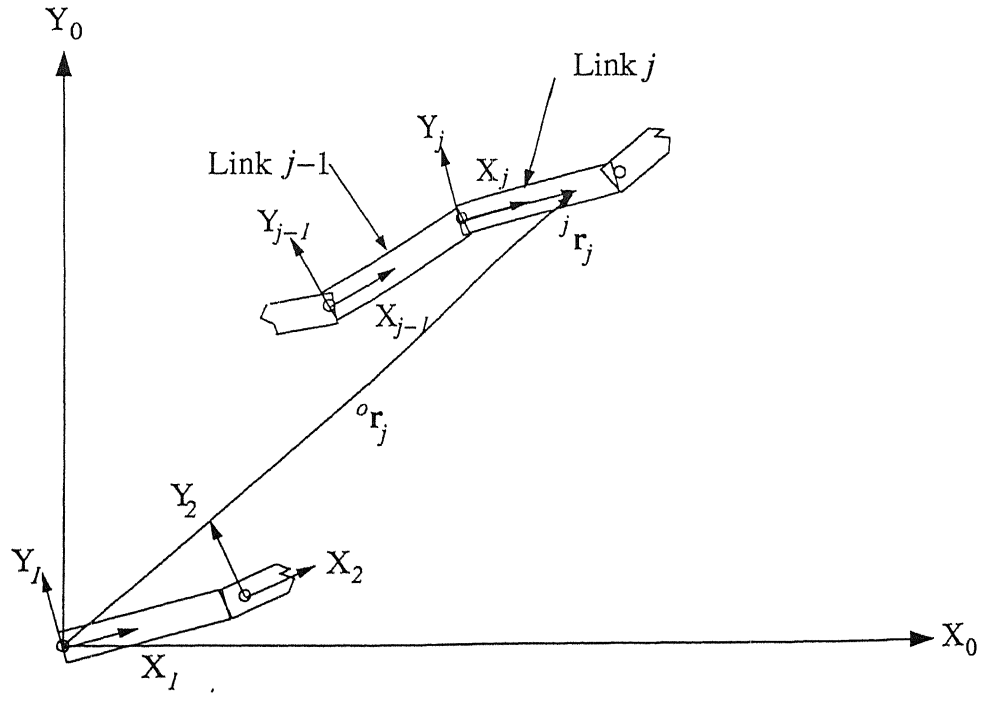

Figure 2.1: Schematic of a multi-link planer manipulator

Position vector of a point on link j in local coordinate frame (X_j, Y_j), $\mathbf{r}_j^j$ is given by:

$$\mathbf{r}_j^j = \begin{bmatrix} x & y & 1 \end{bmatrix}^T \tag{2.2}$$

Therefore position vector of a point on link j in with respect to base coordinate frame (X_0, Y_0), $\mathbf{r}_j^0$ is given by:

$$\mathbf{r}_j^0 = \mathcal{R}_j^0 \mathbf{r}_j^j \tag{2.3}$$

and

$$\mathcal{R}_j^0 = \mathcal{R}_1^0 \mathcal{R}_2^1 \ldots \mathcal{R}_j^{j-1} \tag{2.4}$$

where $\mathcal{R}_j^{j-i}$ is homogeneous coordinate transformation matrix from coordinate system (X_{j-1}, Y_{j-1}) to (X_j, Y_j) and is given by:

$$\mathcal{R}_j^{j-1} = \begin{bmatrix} \cos\theta_j & -\sin\theta_j & L_{j-1}\cos\theta_j \\ \sin\theta_j & \cos\theta_j & L_{j-1}\sin\theta_j \\ 0 & 0 & 1 \end{bmatrix} \tag{2.5}$$

Where L_{j-1} is the length of the $(j-1)th$ link and θ_j is the angle between $(j-1)th$ and jth coordinate frame. Now the velocity at a point on link j with respect to base frame, $\dot{\mathbf{r}}_j^0$ is given by:

$$\begin{aligned} \dot{\mathbf{r}}_j^0 &= \frac{d}{dt}(\mathbf{r}_j^0) = \frac{d}{dt}(\mathcal{R}_j^0 \mathbf{r}_j^j) \\ &= \left(\sum_{i=1}^{j} \frac{\partial \mathcal{R}_j^0}{\partial \mathbf{q}_i} \dot{\mathbf{q}}_i \right) \mathbf{r}_j^j \end{aligned} \tag{2.6}$$

2.1.2 Kinetic Energy of Manipulator

Let dT_j be the kinetic energy of a differential mass dm in the link j, then

$$dT_j = \frac{1}{2}(\dot{x}^2 + \dot{y}^2) = \frac{1}{2} trace(\dot{\mathbf{r}}_j^0 \dot{\mathbf{r}}_j^{0^T}) \tag{2.7}$$

From Equation 2.6, substituting the value of $\dot{\mathbf{r}}_j^0$ we get,

$$\begin{aligned} dT_j &= \frac{1}{2} tr \left[\sum_{p=1}^{j} \frac{\partial \mathcal{R}_j^0}{\partial \mathbf{q}_p} \dot{\mathbf{q}}_p \mathbf{r}_j^j \left(\sum_{r=1}^{j} \frac{\partial \mathcal{R}_j^0}{\partial \mathbf{q}_r} \dot{\mathbf{q}}_r \mathbf{r}_j^j \right)^T \right] dm \\ &= \frac{1}{2} tr \left[\sum_{p=1}^{j} \sum_{r=1}^{j} \frac{\partial \mathcal{R}_j^0}{\partial \mathbf{q}_p} \left(\mathbf{r}_j^j dm \mathbf{r}_j^{j^T} \right) \left(\frac{\partial \mathcal{R}_j^0}{\partial \mathbf{q}_r} \right)^T \dot{\mathbf{q}}_p \dot{\mathbf{q}}_r \right] \end{aligned} \tag{2.8}$$

Integrating to get the total kinetic energy of link j

$$T_j = \frac{1}{2} tr \left[\sum_{p=1}^{j} \sum_{r=1}^{j} \frac{\partial \mathcal{R}_j^0}{\partial \mathbf{q}_p} \left(\int \mathbf{r}_j^j \mathbf{r}_j^{j^T} dm \right) \left(\frac{\partial \mathcal{R}_j^0}{\partial \mathbf{q}_r} \right)^T \dot{\mathbf{q}}_p \dot{\mathbf{q}}_r \right] \tag{2.9}$$

The integral term inside the bracket is defined as Pseudo inertia matrix (J_j) of all points on link j and is given by:

$$J_j = \int \mathbf{r}_j^j \mathbf{r}_j^{j^T} dm = \begin{bmatrix} \int x_j^2 dm & \int x_j y_j dm & \int x_j dm \\ \int x_j y_j dm & \int y_j^2 dm & \int y_j dm \\ \int x_j dm & \int y_j dm & \int dm \end{bmatrix} \tag{2.10}$$

Finally total kinetic energy of manipulator can be found by summing over n links:

$$T = \frac{1}{2} \sum_{j=1}^{n} \sum_{p=1}^{j} \sum_{r=1}^{j} \left[tr \left(\frac{\partial \mathcal{R}_j^0}{\partial \mathbf{q}_p} J_j \left(\frac{\partial \mathcal{R}_j^0}{\partial \mathbf{q}_r} \right)^T \right) \dot{\mathbf{q}}_p \dot{\mathbf{q}}_r \right] \tag{2.11}$$

2.1.3 Potential Energy of Manipulator

In case of a horizontal planer manipulator the gravitation potential energy remains constant, therefore all its derivatives are zero, i.e.

$$\frac{\partial V}{\partial \mathbf{q}} = \frac{\partial V}{\partial \dot{\mathbf{q}}} = 0 \tag{2.12}$$

hence there is no need of calculating the potential energy.

2.1.4 Equations of Motion of a Rigid Robot

From Equations 2.11 and 2.12, the Lagrangian function $\mathcal{L} = T - V$ is given by,

$$\mathcal{L} = \frac{1}{2} \sum_{j=1}^{n} \sum_{p=1}^{j} \sum_{r=1}^{j} \left[tr \left(\frac{\partial \mathcal{R}_j^0}{\partial \mathbf{q}_p} J_j \left(\frac{\partial \mathcal{R}_j^0}{\partial \mathbf{q}_r} \right)^T \right) \dot{\mathbf{q}}_p \dot{\mathbf{q}}_r \right] \tag{2.13}$$

Applying Lagrange's equation yields

$$\begin{aligned}\mathbf{Q}_j &= \frac{d}{dt}\left(\frac{\partial \mathcal{L}}{\partial \dot{\mathbf{q}}}\right) - \frac{\partial \mathcal{L}}{\partial \mathbf{q}} \\ &= \sum_{i=j}^{n}\sum_{k=1}^{i} tr\left(\frac{\partial \mathcal{R}_i^0}{\partial \mathbf{q}_k} J_j \left(\frac{\partial \mathcal{R}_i^0}{\partial \mathbf{q}_j}\right)^T\right)\ddot{\mathbf{q}}_k + \\ &+ \sum_{i=j}^{n}\sum_{k=1}^{i}\sum_{m=1}^{i}\left[tr\left(\frac{\partial^2 \mathcal{R}_i^0}{\partial \mathbf{q}_k \partial \mathbf{q}_m} J_j \left(\frac{\partial \mathcal{R}_i^0}{\partial \mathbf{q}_j}\right)^T\right)\dot{\mathbf{q}}_k \dot{\mathbf{q}}_m\right] \end{aligned} \tag{2.14}$$

For $j = 1, 2, \ldots, n$ above equations can be expressed in the following form:

$$\mathbf{Q}_j = \sum_{k=1}^{n} \mathbf{D}_{jk}\ddot{\mathbf{q}}_k + \sum_{k=1}^{n}\sum_{m=1}^{n} \mathbf{h}_{jkm}\dot{\mathbf{q}}_k \dot{\mathbf{q}}_m \tag{2.15}$$

or in matrix notation form as

$$\mathbf{D}(\mathbf{q}(t))\ddot{\mathbf{q}}(t) + \mathbf{h}(\mathbf{q}(t), \dot{\mathbf{q}}(t)) = \mathbf{Q}(t) \tag{2.16}$$

where:

$$\mathbf{D}_{jk} = \sum_{i=max(j,k)}^{n} tr\left(\frac{\partial \mathcal{R}_i^0}{\partial \mathbf{q}_k} J_j \left(\frac{\partial \mathcal{R}_i^0}{\partial \mathbf{q}_j}\right)^T\right) \tag{2.17}$$

$$\mathbf{h}_{jkm} = \sum_{i=max(j,k,m)}^{n} tr\left(\frac{\partial^2 \mathcal{R}_i^0}{\partial \mathbf{q}_k \partial \mathbf{q}_m} J_j \left(\frac{\partial \mathcal{R}_i^0}{\partial \mathbf{q}_j}\right)^T\right) \tag{2.18}$$

2.2 Dynamics of Multi-Link Flexible Manipulators

A manipulator having flexible links is a continuous dynamic system and therefore has infinite degrees of freedom which is governed by coupled-nonlinear-partial differential equations. However, for a major part of the engineering purposes, a mathematical model should be of finite order. It has been observed that finding the solution of an infinite order system is increasingly difficult or impossible in many cases for e.g. system with complex boundary conditions etc. Moreover certain practical constraints like finite dimensional actuators and sensors make it necessary to discretize the flexible links.

The flexible links may be decritized by using the assumed mode method or finite element method. In the assumed mode method, flexible displacements of each link are expressed as summation of finite number of modal functions. Each term is product of mode shape function, which is a function of displacement along link and time dependent modal amplitude. In the case of finite element method, unlike assumed mode method each of the flexible link is considered as an assemblage of finite number of elements, where each element satisfies the required continuity and convergency conditions (Zienkiewicz 1986). Since the displacement at a junction point (Node) of any two elements is same for both the elements,

the internal forces are balanced so that after assembly we get the model of complete link. Similar to assumed mode method the flexible displacement at any point may be expressed as summation of terms containing the product of polynomial shape functions (different for different continuity requirements) and time dependent nodal displacements.

It has been observed that in the field of flexible manipulator system assumed mode method is more common and finite element method has been somehow disregarded. This is probably due to greater model enlargement in case of finite element modelling i.e. the number of state space equations are more which causes the numerical simulation to take more time compared to the assumed mode method. However owing to simplicity of the shape functions, which are local in nature, less number of mathematical operations are required for inertia matrix computation as compared to that in case of assumed mode method (Rex 1995). The main advantage of finite element method lies in the traceable and natural manner in which the boundary conditions and physical properties may be imposed while deriving the equations of the motion. Hence it is easier to solve complicated problems with different discontinuities of material and shape. Therefore in current work finite element method has been used for the modelling of the flexible arm.

After finding the expression for displacement at any point using any of the discretization method, the dynamic equations of motion can be derived using either of Lagrangian formulation or Newton-Euler formulation. The basic approach in Newton-Euler/finite element method is that the arm is divided into number of elements and a dynamic balance on each element is carried out. However, for a large number of elements clearly it is a tedious process (Fraser and Daniel 1991). In case of Lagrangian formulation, firstly the total kinetic and potential energies are found for all the links in terms of flexible degrees of freedom and joint variables. Then standard Lagrange's equation is applied to get the dynamic equations of motion (Meirovitch 1967). It has been observed that in the case of complex dynamic systems like flexible links manipulator system where mass and elasticity are distributed over the finite regions, it is easier to derive the equations of motion by using Lagrange's method (Rex 1995). Therefore in this thesis Lagrangian formulation has been used to derive the dynamic equations of motion.

2.2.1 Assumptions

In this thesis, basic assumptions for modelling of a flexible manipulator are as follows:

1. Links of the manipulator are equivalent to Euler-Bernoulli beam and axial deformation has been considered during modelling.

2. Bending occurs in one plane.

3. Links are axially symmetric in absence of deformation.

4. Torsional deformations are neglected.

5. Joints are considered to be rigid.

2.2.2 Modelling Procedure

The main objective of the methodology is to derive the dynamic equations of motion in a compact symbolic form. Basic procedure involves the following steps:

1. Division of manipulator link into a number of finite elements of equal length.

2. Calculation of elemental kinetic energy and potential energy.

3. Assembly to get the total kinetic and potential energies for the manipulator.

4. Application of boundary conditions.

5. Application of Lagrange's equation .

2.2.3 Link Kinematics

By convention the links of a planer revolute joint manipulator are numbered consecutively from 0 to n starting from base of the manipulator to tip of the end-effector, where n is the total number of links. We define the coordinate system (X_j, Y_j) on link j with origin O_j at joint j, oriented so that the X_j axis is along the axis of link j. The 2 x 2 rotation matrix from coordinate system (X_{j-1}, Y_{j-1}) to (X_j, Y_j), $\mathcal{R}_j^{j-1}$ is given by (Craig 1999):

$$\mathcal{R}_j^{j-1} = \begin{bmatrix} \cos\hat{\theta}_j & -\sin\hat{\theta}_j \\ -\sin\hat{\theta}_j & \cos\hat{\theta}_j \end{bmatrix} \tag{2.19}$$

where

$$\hat{\theta}_j = \theta_j + \phi_{j-1,tip}$$

θ_j : Angle between $(j-1)th$ and jth links

$\phi_{j-1,tip}$: Angular deflection at the tip (farthest point from base) of the $(j-1)th$ link

Let $\mathcal{R}_j^0$ be the 2 x 2 rotation matrix from the base coordinate system (X_0, Y_0) to (X_j, Y_j) then:

$$\mathcal{R}_j^0 = \mathcal{R}_1^0 \mathcal{R}_2^1 \ldots \mathcal{R}_j^{j-1} \tag{2.20}$$

Using this matrix, the position vector of any material point(s) along the neutral axis of link j can be expressed with respect to base coordinate system (X_0, Y_0) as :

$$\mathbf{r}_j^0 = \mathbf{p}_j^0 + \mathcal{R}_j^0 \mathbf{r}_j^j \tag{2.21}$$

Where $\mathbf{p}_j^0$ is a 2×1 position vector of base point (at jth joint) of jth link with respect to base coordinate system. And the local position vector $\mathbf{r}_j^j$ is given by:

$$\mathbf{r}_j^j = \begin{bmatrix} x \\ 0 \end{bmatrix} + \begin{bmatrix} u_j(x,t) \\ v_j(x,t) \end{bmatrix} \tag{2.22}$$

where

$u_j(x,t)$: axial deformation along X-axis at a distance x and at time t expressed in coordinate frame of link j

$v_j(x,t)$: flexural transverse deflection along Y-axis with reference to neutral axis at a distance x and at time t expressed in coordinate frame of link j

The velocity of a material point on link j can be obtained from the time derivative of the inertial base frame and is given by:

$$\dot{\mathbf{r}}_j = \dot{\mathbf{p}}_j^0 + \dot{\mathcal{R}}_j^0 \mathbf{r}_j^j + \mathcal{R}_j^0 \dot{\mathbf{r}}_j^j \tag{2.23}$$

Where $\dot{\mathbf{r}}_j^j$ is given by:

$$\dot{\mathbf{r}}_j^j = \begin{bmatrix} 0 \\ \dot{v}_j(x,t) \end{bmatrix} \tag{2.24}$$

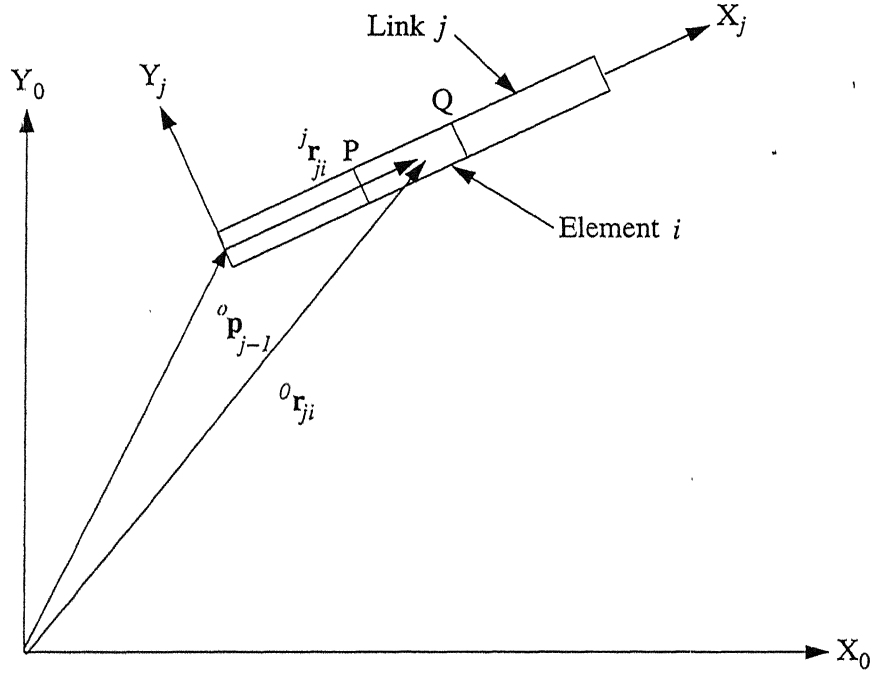

Figure 2.2: A typical finite element i in link j

2.2.4 Discretization

As discussed in Section 2.2, we use finite element method to discritize the flexible links. Each of the links is divided into a number of finite elements of equal lengths. Let PQ be one such element i on link j, with nodes i and $i+1$ as shown in Figure 2.2.

Local position vector of any point along the neutral axis of the *ith* element, expressed in local coordinate system is given by:

$$\mathbf{r}_{ji} = \begin{bmatrix} (i-1)l_j + x_{ji} \\ 0 \end{bmatrix} + \begin{bmatrix} u_{ji}(x,t) \\ v_{ji}(x,t) \end{bmatrix} \tag{2.25}$$

Where l_j is the length of each element of link j and expression for elastic displacements $u_{ji}(x,t)$ and $v_{ji}(x,t)$ are given as:

$$\begin{bmatrix} u_{ji}(x,t) \\ v_{ji}(x,t) \end{bmatrix} = \begin{bmatrix} F_1(x) & 0 & 0 & F_2(x) & 0 & 0 \\ 0 & H_1(x) & H_2(x) & 0 & H_3(x) & H_4(x) \end{bmatrix} \mathbf{q}_{f_{ji}}(t) \tag{2.26}$$

and vector of elemental flexible degrees of freedom, $\mathbf{q}_{f_{ji}}(t)$ is given by:

$$\mathbf{q}_{f_{ji}}(t) = \begin{bmatrix} u_{j,i}(t) & v_{j,i}(t) & vx_{j,i}(t) & u_{j,i+1}(t) & v_{j,i+1}(t) & vx_{j,i+1}(t) \end{bmatrix}^T \tag{2.27}$$

where

$u_{j,i}(t)$: axial deformation along X-axis at *ith* node of *jth* link

$v_{j,i}(t)$: flexural transverse deflection along Y-axis at *ith* node of *jth* link

$vx_{j,i}(t)$: flexural slope along Y-axis at *ith* node of *jth* link

A typical link element '*i*' with its nodal degrees of freedoms has been shown in Figure 2.3.

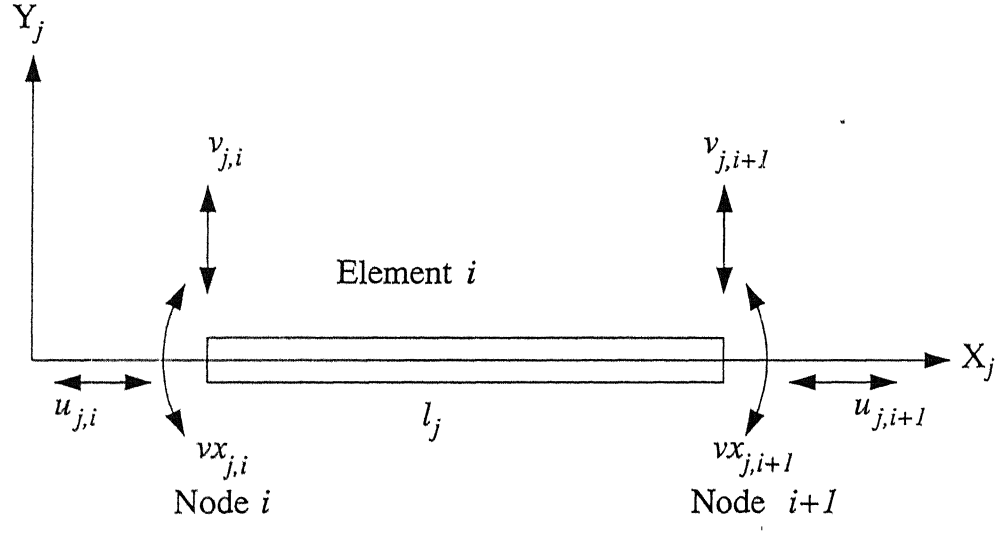

Figure 2.3: Nodal degrees of freedoms of *ith* element of link j

Various shape functions are given as (Zienkiewicz 1986):

$$F_1 = \left(1 - \frac{x}{l_j}\right)$$

$$F_2 = \left(\frac{x}{l_j}\right)$$

$$H_1 = \left(\frac{x}{l_j}\right)^2 + 2\left(\frac{x}{l_j}\right)^3$$

$$H_2 = x\left(\frac{x}{l_j} - 1\right)^2$$

$$H_3 = x\left(\frac{x}{l_j}\right)^2\left(3 - 2\frac{x}{l_j}\right)$$

$$H_4 = \frac{x^2}{l_j}\left(\frac{x}{l_j} - 1\right) \tag{2.28}$$

2.2.5 Calculation of Kinetic and Potential Energies

Kinetic Energy

The total kinetic energy of flexible manipulator system is due to motions of joints and links. The kinetic energy for a revolute joint j, if considered as mass with rotary inertia about the axis of revolution, is given by,

$$T_{joint_j} = \frac{1}{2}I_{h_j}\dot{\theta}_j^2 + \frac{1}{2}m_{h_j}\left(\frac{d\mathbf{p}_j^0}{dt}\right)^T\left(\frac{d\mathbf{p}_j^0}{dt}\right) \tag{2.29}$$

where m_{h_j} and I_{h_j} are the mass and inertia respectively of hub at joint j

$\mathbf{p}_j^0$: position vector of joint j with respect to base frame

$\dot{\theta}_j$: angular velocity of joint j

To calculate the kinetic energy due to flexible link we consider the kinetic energy of a differential mass dm_j, on link j of the manipulator which can be written as:

$$dT_{link_j} = \frac{1}{2}dm_j\left(\frac{d\mathbf{r}_j^0}{dt}\right)^T\left(\frac{d\mathbf{r}_j^0}{dt}\right) \tag{2.30}$$

Kinetic energy of an element i on link j is given by:

$$T_{link_{ji}} = \frac{1}{2}\int_0^{l_j}\rho_j A_j\left(\frac{d\mathbf{r}_j^0}{dt}\right)^T\left(\frac{d\mathbf{r}_j^0}{dt}\right)dx_{ji} \tag{2.31}$$

For constant material density ρ_j and area of cross-section A_j, the above expression can be rewritten as:

$$T_{link_{ji}} = \frac{1}{2}\int_0^{l_j} m_j\left(\frac{d\mathbf{r}_j^0}{dt}\right)^T\left(\frac{d\mathbf{r}_j^0}{dt}\right)dx_{ji} \tag{2.32}$$

where m_j is the mass per unit length for jth link. As assumed for slender beam the total kinetic energy of the flexible link j can be found as:

$$T_{link_j} = \frac{1}{2}\sum_{i=0}^{n_j}\int_0^{l_j} m_j\left(\frac{d\mathbf{r}_j^0}{dt}\right)^T\left(\frac{d\mathbf{r}_j^0}{dt}\right)dx_{ji} \tag{2.33}$$

where n_j is the total number of elements into which link j is discretized.

Potential Energy

The potential energy of flexible manipulator is considered due to axial and transverse deformation of links. Elemental potential energy due to axial deformation of a link is given by:

$$V_{a_{ji}} = \frac{1}{2}\int_0^{l_j} E_j A_j \left(\frac{\partial u_{ji}(x,t)}{\partial x_{ji}}\right)^2 dx_{ji} \tag{2.34}$$

where E_j and A_j are the Young's modulus of elasticity and area of cross- ection of link j respectivly.

Elemental potential energy due to transverse deformation is given by:

$$V_{t_{ji}} = \frac{1}{2}\int_0^{l_j} E_j I_j \left(\frac{\partial^2 v_{ji}(x,t)}{\partial x_{ji}^2}\right)^2 dx_{ji} \tag{2.35}$$

where I_j is the area moment of inertia about neutral axis of link j.

Total potential energy of jth link due to axial and transverse deformation :

$$V_j = \frac{1}{2}\sum_{i=0}^{n_j}\left[\int_0^{l_j} E_j A_j \left(\frac{\partial u_{ji}(x,t)}{\partial x_{ji}}\right)^2 dx_{ji} + \int_0^{l_j} E_j I_j \left(\frac{\partial^2 v_{ji}(x,t)}{\partial x_{ji}^2}\right)^2 dx_{ji}\right] \tag{2.36}$$

2.2.6 Application of Lagrange's Equation

The dynamic equations of motion are obtained by using the Lagrangian formulation of dynamics. The general form of Lagrange's Equation can be written as:

$$\frac{d}{dt}\left(\frac{\partial T}{\partial \dot{\mathbf{q}}}\right) - \frac{\partial T}{\partial \mathbf{q}} + \frac{\partial V}{\partial \mathbf{q}} = \mathbf{Q} \tag{2.37}$$

where T and V are total kinetic and potential energies of manipulator respectively and $\mathbf{q}$ is a vector generalized joint angular displacements and flexible deformation variables. $\mathbf{Q}$ is generalized force vector.

After application of Lagrange's equation we get dynamic equations of motion in the following form:

$$\mathbf{M}\ddot{\mathbf{q}} + \mathbf{f}(\mathbf{q}, \dot{\mathbf{q}}) + \mathbf{K}\mathbf{q} = \mathbf{Q} \tag{2.38}$$

where

$\mathbf{M}$: Generalized Mass Matrix

$\mathbf{f}(\mathbf{q}, \dot{\mathbf{q}})$: Vector of nonlinear functions of $\mathbf{q}$ and $\dot{\mathbf{q}}$

$\mathbf{K}$: Generalized Stiffness Matrix

2.2.7 Damping of the Manipulator

In a flexible manipulator system, damping is present in several possible forms. Depending on the sources, damping can be classified into the following three groups:

1. Structural damping - Due to flexibility of manipulator arms, energy is dissipated within the arm material, that leads to structural damping.

2. Viscous damping/Coulomb damping - This is caused by the friction present at the joints and within the actuator.

3. Air-resistance - External effects, particularly air resistance to the arm motion causes the damping in the manipulator system.

An equivalent damping factor can be considered to model all of the above stated effects (Thomson 1983). Now damping matrix can be found by the following relation:

$$\mathbf{C} = \alpha\mathbf{M} + \beta\mathbf{K} \tag{2.39}$$

where the constants α and β are given by:

$$\alpha = \frac{2\omega_{n_1}\omega_{n_2}(\omega_{n_2}\zeta_1 - \omega_{n_1}\zeta_2)}{\omega_{n_2}^2 - \omega_{n_1}^2} \tag{2.40}$$

$$\beta = \frac{2(\omega_{n_2}\zeta_2 - \omega_{n_1}\zeta_1)}{\omega_{n_2}^2 - \omega_{n_1}^2} \tag{2.41}$$

where ω_{n_1} and ω_{n_2} and are the first and second undamped natural frequencies and ζ_1 and ζ_2 are respective damping factors. The damping factors are determined experimentally by measuring the decrement in the link vibrations, however this method does not take into account the joint and actuator friction. After finding the damping matrix $\mathbf{C}$ the modified equation of motion for a damped system is written as:

$$\mathbf{M}\ddot{\mathbf{q}} + \mathbf{C}\dot{\mathbf{q}} + \mathbf{f}(\mathbf{q}, \dot{\mathbf{q}}) + \mathbf{K}\mathbf{q} = \mathbf{Q} \tag{2.42}$$

2.2.8 Hybrid Damping

Proportional damping, as discussed in previous section is widely used in modelling as it is quite straight forward to incorporate into the model. However, there are few problems faced by this model as discussed below:

1. The fact, that quite a few applications demand for the lightweight of the flexible manipulator links, discourages the use of metallic links. With the development of composite materials, manipulators made of composite laminates have come out as a viable alternate. However, composite materials exhibit non proportional damping.

2. In the case of coulomb damping the equivalent damping factor is a function of the amplitude of oscillations, leading to nonlinear system model (Fraser and Anthony 1991), thereby making the linear control design difficult.

To avoid the above stated problems a hybrid damping scheme is proposed (Bhattacharya, Vidyashankar and Tomlinson 2000). Hybrid damping refers to the combined passive damping and active damping strategy. In current work, a strain dependent passive damping is proposed. It has been found that ceremic and ferromagnetic coatings yield significant damping over a wide range of frequency. The vibrational energy in these alloys is dissipated through magneto-elastic coupling. During vibration, the coatings of such materials undergo a change of strain, initiating a movement of magnetic domains thereby dissipating the mechanical energy through hysteresis. It is observed that ferromagnetic materials show high damping at low strain levels (around 50-100 μ-strain) only, however for structural vibration control, induced strains are often at least one order higher in magnitude. Hence, if only ferromagnetic material is used the extent of damping achieved may be negligible. Therefore an active damping scheme is employed to limit the induced strains to low level in the passive damping coating. Smart magnetostrictive material layer like the Terfenol-D (Bhattacharya, Vidyashankar and Tomlinson 2000)is used to achieve active damping in the links. Usually smart materials, in the form of point actuators, are used to control the vibrations. However with the advent of magnetostrictive composites, such material can be used as distributed layer over the links to introduce distributed control of vibration. A series of closely packed coils enclose the magnetostrictive layer through out the link length. By driving the required current, a distributed active strain is generated in the magnetostrictive layer.

Model

A typical laminated composite link is shown in Figure 2.4. In general the link is made up of n_l layers or plies along with a layer each of magnetostrictive material and passive damping alloy.

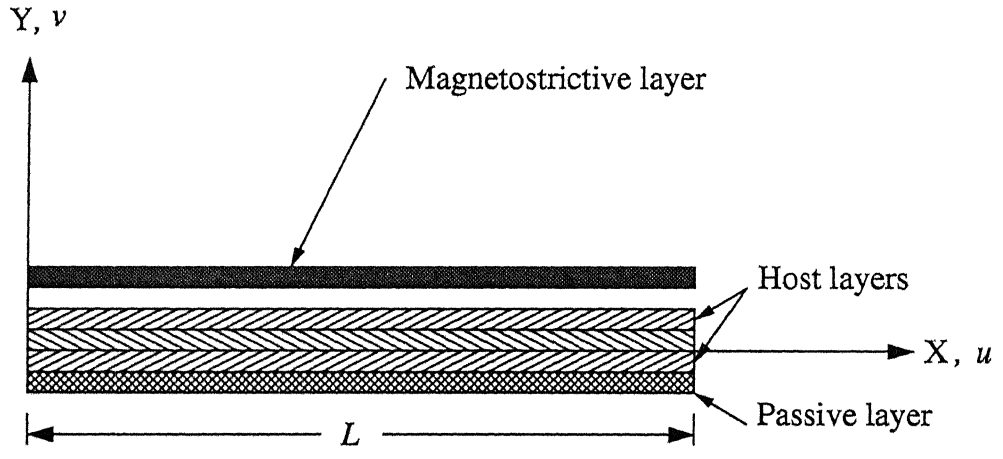

Figure 2.4: Laminated composite beam with embedded active and passive damping layer

From laminated beam theory, the total strain in terms of displacements is given by,

$$\varepsilon_x = \frac{\partial u}{\partial x} - y\frac{\partial^2 v}{\partial x^2} \tag{2.43}$$

where

y : Distance from the neutral axis

u, v : Mid-plane displacements along X and Y axes respectively

Elemental Strain and Loss Factor Calculation

Elemental strain in ith element of the jth link may be written in matrix form as:

$$\begin{aligned}
\varepsilon_{j,i} &= \left[\begin{array}{cc} \frac{\partial}{\partial x} & -y\frac{\partial^2 v}{\partial x^2} \end{array}\right] \left[\begin{array}{cccccc} F_1(x) & 0 & 0 & F_2(x) & 0 & 0 \\ 0 & H_1(x) & H_2(x) & 0 & H_3(x) & H_4(x) \end{array}\right] \mathbf{q}_{f_{ji}}(t) \\
&= \left[\begin{array}{cccccc} -1 & 0 & 0 & 1 & 0 & 0 \\ 0 & \frac{y}{l_j}\left(6-\frac{12x}{l_j}\right) & y\left(4-\frac{6x}{l_j}\right) & 0 & \frac{y}{l_j}\left(6-\frac{12x}{l_j}\right) & y\left(2-\frac{6x}{l_j}\right) \end{array}\right] \mathbf{q}_{f_{ji}}(t)
\end{aligned} \tag{2.44}$$

Since strain in an element is varying linearly with the distance along X-axis, the average strain in an element is taken as the mean of the strains at the two nodes. After solving we get:

$$\varepsilon_{j,i} = \frac{1}{l_j}\left[(u_{j,i+1} - u_{j,i}) + \frac{y}{l_j}(vx_{j,i+1} - vx_{j,i})\right] \tag{2.45}$$

Next, the strain value calculated, may be used to determine the loss factor for passive layer (η_p) by using the strain vs damping data (Bhattacharya 2000). A typical curve showing relationship between material loss factor (for Fe-16Cr-4Al material) and strain is shown in Figure 2.5. The loss factors for host layer (η_h) and magnetostrictive layer (η_m) are kept constant and equal to 0.001.

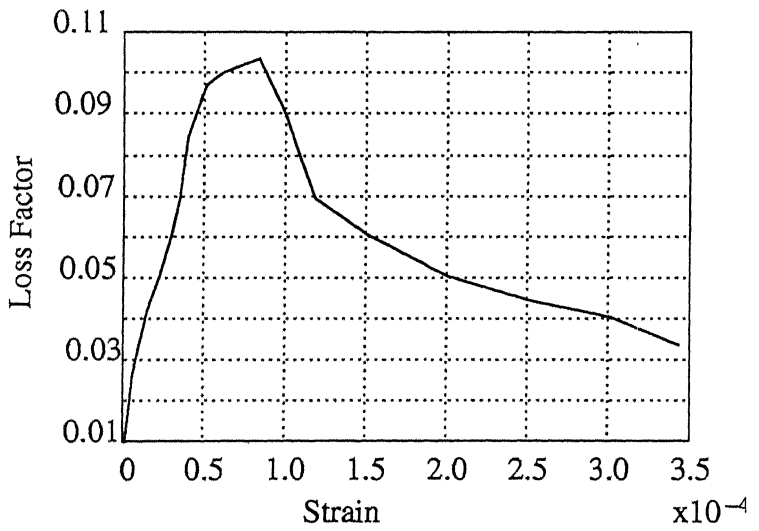

Figure 2.5: Material loss factor in passive damping layer as a function of strain

Modification in Elemental Stiffness Matrix

As each of the link is made up of a number of layers of different mater als, the various material properties vary as we move from one layer to other in transverse direction. Hence various elements of stiffness matrix get modified. The modified elemental stiffness matrix is calculated in the following manner:

First we calculate the equivalent flexural rigidity for complete link thickness as:

$$EI = \sum_{i=1}^{n_l} \int_{t_i}^{t_{i+1}} \overline{Q}_{11}^{i} w t^2 dt \tag{2.46}$$

where

w : Width of the link

t : Distance of a layer from the neutral axis

η_i : Loss factor corresponding to the ith layer

n_l : number of layers

$\overline{Q}_{11}^{i}$: First diagonal element of the stiffness matrix in the stress-strain relationship for an orthotropic lamina referred to an arbitrary axis (Agarwal and Lawerence 1990).

$\overline{Q}_{11}^{i}$ is calculated for each layer in the following manner:

- For magnetostrictive layer

$$\overline{Q}_{11}^{i} = \frac{\overline{E}_m}{1 - \nu_m^2}$$

and

$$\overline{E}_m = (1 + \eta_m j) E_m \tag{2.47}$$

where

ν_m : Poisson's ratio for magnetostrictive material

η_m : Loss factor for magnetostrictive layer

E_m : Modulus of elasticity for magnetostrictive material

- For passive layer

$$\overline{Q}_{11}^{i} = \frac{\overline{E}_p}{1 - \nu_p^2}$$

and

$$\overline{E}_p = (1 + \eta_p j) E_p \tag{2.48}$$

where

ν_p : Poisson's ratio for passive material

η_p : Loss factor for passive layer

E_p : Modulus of elasticity for passive material

- For Host layers

$$\overline{Q}^i_{11} = Q^i_{11}\cos^4\psi_i + 2(Q^i_{12} + 2Q^i_{66})\cos^2\psi_i \sin^2\psi_i + Q^i_{22}\sin^4\psi_i \tag{2.49}$$

where

ψ_i : the angle which the principal material axis of an orthographic lamina makes with the reference coordinate frame.

$Q^i_{11}, Q^i_{12}, Q^i_{21}, Q^i_{22}, Q^i_{66}$ are the elements of the stiffness matrix in the stress-strain relationship for a two dimensional orthotropic case (Agarwal and Lawerence 1990) and are calculated as:

$$Q^i_{11} = \frac{\overline{E}^i_L}{1 - \nu^i_{LT}\nu^i_{TL}}$$

$$Q^i_{12} = Q^i_{21} = \frac{\overline{E}^i_L \nu^i_{TL}}{1 - \nu^i_{LT}\nu^i_{TL}}$$

$$Q^i_{22} = \frac{\overline{E}^i_T}{1 - \nu^i_{LT}\nu^i_{TL}}$$

$$Q^i_{66} = G^i_{LT}$$

$$\overline{E}^i_L = E^i_L(1 + \eta_h j)$$

and

$$\overline{E}^i_T = E^i_T(1 + \eta_h j)$$

where

E^i_L and E^i_T : Elastic modulii in the longitudinal and transverse direction respectively.

ν^i_{LT} : Major Poisson ratio, giving the transverse strain caused by the longitudinal stress

ν^i_{LT} : Minor Poisson ratio, giving the longitudinal strain caused by the transverse stress

G^i_{LT} : Shearing modulus associated with the axis of symmetry.

In addition, for calculation of stiffness matrix elements corresponding to axial deformation, equivalent EA for complete link thickness as:

$$EA = \sum_{i=1}^{n_l} \int_{t_i}^{t_{i+1}} \overline{Q}^i_{11} w dt \tag{2.50}$$

Values of EI and EA, calculated by the above discussed procedure, are used while calculating the elemental stiffness matrix $\mathbf{K}_p$ for a passive damped system.

Calculation of Active damping

Active damping matrix is calculated as (Bhattacharya 1997):

$$\mathbf{C}_{a_{j,i}} = \begin{bmatrix} 0 & -\frac{F_1}{2} & -\frac{F_1 l_j}{12} & 0 & -\frac{F_1}{2} & \frac{F_1 l_j}{12} \\ 0 & \frac{6F_2}{5l_j} & \frac{F_2}{10} & 0 & -\frac{6F_2}{5l_j} & \frac{F_2}{10} \\ 0 & \frac{11F_2}{10} & \frac{2F_2 l_j}{15} & 0 & -\frac{F_2}{10} & -\frac{F_2 l_j}{30} \\ 0 & \frac{F_1}{2} & \frac{F_1 l_j}{12} & 0 & \frac{F_1}{2} & -\frac{F_1 l_j}{12} \\ 0 & -\frac{6F_2}{5l_j} & -\frac{F_2}{10} & 0 & \frac{6F_2}{5l_j} & -\frac{F_2}{10} \\ 0 & -\frac{F_2}{10} & -\frac{F_2 l_j}{30} & 0 & -\frac{11F_2}{10} & \frac{2F_2 l_j}{15} \end{bmatrix} \tag{2.51}$$

where F_1 and F_2 are given by:

$$F_1 = \int_{t_m}^{t_{m+1}} \overline{C} dt$$

and

$$F_2 = \int_{t_m}^{t_{m+1}} \overline{C} t dt$$

where

t_m, t_{m+1} : Distances of the magnetostrictive layer from neutral axis

$$\overline{C} = -d_m k_1 cc E_m w$$

d_m : Magneto-Mechanic constant (meter/Ampere)

k_1 : Gain of controller

cc is coil-constant which is calculated as:

$$cc = \frac{n_c}{\sqrt{w^2 + 4r_c^2}}$$

where

n_c : Number of coils

w : Width of the link

r_c : Radius of coil wire

Once we find the modified stiffness matrix $\mathbf{K}_p$ and active damping matrix $\mathbf{C}_a$ the modified equation of motion for a hybrid damped system is written as:

$$\mathbf{M}\ddot{\mathbf{q}} + \mathbf{C}_a\dot{\mathbf{q}} + \mathbf{f}(\mathbf{q}, \dot{\mathbf{q}}) + \mathbf{K}_p\mathbf{q} = \mathbf{Q} \tag{2.52}$$

A flow-chart for finding the system time response with hybrid damping is shown in Figure 2.6.

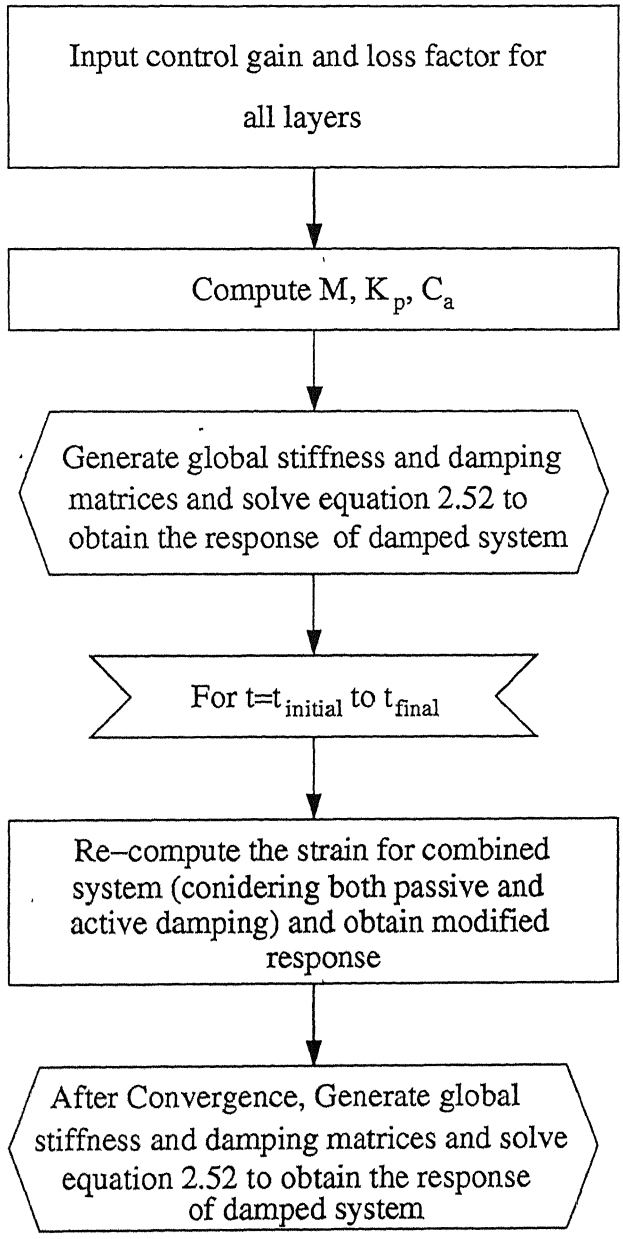

Figure 2.6: A flow-chart for finding the system response with hybrid damping

Chapter 3

Dynamic Model Derivation and Simulation of Single-Link Manipulator

In this chapter, first the closed form undamped dynamic equations of motion are derived for single-link rigid and flexible manipulators from the formulation given in Chapter 2. Later damping is introduced into the model. Proportional and hybrid dampings are considered. Finally numerical simulation of this dynamic system is carried out and various results are discussed.

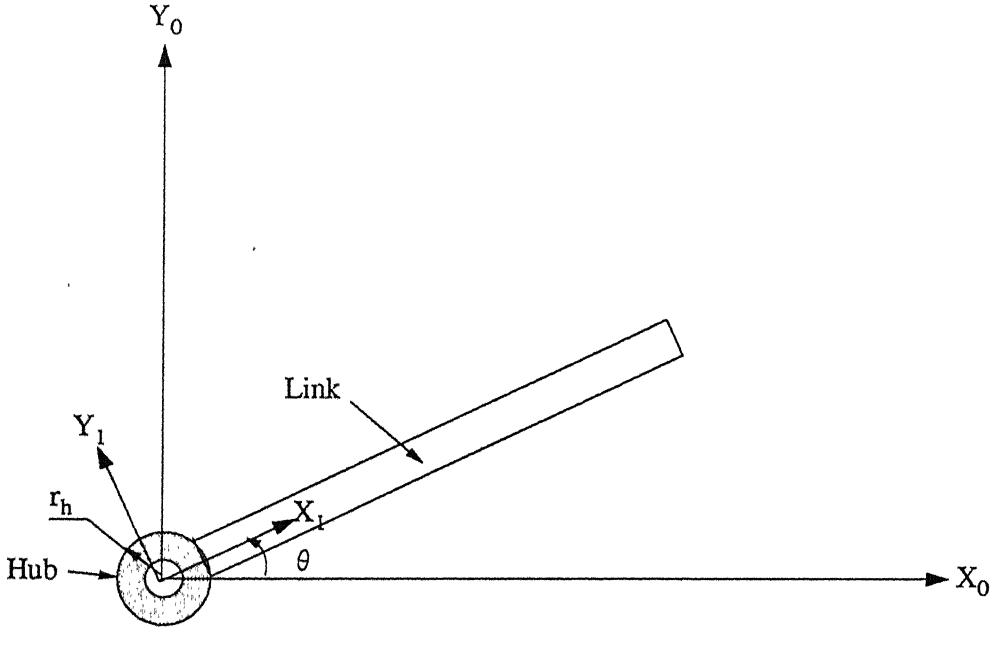

Figure 3.1: A schematic of a single-link manipulator

3.1 Rigid Single-Link Manipulator

In this section, the dynamic equations of motion for a single-link rigid manipulator are derived in matrix form. A single-link revolute joint manipulator is shown in Figure 3.1.

We assume joint variable= θ; mass of link= M; length of link= L. From Equation 2.5, the homogeneous transformation matrice is obtained as:

$$\mathcal{R}_1^0 = \begin{bmatrix} \cos\theta & -\sin\theta & L\cos\theta \\ \sin\theta & \cos\theta & L\sin\theta \\ 0 & 0 & 1 \end{bmatrix} \tag{3.1}$$

Therefore we can find:

$$\frac{\partial \mathcal{R}_1^0}{\partial \theta} = \begin{bmatrix} -\sin\theta & -\cos\theta & -L\sin\theta \\ \cos\theta & -\sin\theta & L\cos\theta \\ 0 & 0 & 0 \end{bmatrix} \tag{3.2}$$

Using Equation 2.10, assuming all the products of inertia are zero (Fu, Gonzalez and Lee 1987), we can derive the pseudo inertia matrix J:

$$J = \begin{bmatrix} \frac{1}{3}ML^2 & 0 & 0 & \frac{1}{3}ML \\ 0 & 0 & 0 & 0 \\ 0 & 0 & 0 & 0 \\ -\frac{1}{3}ML^2 & 0 & 0 & M \end{bmatrix} \tag{3.3}$$

Then using Equation 2.17, the inertia term is given as:

$$D = Tr\left(\frac{\partial \mathcal{R}_1^0}{\partial \theta} J \left(\frac{\partial \mathcal{R}_1^0}{\partial \theta}\right)^T\right)$$

Substituting values of $\frac{\partial \mathcal{R}_1^0}{\partial \theta}$ and J from Equations 3.2 and 3.3, we get

$$D = \frac{1}{3}ML^2 \tag{3.4}$$

Using Equation 2.15, vector of Coriolis and Centrifugal terms is given as:

$$\begin{aligned} h &= \sum_{k=1}^{1}\sum_{m=1}^{1} h_{1km}\dot{\theta}_k\dot{\theta}_m \\ &= h_{111}\dot{\theta}^2 \end{aligned} \tag{3.5}$$

Using Equation 2.18, we can obtain the value of h_{111}, therefore

$$h = 0$$

Substituting in Equation 2.16, final dynamic equation is given as:

$$\frac{1}{3}ML^2\ddot{\theta} = \tau \tag{3.6}$$

where τ is the external torque applied at the joint.

3.2 Flexible Single-Link Manipulator

The dynamic equations of motion for a single-link flexible manipulator are derived us finite element discretization model developed in Chapter 2. Lagrangian formulation used for deriving equations of motion. Numerical results of simulation of this system a presented in Section 3.3 and the effect of damping is brought out.

3.2.1 Calculation of Elemental Kinetic Energy

We define the joint and link coordinate system according to Section 2.2.3. Therefore th position vector of any material point(s) along the neutral axis of link can be expressed wit respect to base coordinate system (X_0, Y_0) as:

$$\mathbf{r}_1^0 = \mathbf{p}_1^0 + \mathcal{R}_1^0 \mathbf{r}_1^1 \tag{3.7}$$

Here $\mathbf{p}_1^0$ is a null vector (as joint is at the origin of base coordinate system) and $\mathcal{R}_1^0$ is given by

$$\mathcal{R}_1^0 = \begin{bmatrix} \cos\theta & -\sin\theta \\ -\sin\theta & \cos\theta \end{bmatrix} \tag{3.8}$$

From Figure 2.2, local position vector $\mathbf{r}_1^1$ is given by:

$$\mathbf{r}_1^1 = \begin{bmatrix} (i-1)l + x_i + u_i(x,t) + r_h \\ v_i(x,t) \end{bmatrix} \tag{3.9}$$

where

r_h : radius of joint-hub

$u_i(x,t)$: axial deformation along X-axis at a distance x and at time t in the *ith* element of link expressed in coordinate frame of link

$v_i(x,t)$: flexural transverse deflection along Y-axis with reference to neutral axis at a distance x and at time t in the *ith* element of link expressed in coordinate frame of link

and $u_i(x,t)$ and $v_i(x,t)$ are given as

$$\begin{bmatrix} u_i(x,t) \\ v_i(x,t) \end{bmatrix} = \begin{bmatrix} F_1(x) & 0 & 0 & F_2(x) & 0 & 0 \\ 0 & H_1(x) & H_2(x) & 0 & H_3(x) & H_4(x) \end{bmatrix} \mathbf{q}_{f_i}(t) \tag{3.10}$$

Where

$$\mathbf{q}_{f_i}(t) = \begin{bmatrix} u_i(t) & v_i(t) & vx_i(t) & u_{i+1}(t) & v_{i+1}(t) & vx_{i+1}(t) \end{bmatrix}^T$$

and

$u_i(t)$: axial deformation along X-axis at *ith* node of link

$v_i(t)$: flexural transverse deflection along Y-axis at *ith* node of link

$vx_i(t)$: flexural slope along Y-axis at *ith* node of link

Various shape functions are given as in Equation 2.28.

The general expression for kinetic energy due to inertia of joint

$$T_{joint} = \frac{1}{2} I_h \dot{\theta}^2 \tag{3.11}$$

where I_h is the inertia of the joint. Now general expression for kinetic energy of the ith element of link

$$T_{link_i} = \frac{1}{2} \int_0^l m \left(\frac{d\mathbf{r}_1^0}{dt} \right)^T \left(\frac{d\mathbf{r}_1^0}{dt} \right) dx_i \tag{3.12}$$

we can also write:

$$\frac{d\mathbf{r}_1^0}{dt} = \frac{\partial \mathbf{r}_1^0}{\partial \mathbf{q}_i} \frac{\partial \mathbf{q}_i}{\partial t}$$

$$= \left[\begin{array}{ccccccc} \frac{\partial \mathbf{r}_1^0}{\partial \theta} & \frac{\partial \mathbf{r}_1^0}{\partial u_i} & \frac{\partial \mathbf{r}_1^0}{\partial v_i} & \frac{\partial \mathbf{r}_1^0}{\partial vx_i} & \frac{\partial \mathbf{r}_1^0}{\partial u_{i+1}} & \frac{\partial \mathbf{r}_1^0}{\partial v_{i+1}} & \frac{\partial \mathbf{r}_1^0}{\partial vx_{i+1}} \end{array} \right] \dot{\mathbf{q}}_i \tag{3.13}$$

Where elemental degrees of freedom vector is given by

$$\mathbf{q}_i(t) = \left[\begin{array}{ccccccc} \theta & u_i(t) & v_i(t) & vx_i(t) & u_{i+1}(t) & v_{i+1}(t) & vx_{i+1}(t) \end{array} \right]^T$$

From Equation 3.12 and Equation 3.13 the kinetic energy of ith element is found and written in the following form

$$T_{link_i} = \frac{1}{2} \dot{\mathbf{q}}_i^T \mathbf{M}_i \dot{\mathbf{q}}_i \tag{3.14}$$

Where $\mathbf{M}_i$ is a symmetric 7 x 7 size elemental mass matrix of the following form

$$\mathbf{M}_i = \left[\begin{array}{ccccc} \mathbf{M}_i(1,1) & \mathbf{M}_i(1,2) & \dots & \mathbf{M}_i(1,7) \\ \mathbf{M}_i(2,1) & & & \\ \vdots & & [\mathbf{P}_i]_{6x6} & \\ \mathbf{M}_i(7,1) & & & \end{array} \right]_{7x7} \tag{3.15}$$

Elements of the above mass matrix are calculated as

$$\mathbf{M}_i(j,k) = \int_0^l m \left(\frac{\partial \mathbf{r}_1^0}{\partial \mathbf{q}_{i,j}} \right)^T \left(\frac{\partial \mathbf{r}_1^0}{\partial \mathbf{q}_{i,k}} \right) dx_i \tag{3.16}$$

Where $\mathbf{q}_{i,j}$ is the jth element of vector $\mathbf{q}_i$.

After integration, all the matrix elements are derived and given in final form as:

$$\mathbf{P}_i = \frac{ml}{420} \left[\begin{array}{cccccc} 140 & 0 & 0 & 70 & 0 & 0 \\ 0 & 156 & 22l & 0 & 54 & -13l \\ 0 & 22l & 4l^2 & 0 & 13l & -3l^2 \\ 70 & 0 & 0 & 140 & 0 & 0 \\ 0 & 54 & 13l & 0 & 156 & -22l \\ 0 & -13l & -3l^2 & 0 & -22l & 4l^2 \end{array} \right] \tag{3.17}$$

$$\begin{aligned} \mathbf{M}_i(1,1) &= ml \left[l^2 \left(i^2 - i + \frac{1}{3} \right) + lr_h(2i-1) + r_h^2 \right] + \mathbf{q}_{f_i}^T \mathbf{P}_i \mathbf{q}_{f_i} + \\ &+ 2m \left[\begin{array}{cc} \left(\frac{il^2}{2} - \frac{l^3}{3} + \frac{r_h l}{2} \right) & \left(\frac{il^2}{2} - \frac{l^3}{6} + \frac{r_h l}{2} \right) \end{array} \right] \left[\begin{array}{c} u_i \\ u_{i+1} \end{array} \right] \end{aligned} \tag{3.18}$$

$$\mathrm{M}_i(1,2) = -\frac{ml}{20}\begin{bmatrix} 7 & l & 3 & -l \end{bmatrix}\begin{bmatrix} v_i \\ vx_i \\ v_{i+1} \\ vx_{i+1} \end{bmatrix} \tag{3.19}$$

$$\mathrm{M}_i(1,3) = \frac{ml}{20}(10il - 7l + 10r_h) + \frac{ml}{20}\begin{bmatrix} -13 & 3 \end{bmatrix}\begin{bmatrix} u_i \\ u_{i+1} \end{bmatrix} \tag{3.20}$$

$$\mathrm{M}_i(1,4) = \frac{ml^2}{60}(5il - 3l + 5r_h) + \frac{ml^2}{20}\begin{bmatrix} 1 & 4 \end{bmatrix}\begin{bmatrix} u_i \\ u_{i+1} \end{bmatrix} \tag{3.21}$$

$$\mathrm{M}_i(1,5) = -\frac{ml}{60}\begin{bmatrix} 9 & 2l & 21 & 3l \end{bmatrix}\begin{bmatrix} v_i \\ vx_i \\ v_{i+1} \\ vx_{i+1} \end{bmatrix} \tag{3.22}$$

$$\mathrm{M}_i(1,6) = \frac{ml}{20}(10il - 3l + 10r_h) + \frac{ml}{20}\begin{bmatrix} 17 & 7 \end{bmatrix}\begin{bmatrix} u_i \\ u_{i+1} \end{bmatrix} \tag{3.23}$$

$$\mathrm{M}_i(1,7) = -\frac{ml^2}{60}(5il - 2l + 5r_h) + \frac{ml^2}{20}\begin{bmatrix} -2 & 3 \end{bmatrix}\begin{bmatrix} u_i \\ u_{i+1} \end{bmatrix} \tag{3.24}$$

3.2.2 Calculation of Elemental Potential Energy

The elastic potential energy of flexible link is considered due to axial and transverse deformation of link. Elemental potential energy due to axial deformation is given by:

$$V_{a_i} = \frac{1}{2}\int_0^l EA\left(\frac{\partial u_i(x,t)}{\partial x_i}\right)^2 dx_i \tag{3.25}$$

where E and A are Young's modulus of elasticity and area of cross-section for link and $u_i(x,t)$ is given by

$$u_i(x,t) = \begin{bmatrix} F_1(x) & F_2(x) \end{bmatrix}\begin{bmatrix} u_i \\ u_{i+1} \end{bmatrix} \tag{3.26}$$

From Equation 3.25 and Equation 3.26, V_{a_i} is written as:

$$V_{a_i} = \frac{1}{2}\begin{bmatrix} u_i & u_{i+1} \end{bmatrix}^T \mathrm{K}_{a_i}\begin{bmatrix} u_i \\ u_{i+1} \end{bmatrix} \tag{3.27}$$

where

$$\mathrm{K}_{a_i} = \int_0^l EA\begin{bmatrix} \frac{1}{l^2} & -\frac{1}{l^2} \\ -\frac{1}{l^2} & \frac{1}{l^2} \end{bmatrix} dx_i \tag{3.28}$$

$$\mathrm{K}_{a_i} = \frac{EA}{l}\begin{bmatrix} 1 & -1 \\ -1 & 1 \end{bmatrix} \tag{3.29}$$

Elemental potential energy due to transverse deformation is given by:

$$V_{t_i} = \frac{1}{2}\int_0^l EI\left(\frac{\partial^2 v_i(x,t)}{\partial x_i^2}\right)^2 dx_i \tag{3.30}$$

where I is area moment of inertia of link about neutral axis and v_i is given by

$$v_i(x,t) = \begin{bmatrix} H_1(x) & H_2(x) & H_3(x) & H_4(x) \end{bmatrix} \begin{bmatrix} v_i \\ vx_i \\ v_{i+1} \\ vx_{i+1} \end{bmatrix} \tag{3.31}$$

From Equation 3.30 and Equation 3.31, V_{t_i} can be written as

$$V_{t_i} = \frac{1}{2} \begin{bmatrix} v_i & vx_i & v_{i+1} & vx_{i+1} \end{bmatrix}^T \mathbf{K}_{t_i} \begin{bmatrix} v_i \\ vx_i \\ v_{i+1} \\ vx_{i+1} \end{bmatrix} \tag{3.32}$$

where

$$\mathbf{K}_{t_i} = \frac{EI}{l^3} \begin{bmatrix} 12 & 6l & -12 & 6l \\ 6l & 4l^2 & -6l & 2l^2 \\ -12 & -6l & 12 & -6l \\ 6l & 2l^2 & -6l & 4l^2 \end{bmatrix} \tag{3.33}$$

Therefore total potential energy of link due to axial and transverse deformation can be written in matrix form as:

$$V_i = \frac{1}{2} \mathbf{q}_{f_i}^T \mathbf{K}_i \mathbf{q}_{f_i} \tag{3.34}$$

where combined stiffness matrix K_i is given by:

$$\mathbf{K}_i = \frac{E}{l} \begin{bmatrix} A & 0 & 0 & -A & 0 & 0 \\ 0 & \frac{12I}{l^2} & \frac{6I}{l} & 0 & -\frac{12I}{l^2} & \frac{6I}{l} \\ 0 & \frac{6I}{l} & 4I & 0 & -\frac{6I}{l} & 2I \\ -A & 0 & 0 & A & 0 & 0 \\ 0 & -\frac{12I}{l^2} & -\frac{6I}{l} & 0 & \frac{12I}{l^2} & -\frac{6I}{l} \\ 0 & \frac{6I}{l} & 2I & 0 & -\frac{6I}{l} & 4I \end{bmatrix} \tag{3.35}$$

3.2.3 Assembly Procedure

The total kinetic and potential energies are calculated by adding the elemental kinetic and potential energies which involves the assembling of various vectors and matrices. Let n be the number of elements into which link is discretized.

Kinetic Energy

Reduced kinetic energy of the manipulator link, T^*_{link} is given by

$$\begin{aligned} T^*_{link} &= \sum_{i=1}^{n} \frac{1}{2} \dot{\mathbf{q}}_i^T \mathbf{M}_i^* \dot{\mathbf{q}}_i \\ &= \frac{1}{2} \dot{\mathbf{q}}^T \mathbf{M}^*_{link} \dot{\mathbf{q}} \end{aligned} \tag{3.36}$$

Here $\mathbf{M}_i^*$ is found by dropping out the term containing second power of flexible degrees of freedom (i.e. the term containing $\mathbf{q}_{f_i}^T \mathbf{P}_i \mathbf{q}_{f_i}$) from actual elemental mass matrix $\mathbf{M}_i$. This

dropped out term is assembled separately for convenience in applying the Lagrange's equation in the following step. Thus the reduced mass matrix $\mathbf{M}^*_{link}$ is obtained by assembling the elemental mass matrices $\mathbf{M}^*_i$. For n elements there will be $(n+1)$ nodes with 3 nodal degrees of freedom and there is one additional degree of freedom in the form of angular displacement. Hence the size of reduced mass matrix $\mathbf{M}^*_{link}$ before application of boundary conditions is $[3(n+1)+1]$ x $[3(n+1)+1]$.

$\mathbf{q}$ is the generalized variable vector for the link and $\mathbf{q}_f$ is its sub-vector which consists of flexible motion variables of the link. These are given by:

$$\mathbf{q} = \begin{bmatrix} \theta & u_1 & v_1 & vx_1 & \dots & u_{n+1} & v_{n+1} & vx_{n+1} \end{bmatrix}^T_{3(n+1)+1} \tag{3.37}$$

$$\mathbf{q}_f = \begin{bmatrix} u_1 & v_1 & vx_1 & \dots & u_{n+1} & v_{n+1} & vx_{n+1} \end{bmatrix}^T_{3(n+1)} \tag{3.38}$$

The left out term (i.e. the term containing $\mathbf{q}^T_{f_i}\mathbf{P}_i\mathbf{q}_{f_i}$)) is assembled separately in the following manner:

$$\mathbf{q}^T_f\mathbf{P}\mathbf{q}_f = \sum_{i=1}^{n} \mathbf{q}^T_{f_i}\mathbf{P}_i\mathbf{q}_{f_i} \tag{3.39}$$

We can write the contribution of this term in the total kinetic energy as

$$S = \mathbf{q}^T_f\mathbf{P}\mathbf{q}_f\dot{\theta}^2 \tag{3.40}$$

Hence total kinetic energy of the manipulator link is given as

$$T_{link} = \frac{1}{2}\left(\dot{\mathbf{q}}^T_f\mathbf{M}^*_{link}\dot{\mathbf{q}}_f + S\right) \tag{3.41}$$

From Equation 3.11 and Equation 3.41 the total kinetic energy of manipulator T is found as:

$$\begin{aligned} T &= T_{link} + T_{joint} \\ &= \frac{1}{2}\left(\dot{\mathbf{q}}^T\mathbf{M}^*_{link}\dot{\mathbf{q}} + S\right) + \frac{1}{2}I_h\dot{\theta}^2 \\ &= \frac{1}{2}\left(\dot{\mathbf{q}}^T\mathbf{M}^*\dot{\mathbf{q}} + S\right) \end{aligned} \tag{3.42}$$

where $\mathbf{M}^*$ is found by including I_h in the reduced mass matrix of the link $\mathbf{M}^*_{link}$.

Potential Energy

Potential energy of the link, V is given by

$$\begin{aligned} V &= \sum_{i=1}^{n} \frac{1}{2}\mathbf{q}^T_{f_i}\mathbf{K}_i\mathbf{q}_{f_i} \\ &= \frac{1}{2}\mathbf{q}^T_f\mathbf{K}^*\mathbf{q}_f \end{aligned} \tag{3.43}$$

Here $\mathbf{q}_f$ is given by Equation 3.38. $\mathbf{K}^*$ is the stiffness matrix of size $3(n+1)$. We define $\mathbf{K}$, which is obtained by adding a zero row and column to $\mathbf{K}^*$, as:

$$\mathbf{K} = \begin{bmatrix} 0 & \dots & 0 \\ \vdots & \mathbf{K}^* & \\ 0 & & \end{bmatrix} \tag{3.44}$$

Thus total potential energy of the manipulator is rewritten as:

$$V = \frac{1}{2}\mathbf{q}^T\mathbf{K}\mathbf{q} \tag{3.45}$$

where $\mathbf{K}$ is the global stiffness matrix. The size of stiffness matrix before application of boundary conditions is equal to that of mass matrix, i.e. $[3(n+1)+1]$ x $[3(n+1)+1]$.

3.2.4 Boundary Conditions

We assume that link is clamped rigidly with the actuator hub at the joint, therefore any displacement at node 1 of this link is constrained. This boundary condition is included into the model by setting the all flexible degrees of freedoms at node-1 to zero, i.e.

$$u_1 = 0, v_1 = 0, vx_1 = 0 \tag{3.46}$$

These nodal degrees of freedoms are eliminated from the generalized variable vector $\mathbf{q}$. Thus final $\mathbf{q}$ of size $3n+1$ is given by:

$$\mathbf{q} = \begin{bmatrix} \theta & u_2 & v_2 & vx_2 & \dots & u_{n+1} & v_{n+1} & vx_{n+1} \end{bmatrix}^T_{3n+1} \tag{3.47}$$

Consequently mass and stiffness matrices are reduced by trimming the corresponding rows and columns.

3.2.5 Application of Lagrange's Equation

The final equations of motions are derived in the matrix form by applying the Lagrange's equation. From Equations 2.1, 3.42 and 3.45

$$\mathcal{L} = \frac{1}{2}\left(\dot{\mathbf{q}}^T\mathbf{M}^*\dot{\mathbf{q}} + S - \mathbf{q}^T\mathbf{K}\mathbf{q}\right) \tag{3.48}$$

To get dynamic equations we first find $\frac{\partial \mathcal{L}}{\partial \mathbf{q}}$ and $\frac{d}{dt}\left(\frac{\partial \mathcal{L}}{\partial \dot{\mathbf{q}}}\right)$. Here again the term containing the second power of variables (i.e. S) is considered separately. Now

$$\frac{\partial \mathcal{L}}{\partial \mathbf{q}} = \frac{1}{2}\left(\dot{\mathbf{q}}^T\frac{\partial \mathbf{M}^*}{\partial \mathbf{q}}\dot{\mathbf{q}} - \mathbf{K}\mathbf{q} - \mathbf{q}^T\mathbf{K}\right) \tag{3.49}$$

And

$$\frac{\partial \mathcal{L}}{\partial \dot{\mathbf{q}}} = \frac{1}{2}\left(\mathbf{M}^*\dot{\mathbf{q}} + \dot{\mathbf{q}}^T\mathbf{M}^*\right) \tag{3.50}$$

Therefore

$$\begin{aligned}\frac{d}{dt}\frac{\partial \mathcal{L}}{\partial \dot{\mathbf{q}}} &= \frac{1}{2}\left[\mathbf{M}^*\ddot{\mathbf{q}} + \ddot{\mathbf{q}}^T\mathbf{M}^* + \sum_{k=1}^{3n+1}\left(\dot{\mathbf{q}}_k^T\frac{\partial \mathbf{M}^*}{\partial \dot{\mathbf{q}}_k}\dot{\mathbf{q}} + \dot{\mathbf{q}}^T\frac{\partial \mathbf{M}^*}{\partial \dot{\mathbf{q}}_k}\dot{\mathbf{q}}_k\right)\right] \\ &= \left[\mathbf{M}^*\ddot{\mathbf{q}} + \sum_{k=1}^{3n+1}\left(\dot{\mathbf{q}}_k^T\frac{\partial \mathbf{M}^*}{\partial \dot{\mathbf{q}}_k}\dot{\mathbf{q}}\right)\right] \end{aligned} \tag{3.51}$$

Left-out term (S) is considered in the following manner:

From Equation 3.40

$$S = \mathbf{q}_f^T\mathbf{P}\mathbf{q}_f\dot{\theta}^2 \tag{3.52}$$

$$\begin{aligned}\frac{1}{2}\left[\frac{d}{dt}\left(\frac{\partial S}{\partial \dot{\mathbf{q}}}\right) - \frac{\partial S}{\partial \mathbf{q}}\right] &= \frac{1}{2}\left[\frac{d}{dt}\left(\frac{\partial}{\partial \dot{\mathbf{q}}}\left(\mathbf{q}_f^T\mathbf{P}\mathbf{q}_f\dot{\theta}^2\right)\right) - \frac{\partial}{\partial \mathbf{q}}\left(\mathbf{q}_f^T\mathbf{P}\mathbf{q}_f\dot{\theta}^2\right)\right] \\ &= \left[\begin{array}{cccccccc}\mathbf{q}_f^T\mathbf{P}\mathbf{q}_f & 0 & \ldots & 0 & 0 & 0 & \ldots & 0\end{array}\right]^T\ddot{\theta} + \\ &+ \left[\begin{array}{cccccccc}2\mathbf{q}_f^T\mathbf{P}\dot{\mathbf{q}}_f & 0 & \ldots & 0 & 0 & 0 & \ldots & 0\end{array}\right]^T\dot{\theta} - \\ &- \left[\begin{array}{cc}0 & \left[\mathbf{P}\mathbf{q}_f\right]^T\end{array}\right]^T\dot{\theta}^2 \end{aligned} \tag{3.53}$$

Now the term containing the second derivative of general variables (i.e. term containing $\ddot{\theta}$ in the right hand side of Equation 3.53) is assembled with the inertia term $\mathbf{M}^*\ddot{\mathbf{q}}$ to get the final inertia term in the form of $\mathbf{M}\ddot{\mathbf{q}}$, where $\mathbf{M}$ is the global mass matrix.

Rest of the terms (i.e. terms containing up-to first derivative of variables in Equation 3.53) are assembled to get the vector $\mathbf{f}(\dot{\mathbf{q}}, \mathbf{q})$ of nonlinear terms.

Now from the Equations 2.1, 3.49, 3.51 and 3.53 the dynamic equations in the matrix form are given as:

$$\mathbf{M}\ddot{\mathbf{q}} + \sum_{k=1}^{3n+1}\left(\dot{\mathbf{q}}_k^T\frac{\partial \mathbf{M}^*}{\partial \mathbf{q}_k}\dot{\mathbf{q}}\right) - \frac{1}{2}\dot{\mathbf{q}}^T\frac{\partial \mathbf{M}^*}{\partial \mathbf{q}}\dot{\mathbf{q}} - \mathbf{K}\mathbf{q} + \mathbf{f} = \mathbf{Q} \tag{3.54}$$

Let

$$\mathbf{F} = \sum_{k=1}^{3n+1}\left(\dot{\mathbf{q}}_k^T\frac{\partial \mathbf{M}^*}{\partial \mathbf{q}_k}\dot{\mathbf{q}}\right) - \frac{1}{2}\dot{\mathbf{q}}^T\frac{\partial \mathbf{M}^*}{\partial \mathbf{q}}\dot{\mathbf{q}} + \mathbf{f}(\dot{\mathbf{q}}, \mathbf{q}) \tag{3.55}$$

We get the final equation in the form as:

$$\mathbf{M}\ddot{\mathbf{q}} + \mathbf{F}(\dot{\mathbf{q}}, \mathbf{q}) + \mathbf{K}\mathbf{q} = \mathbf{Q} \tag{3.56}$$

where $\mathbf{M}$ is the mass matrix, $\mathbf{F}$ the vector consisting of cetrifugal and coriolis forces, $\mathbf{K}$ the stiffness matrix and $\mathbf{Q}$ the force vector and $\mathbf{q}$ represents genralized degrees of freedom.

Now defining a state vector $\mathbf{z} = \left[\begin{array}{cc}\mathbf{q} & \dot{\mathbf{q}}\end{array}\right]^T$, Equation 3.56 can be re-written in the form:

$$\dot{\mathbf{z}} = \left[\begin{array}{c}\dot{\mathbf{q}} \\ \mathbf{M}^{-1}[\mathbf{Q} - \mathbf{F} - \mathbf{K}\mathbf{q}]\end{array}\right] \tag{3.57}$$

The above equation gives a system of first order differential equations which can be integrated to get the time response of the system.

3.2.6 Damping Matrix

From Equation 2.39 viscous damping matrix can be found by the following relation:

$$\mathbf{C} = \alpha\mathbf{M} + \beta\mathbf{K} \tag{3.58}$$

where the constants α and β are given by:

$$\alpha = \frac{2\omega_{n_1}\omega_{n_2}(\omega_{n_2}\zeta_1 - \omega_{n_1}\zeta_2)}{\omega_{n_2}^2 - \omega_{n_1}^2} \tag{3.59}$$

$$\beta = \frac{2(\omega_{n_2}\zeta_2 - \omega_{n_1}\zeta_1)}{\omega_{n_2}^2 - \omega_{n_1}^2} \tag{3.60}$$

where ω_{n_1} and ω_{n_2} and are the first and second natural undamped frequencies of link and ζ_1 and ζ_2 are respective damping factors

ω_{n_1} and ω_{n_2} are found as (Meirovitch 1967):

$$\begin{aligned} \omega_{n_1} &= 1.875^2\sqrt{\frac{EI}{mL^4}} \\ \omega_{n_2} &= 4.694^2\sqrt{\frac{EI}{mL^4}} \end{aligned} \tag{3.61}$$

In the past study, experimentally determined values of ζ_1 and ζ_2 (both equal to 0.01) are chosen (Petric 1995) for the identical conditions. After finding the damping matrix $\mathbf{C}$, the modified final equation of motion for damped system is written as:

$$\mathbf{M}\ddot{\mathbf{q}} + \mathbf{C}\dot{\mathbf{q}} + \mathbf{F}(\mathbf{q}, \dot{\mathbf{q}}) + \mathbf{K}\mathbf{q} = \mathbf{Q} \tag{3.62}$$

3.2.7 Hybrid Damping

Various material properties of the hybrid damped links are given in Table 3.1. From Equation 2.45 average elemental strain in *ith* element of the link can be written as:

$$\varepsilon_i = \frac{1}{l}\left[(u_{i+1} - u_i) + \frac{y}{l}(vx_{i+1} - vx_i)\right] \tag{3.63}$$

After computing the strain values, the strain vs damping data (Bhattacharya 2000) may be used to determine the loss factor for passive layer (η_p). The loss factors for host layer (η_h) and magnetostrictive layer (η_m) are kept constant and equal to 0.001. Once we find the loss factor η, the equivalent values of EA and EI for total link thickness are calculated with the help of Equations 2.46 to 2.50. Hence elemental stiffness matrix given by Equation 3.35 is modified into the following form to get elemental stiffness matrix for passive damped system.

$$\mathbf{K}_{p_i} = \begin{bmatrix} \frac{EA}{l} & 0 & 0 & -\frac{EA}{l} & 0 & 0 \\ 0 & \frac{12EI}{l^3} & \frac{6EI}{l^2} & 0 & -\frac{12EI}{l^3} & \frac{6EI}{l^2} \\ 0 & \frac{6EI}{l^2} & \frac{4EI}{l} & 0 & -\frac{6EI}{l} & \frac{2EI}{l} \\ -\frac{EA}{l} & 0 & 0 & \frac{EA}{l} & 0 & 0 \\ 0 & -\frac{12EI}{l^3} & -\frac{6EI}{l^2} & 0 & \frac{12EI}{l^3} & -\frac{6EI}{l^2} \\ 0 & \frac{6EI}{l^2} & \frac{2EI}{l} & 0 & -\frac{6EI}{l^2} & \frac{4EI}{l} \end{bmatrix} \tag{3.64}$$

	Aluminium	Terfenol-D	Fe-Cr-Al Alloy
Thickness (t)	0.01	$150x10^{-6}$	$150x10^{-6}$
Elastic Modulus (E)	70 GPa	35 GPa	200 GPa
Density (ρ)	$2700Kg/m^3$	$9250Kg/m^3$	$7000Kg/m^3$
Poisson's Ratio (ν)	0.33	0.25	0.28
Loss-Factor (η)	0.001	0.001	(from Figure 2.5)

Table 3.1: Geometric and material properties of the hybrid damped links

Physical system parameters	Value
Mass per unit of length of link (m)	4.93 kg/m
Length of link (L)	1.0 m
Hub radius (r_h)	0.02 m
Hub Inertia (I_h)	0.0044 kgm^2
Width of link (w)	50 mm
Thickness of link (t)	10 mm
Modulus of elasticity (E)	200 GPa

Table 3.2: Physical system parameters for single link mainipulator

Elemental stiffness matrix $\mathbf{K}_{p_i}$ is assembled to get the global stiffness matrix $\mathbf{K}_p$ for passive damped system.

Calculation of Active Damping

Elemental active damping matrix is calculated from Equation 2.51 and assembled to get the global active damping matrix $\mathbf{C}_a$.

Thus calculated values of $\mathbf{K}_p$ and $\mathbf{C}_a$ are included into the model which gives the following dynamic equation for hybrid damped system.

$$\mathbf{M}\ddot{\mathbf{q}} + \mathbf{C}_a\dot{\mathbf{q}} + \mathbf{F}(\mathbf{q}, \dot{\mathbf{q}}) + \mathbf{K}_p\mathbf{q} = \mathbf{Q} \tag{3.65}$$

3.3 Results And Discussion

Numerical simulations of single-link rigid and flexible manipulator dynamics were performed. All the programs were developed in MATLAB and to solve the system of first order differential equations in state space form (see Equation 3.57) MATLAB routine "ode45" is used which is based on the 4th and 5th order Runga-Kutta scheme with adaptive step-size. The physical properties of the manipulator are given in Table 3.2. Later to study the effect of variation of these parameters, results are obtained with different values of parameters which are given in corresponding figures. In all cases considered, a torque is applied at the joint and time-reponse of manipulator unconstrained link is studied.

3.3.1 Rigid Manipulator Results

To study the basic behaviour of the single link manipulator, results for rigid link are discussed so that later a comparison can be made with the flexible link manipulator response under similar conditions. For the given input torque at the joint, the variation of joint rate and angular displacement for rigid manipulator are shown by blue coloured curves for all the cases.

1. **Time-Response Under Different Types of Input Torques**

   Three types of torques namely sine wave, cosine wave and square wave, of equal peak values and frequencies are considered and the time response for each case is discussed below.

   Time response under sine wave input torque is shown in Figure 3.2. The continuously varying torque gives rise to a joint rate which again varies along a sine curve with 90 degrees phase lag with the input torque. It varies between zero and a positive peak value (Figure 3.2B). Since the joint rate is positive at all the instants, the angular displacement follows a continuously increasing curve (Figure 3.2C).

   Time response under cosine wave input torque is shown in Figure 3.3. The continuously varying torque causes the joint rate to vary as a sine wave about a zero mean position (Figure 3.3B). Due to this alternating joint rate the angular displacement varies between zero and a peak value in the form of a cosine wave which is 180 degrees out of phase with input torque.

   Time response under square wave input torque is shown in Figure 3.4. The torque variation is sudden and discontinuous. Here we observe a linear variation of joint rate with discontinuities at the peak points (Figure 3.4B). However, the joint rate remains positive at all instants that gives rise to a continuously increasing angular displacement (Figure 3.4C).

2. **Variation in Time Response With Respect to Change in Input Torque-Frequency**

   Time responses under cosine wave input torque with frequency equal to 1 Hz, 2 Hz, 4 Hz and 8 Hz are shown in Figures 3.5, 3.3, 3.6 and 3.7 respectively. It is observed that due to perfectly rigid link, there is absolutely no effect of frequency variation on the basic shape of the time response curves for joint rate and angular displacement. However with decrease in frequency i.e. with increase in time period, the joint rate and angular displacement varies between peaks of larger magnitude, as

at lower frequency the link gets more time to attain a higher joint rate which in turn causes angular displacement to attain larger value.

3.3.2 Flexible Manipulator Results

Here in addition to the joint rate and angular displacement, the variation of flexural transverse deflection and slope at the tip of flexible link are studied with respect to variation of frequency of torque, size of meshing, link material properties and slenderness-ratio of link. In all the figures flexible manipulator results are shown by red coloured curves.

1. **Time Response Under Different Types of Input Torque**

   As in the case of rigid manipulator sine wave, cosine wave and square wave of equal peak values and frequencies, are considered and the time response for each case is discussed below.

   Time response under sine wave input torque is shown in Figure 3.2. Similar to rigid link manipulator case, the joint rate again varies between zero and a positive peak value (Figure 3.2B) and gives rise to a continuously increasing angular displacement (Figure 3.2C). The effect of link flexibility is observed in the form of zigzag behaviour of joint rate and angular displacement variation. However the manipulator still tends to follow the basic behaviour of rigid manipulator, shown by the blue coloured curves. The transverse deflection and slope, with respect to neutral axis of link, are shown in Figure 3.2D and 3.2E. Both deflection and slope varies along a curve similar to a sine wave and is 180 degrees out of phase with input torque.

   Time response under cosine wave input torque is shown in Figure 3.3. In this case also there is a smooth variation of torque. However, the input torque starts from an initial peak value that acts like an impact for a flexible link. Similar to sine wave case, the joint rate and angular displacement tends to follow the rigid link behaviour with greater zigzag behaviour as a result of impact for cosine wave (Figure 3.3B and 3.3C). Tip deflection and slope vibration show two modes of oscillations. A relatively fast mode with high frequency superimposed on a relatively slower oscillatory mode which follows a curve 180 degrees out of phase with input torque (Figure 3.2D and 3.2E). It is noticed that frequency of fast mode is equal to the natural frequency of flexible link, while slower mode has frequency equal to the exitation torque frequency. The peak values of deflection and slope are higher than those in case of sine wave.

   Time response under square wave input torque is shown in Figure 3.4. A square wave input torque exhibits a sudden change in torque at finite number of points. Due of this, joint rate and angular displacement tend to deviate from the rigid manipulator

Frequency of input torque (Hz)	Error ratio	Tip deflection amplitude
1	0.050	1.1
2	0.167	1.1
4	0.33	1.1
8	0.98	1.1

Table 3.3: Frequency variation results

response more as compared to previous cases (Figure 3.4B and 3.4C). Deflection and slope variation, again show two modes of oscillations with slower mode follows a curve 180 degrees out of phase with input torque (Figure 3.4D and 3.4E). In addition, the amplitude of deflection and slope variation is dependent on the amount of sudden change in input torque, which is clear from the comparison of vibration-amplitudes between time intervals 0 to 0.5 and 0.5 to 1.0 seconds.

2. **Variation in Time Response With Respect to Change in Input Torque-Frequency**

Time responses under cosine wave input torque with frequency equal to 1 Hz, 2 Hz, 4 Hz and 8 Hz are shown in Figures 3.5, 3.3, 3.6 and 3.7 respectively. To study the effect of frequency variation on angular displacement at the joint, error ratio is found by the following formula:

$$error\ ratio = \frac{amplitude\ of\ deviation\ from\ rigid\ manipulator\ angular\ displacement}{amplitude\ of\ angular\ displacement\ of\ rigid\ manipulator}$$

Error ratio at time instant $T_p/4$ (where T_p is the time period of input torque) is found at all frequencies and are given in Table 3.3. It is found that with the increase in the frequency of input torque error ratio in angular displacement increase. However the tip deflection and slope remains unaffected by the variation in input torque frequency. The high frequency mode oscillations are observed as the zigzag pattern in the tip deflection and slope variation. Non-dimensional amplitude of tip deflection is found for each frequency by following relation and given in Table 3.3.

$$non-dimensional\ tip\ defletion\ amplitude = \frac{amplitude\ of\ tip\ defletion\ variation}{thickness\ of\ link}$$

3. **Variation in Time Response With Respect to Change in Number of Elements - Convergence Test**

To ensure the convergence, results are obtained for different mesh sizes and the results are compared. Time responses under cosine wave input torque with frequency of

Material	E (GPa)	E/ρ (m^2/sec^2)	Error ratio	Tip deflection amplitude
Steel	200	20.31	0.167	1.1
Aluminium	70	25.13	0.130	3.2
CFRP	300	130.44	0.057	0.8

Table 3.4: Material properties variation results

2.0 Hz and with total number of elements equal to 2, 3, 4, 5 and 6 are compared. Angular diplacement and tip deflection response with increasing mesh size is shown in Figure 3.8. It is observed that with the increase in meshing the change in the response for consecutive mesh size values is lesser. Hence the model is converging.

4. **Performance of Link Materials Having Different Modulus of Elasticity and Density**

Performance of manipulators having link made up of Aluminium, Steel and Carbon Fibre Reinforced Plastic (CFRP) Laminates is compared. Time responses of the same are shown in Figures 3.9, 3.3 and 3.10 respectively.

Error ratio at time instant $t = 0.125$ sec is obtained and given in Table 3.4. It is observed that error ratio in angular displacement reduces with increase in specific modulus of elasticity (E/ρ) (Figure 3.11A). Therefore material having higher specific modulus of elasticity i.e. CFRP shows the smoothest angular displacement variation. Tip deflection amplitude is found to be independent of link material density and decreases uniformly with increase in the modulus of elasticity (Figure 3.11B).

5. **Variation in Time Response With Respect to Change in Slenderness Ratio (L/T) of Link**

Time response of links with lengths equal to 2.0 meters, 1.0 meters and 0.5 meters are shown in Figures 3.12, 3.3 and 3.13 respectively. The thickness of link is kept constant in all the cases. Error ratio at time instant $t = 0.125$ sec is found and given in Table 3.5. With longer link, the effect of flexibility is more pronounced on the joint angular motion as observed by the increase in the error ratio in angular displacement. However the frequency of the zigzag pattern in angular displacement (Figure 3.12C) is less for longer link as natural frequency of a beam is inversely proportional to square of the length of beam. Similar response is observed in the tip deflection and slope variation. Tip deflection amplitude is found to be increasing with length of link, as shown by Table 3.5.

Link length L (m)	Error ratio	Tip deflection amplitude
2.0	0.944	5.0
1.0	0.167	1.1
0.5	0.028	0.3

Table 3.5: Slenderness ratio variation results

Resonant Frequency (ω_r)(Hz)	From Petric (1995)	From Simulation Results
First	4.93	5.01
Second	14.21	14.61
Third	30.16	30.24

Table 3.6: System resonant frequencies

6. Time Response With Proportional Damping

Firstly the response of an undamped and damped single link manipulator of very small thickness under a sine wave input torque are shown in Figures 3.14 and 3.15 respectively. In Figure 3.16 the result from an earlier work (Petric 1995) with identical parameters is shown. The simulation results in Figure 3.15 are found to be in agreement with the experimental results in Figure 3.16. Further a linear model is obtain by dropping out the second power term of elastic variables (i.e. S) in equation 3.48 and system resomant frequencies are calculated, which are given in Table 3.6.

It is observed that the proportional damping is able to damp-out the link vibrations effectively and the result obtained matches with the given results in Figure 3.16. In all the results presented above the damping of joint angular motion is considered.

In Figure 3.17, results for similar manipulator without any damping of joint motion is shown. In comparison with rigid link response it is shown that in the latter case link follows the rigid manipulator behaviour far more closely than earlier cases, which is desirable from practical applications point of view.

In Figure 3.18, results for manipulator with physical parameters given in Table 3.2, without any damping of joint motion is shown. On comparison with undamped and rigid link response with same input parameters (shown in Figure 3.3), again it is observed that the proportional damping is able to damp-out the link vibrations effectively. Logarithmic decrement in tip slope variation is calculated by taking the natural logarithm of the ratio of one amplitude to that of the next amplitude of the same and is equal to 0.2231.

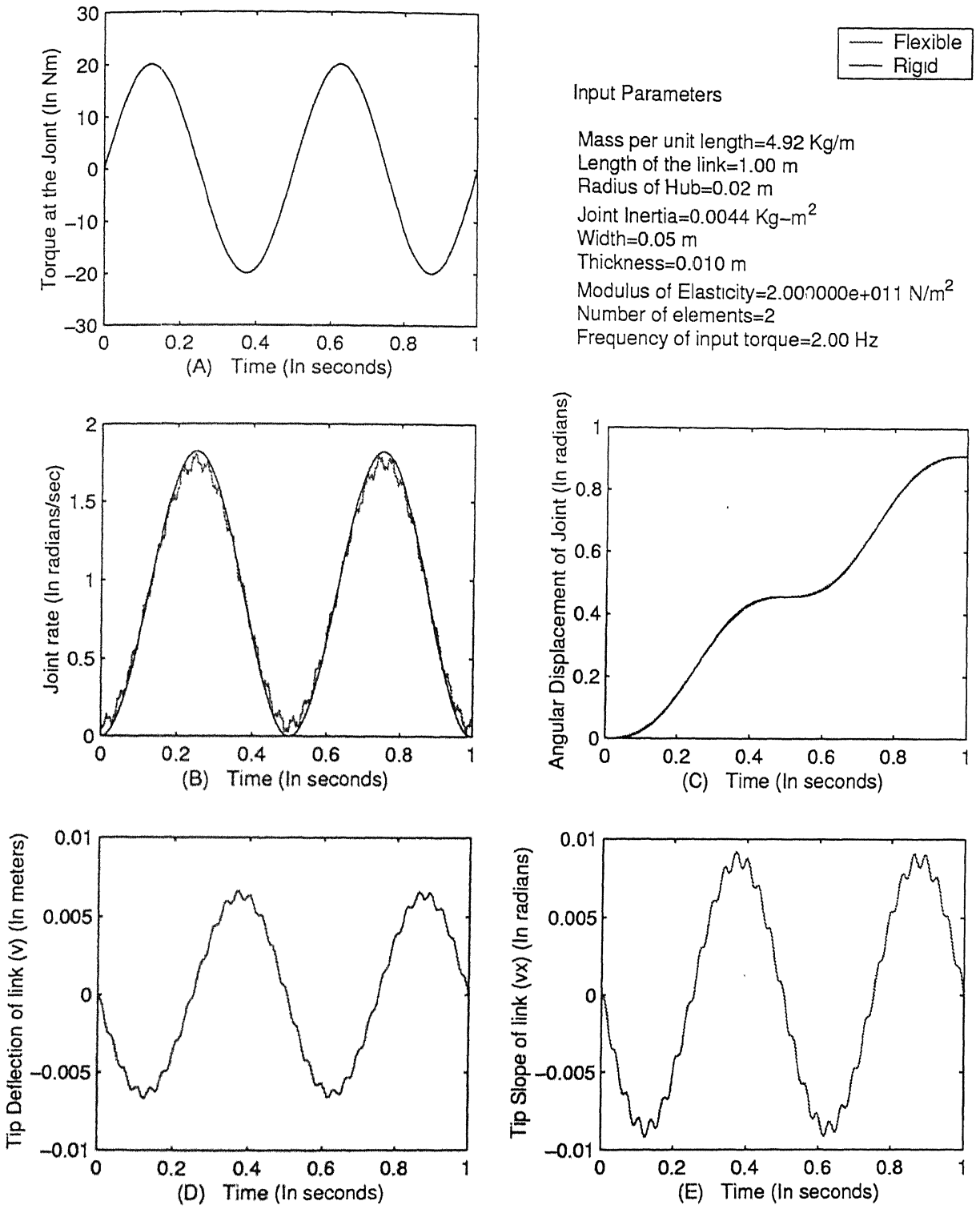

Figure 3.2: Time response under sine wave input torque

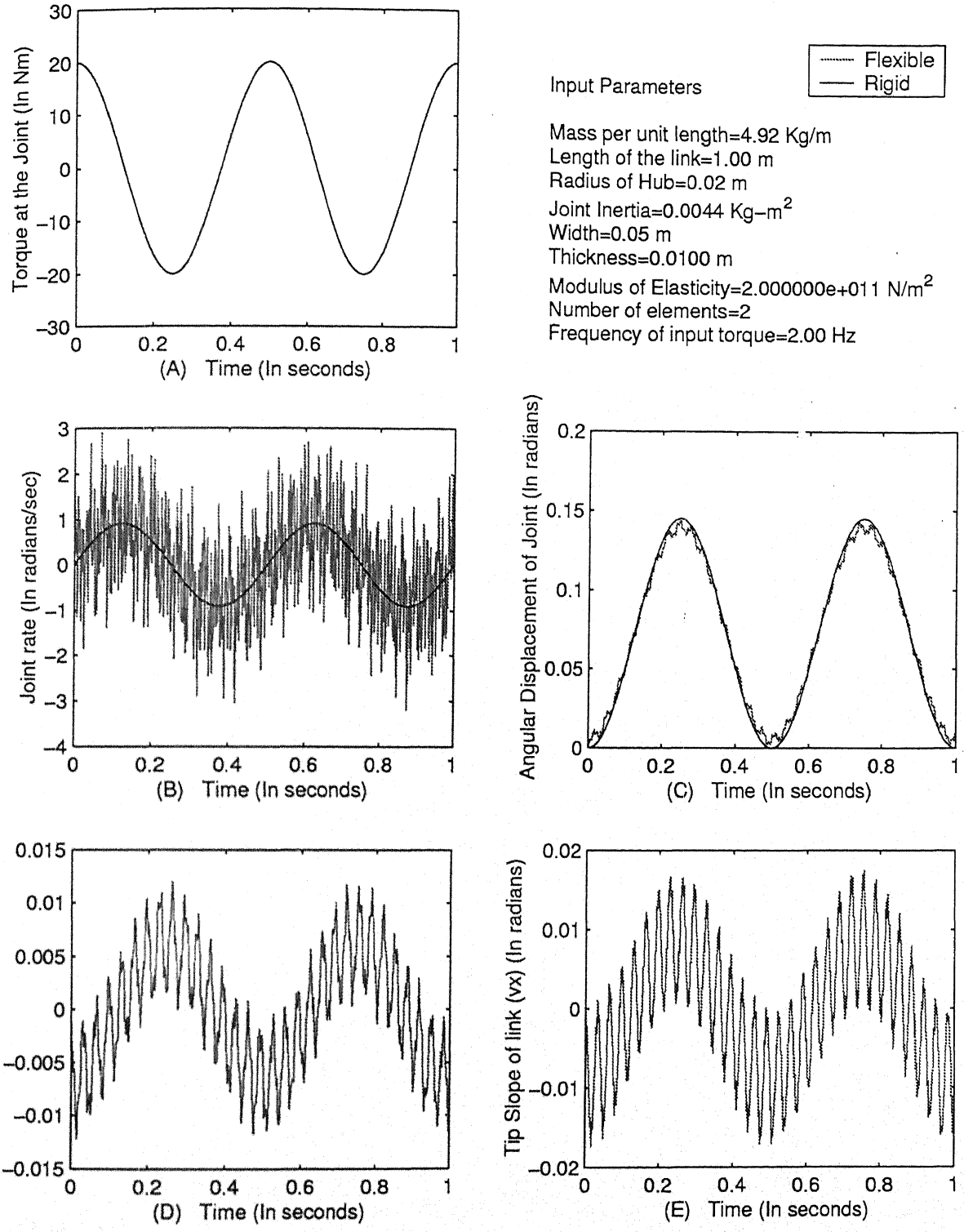

Figure 3.3: Time response under cosine wave input torque

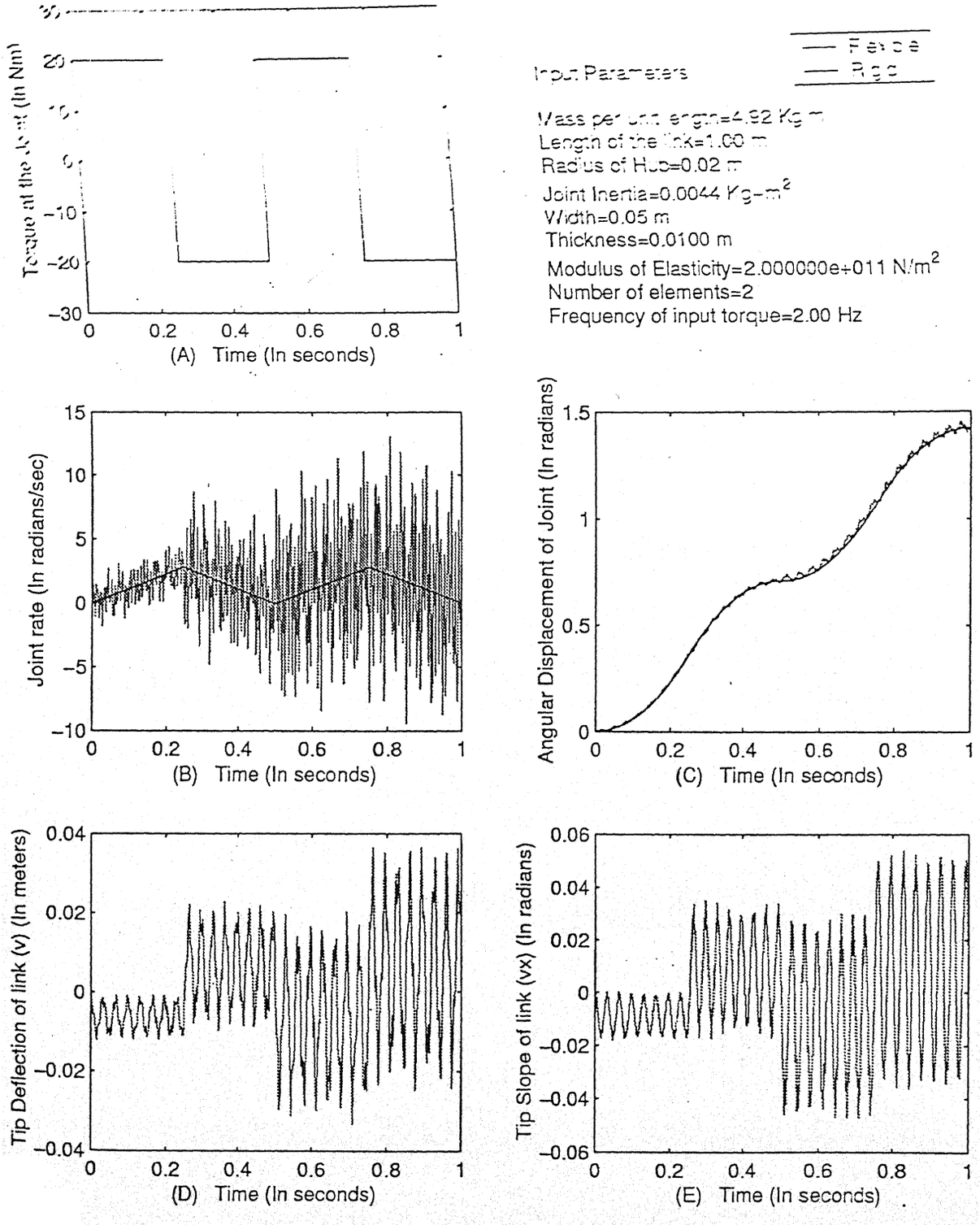

Figure 3.4: Time response under square wave input torque

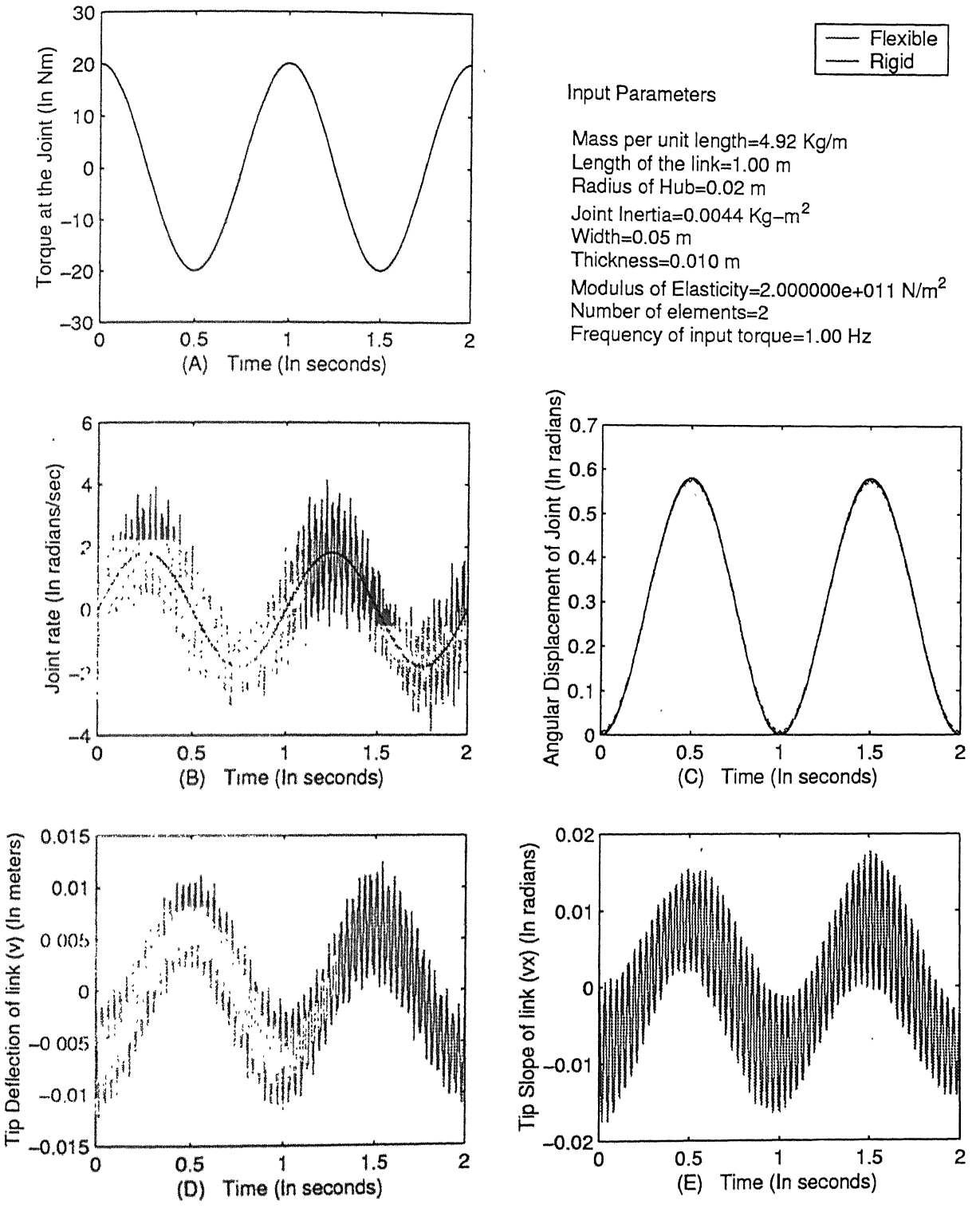

Figure 3.5: Time response under cosine wave input torque of frequency=1.0 Hz

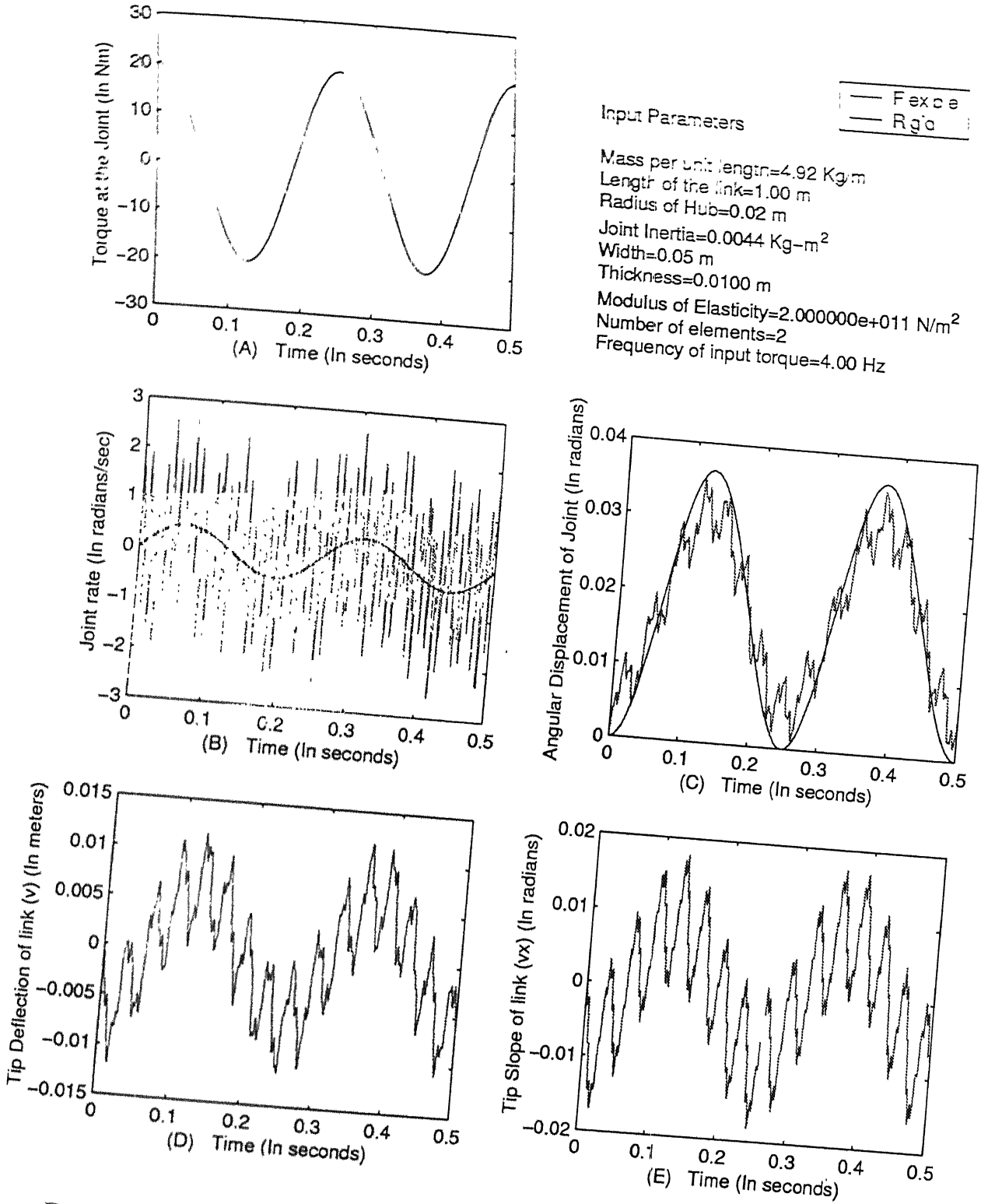

Figure 3.6: Time response under cosine wave input torque of frequency=4.0 Hz

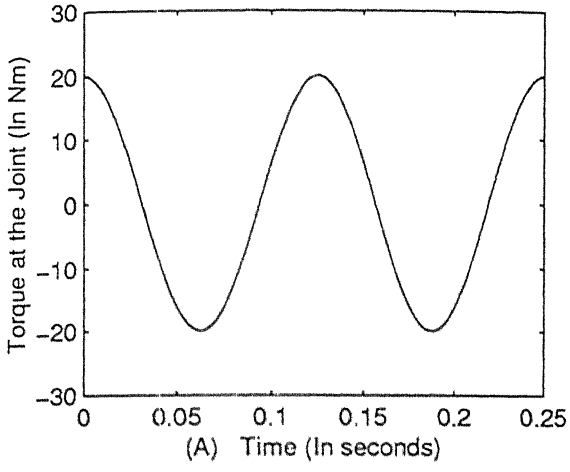

Input Parameters

Mass per unit length=4.92 Kg/m
Length of the link=1.00 m
Radius of Hub=0.020 m
Joint Inertia=0.0044 Kg–m^2
Width=0.05 m
Thickness=0.010 m
Modulus of Elasticity=2.000000e+011 N/m^2
Number of elements=2
Frequency of input torque=8.00 Hz

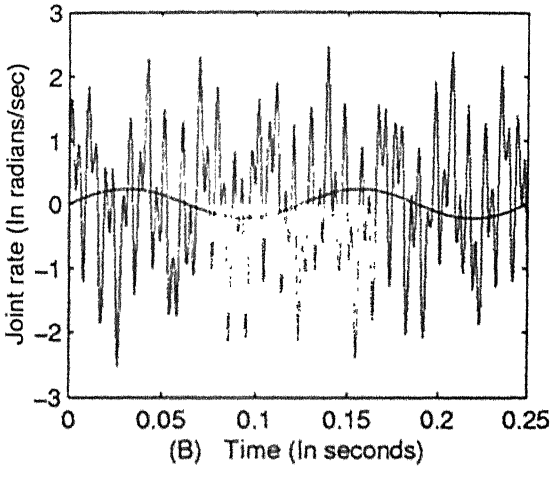

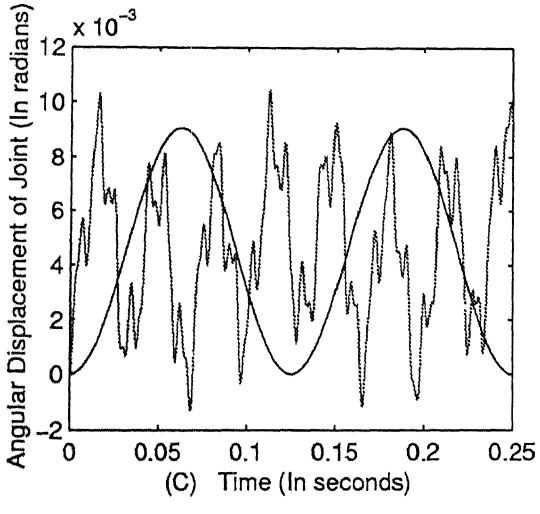

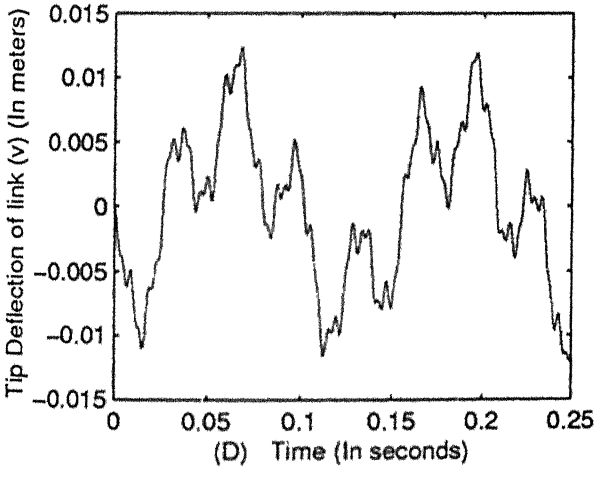

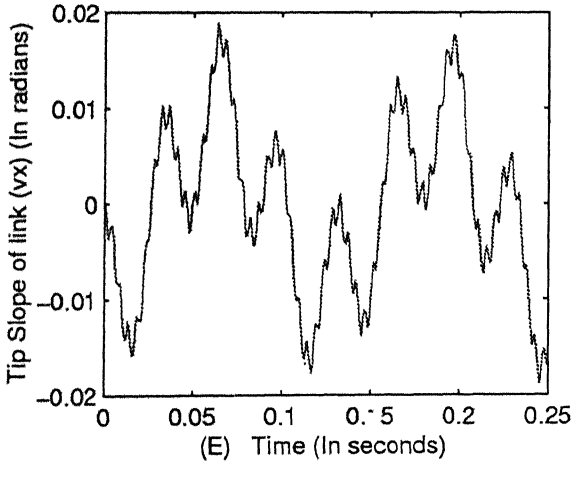

Figure 3.7: Time response under cosine wave input torque of frequency=8.0 Hz

Input Parameters

Mass per unit length=4.92 Kg/m
Length of the link=1.00 m
Radius of Hub=0.020 m
Joint Inertia=0.0044 Kg-m^2
Width=0.05 m
Thickness=0.010 m
Modulus of Elasticity=2.000000e+011 N/m^2
Frequency of input torque=2.00 Hz

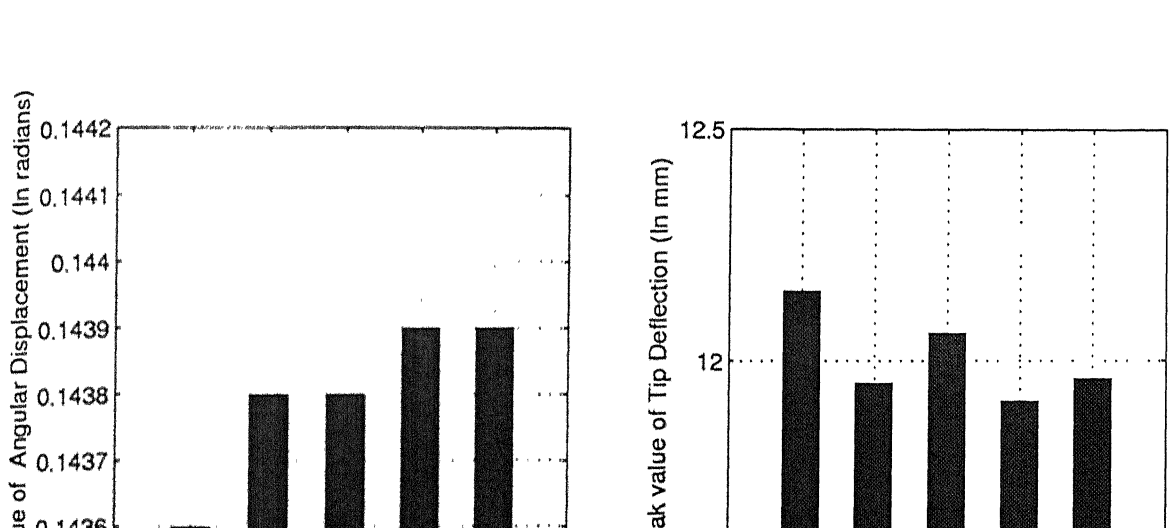

Figure 3.8: Variation of output variables with number of elements

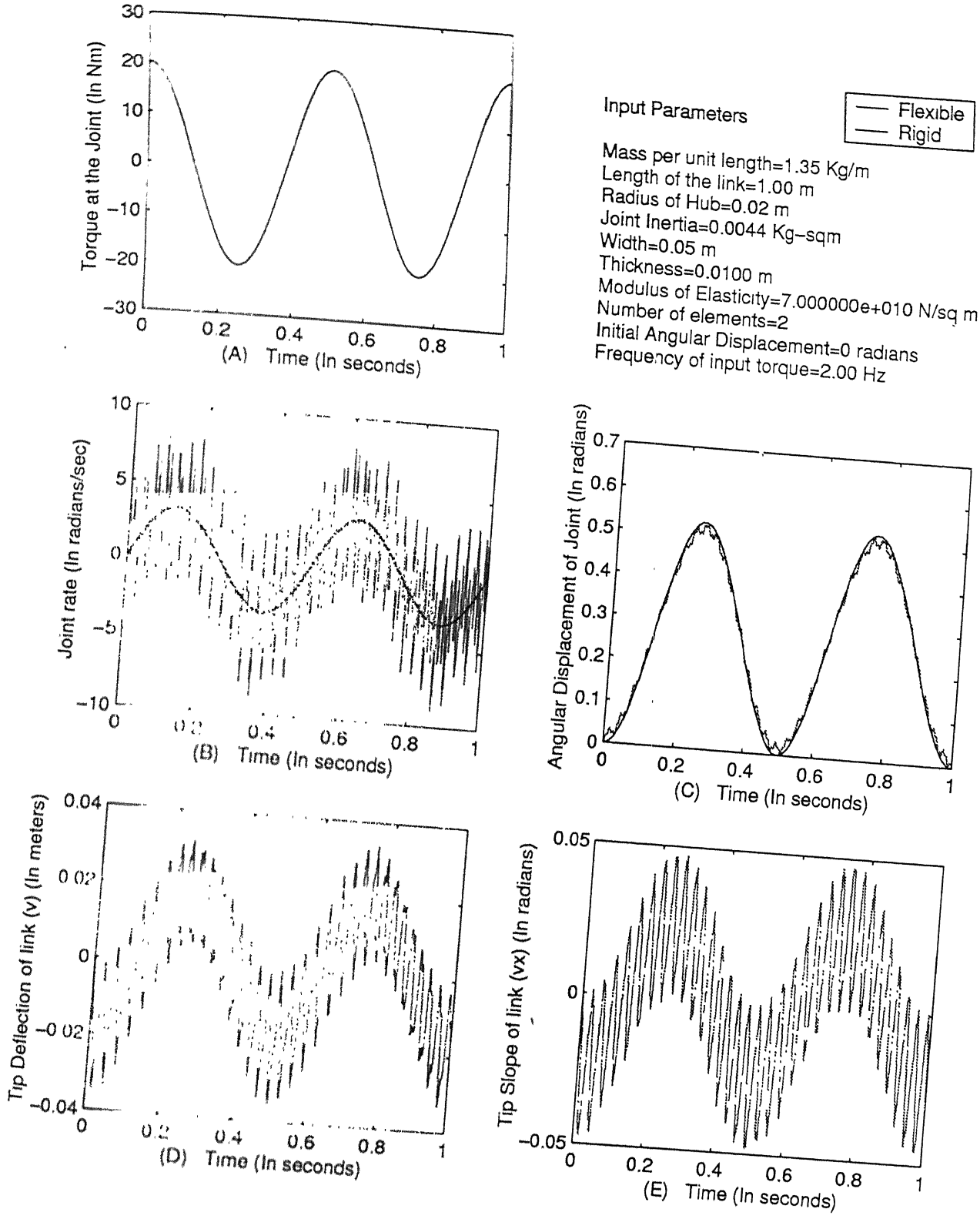

Figure 3.9: Time response of an Aluminium link manipulator

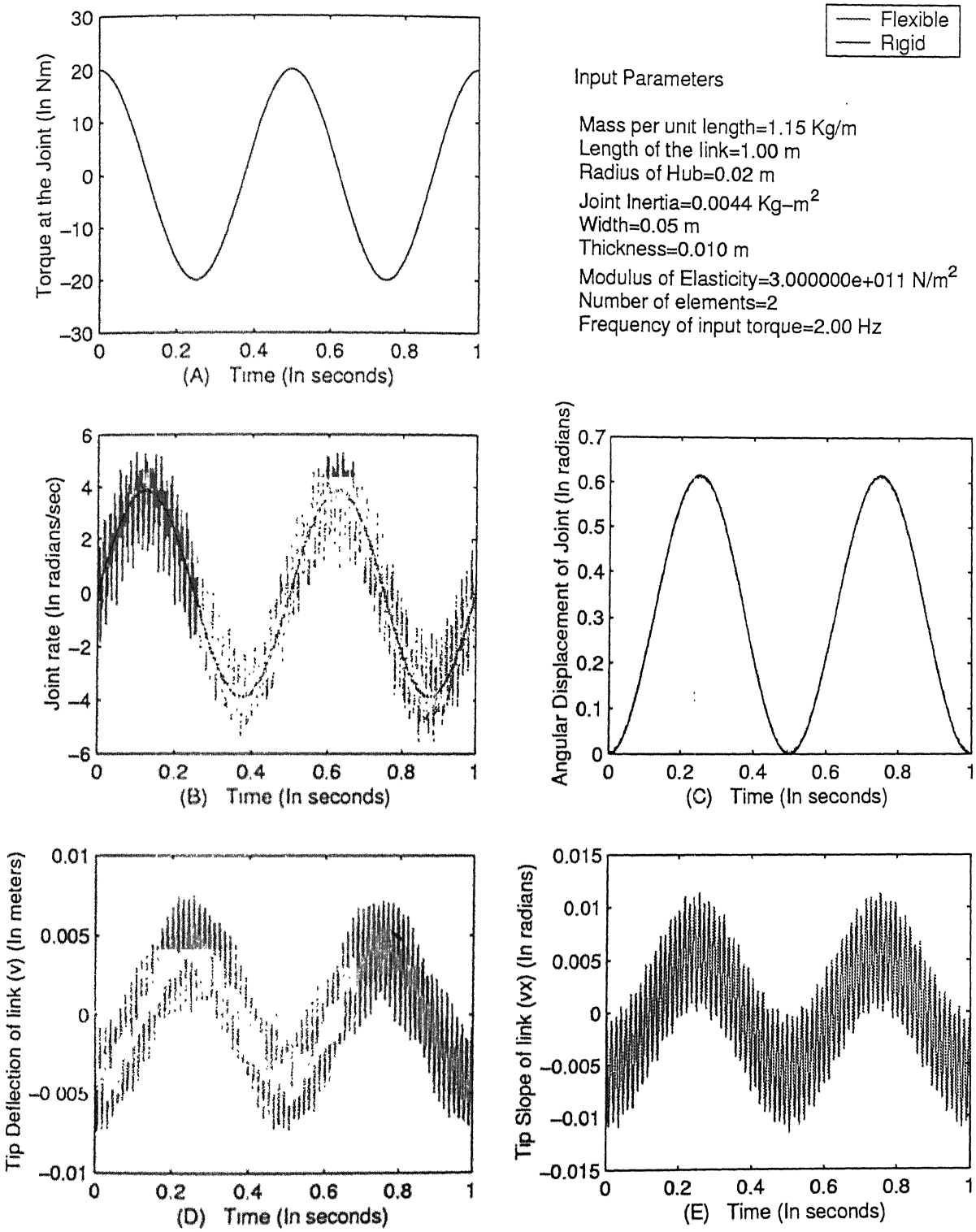

Figure 3.10: Time response of a CFRP link manipulator

Input Parameters

Length of the link=1.00 m
Radius of Hub=0.020 m
Joint Inertia=0.0044 Kg–m^2
Width=0.05 m
Thickness=0.010 m
Number of elements=2
Frequency of input torque=2.00 Hz

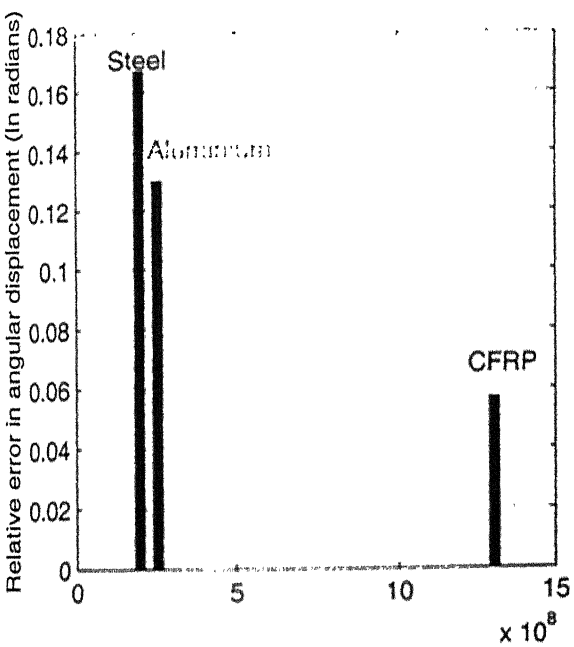

(A) Specific Modulus of Elasticity (In m^2/sec^2)

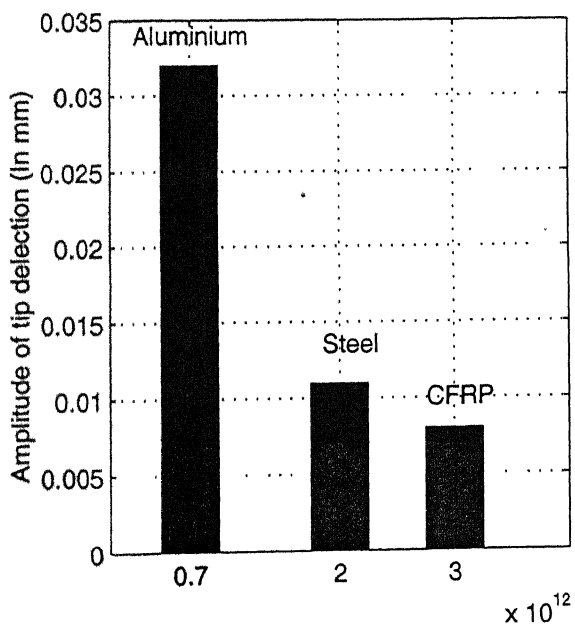

(B) Modulus of Elasticity (In GPa)

Figure 3.11: Variation of output variables meterial properties

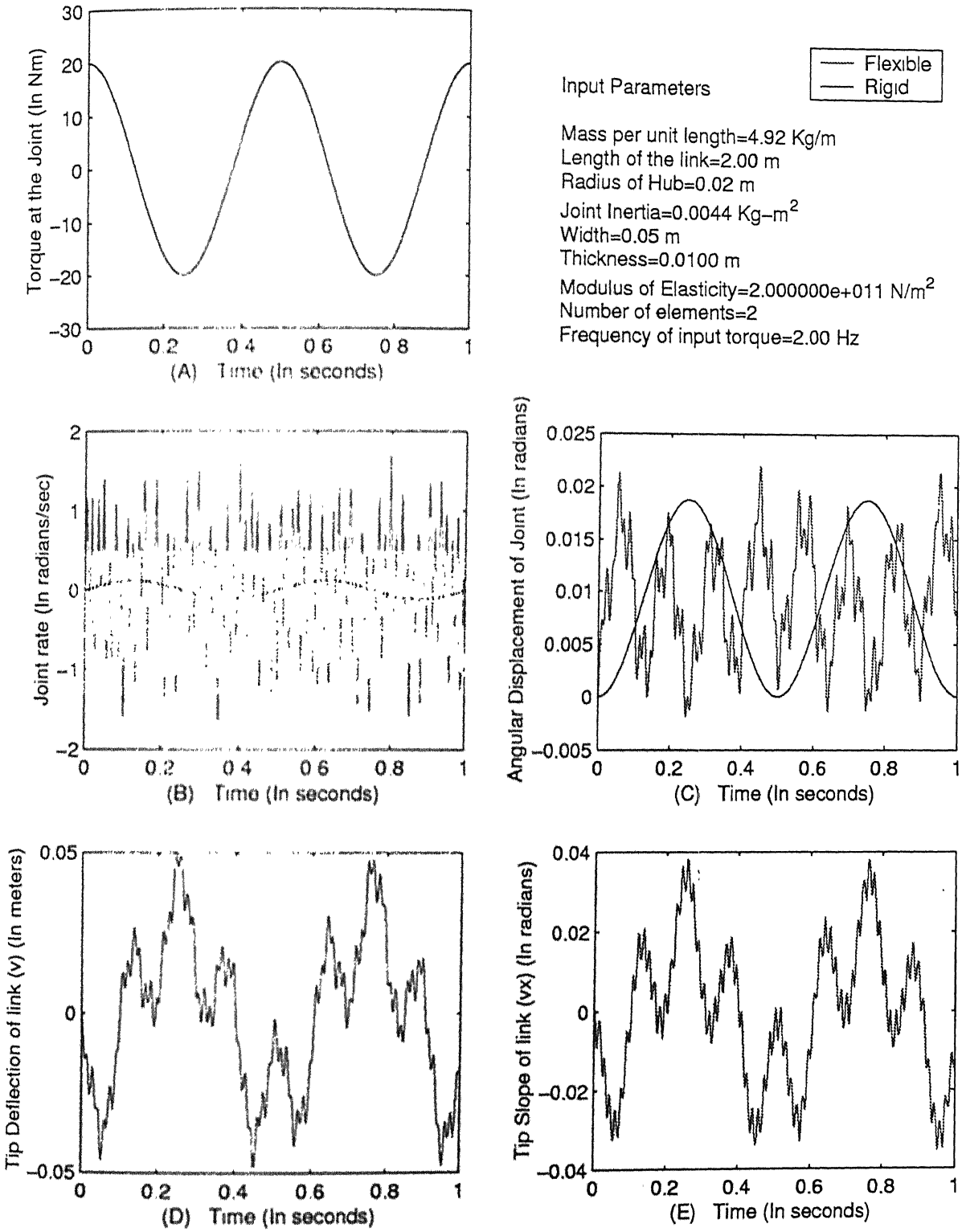

Figure 3.12: Time response of manipulator having Link length=2.0 meters

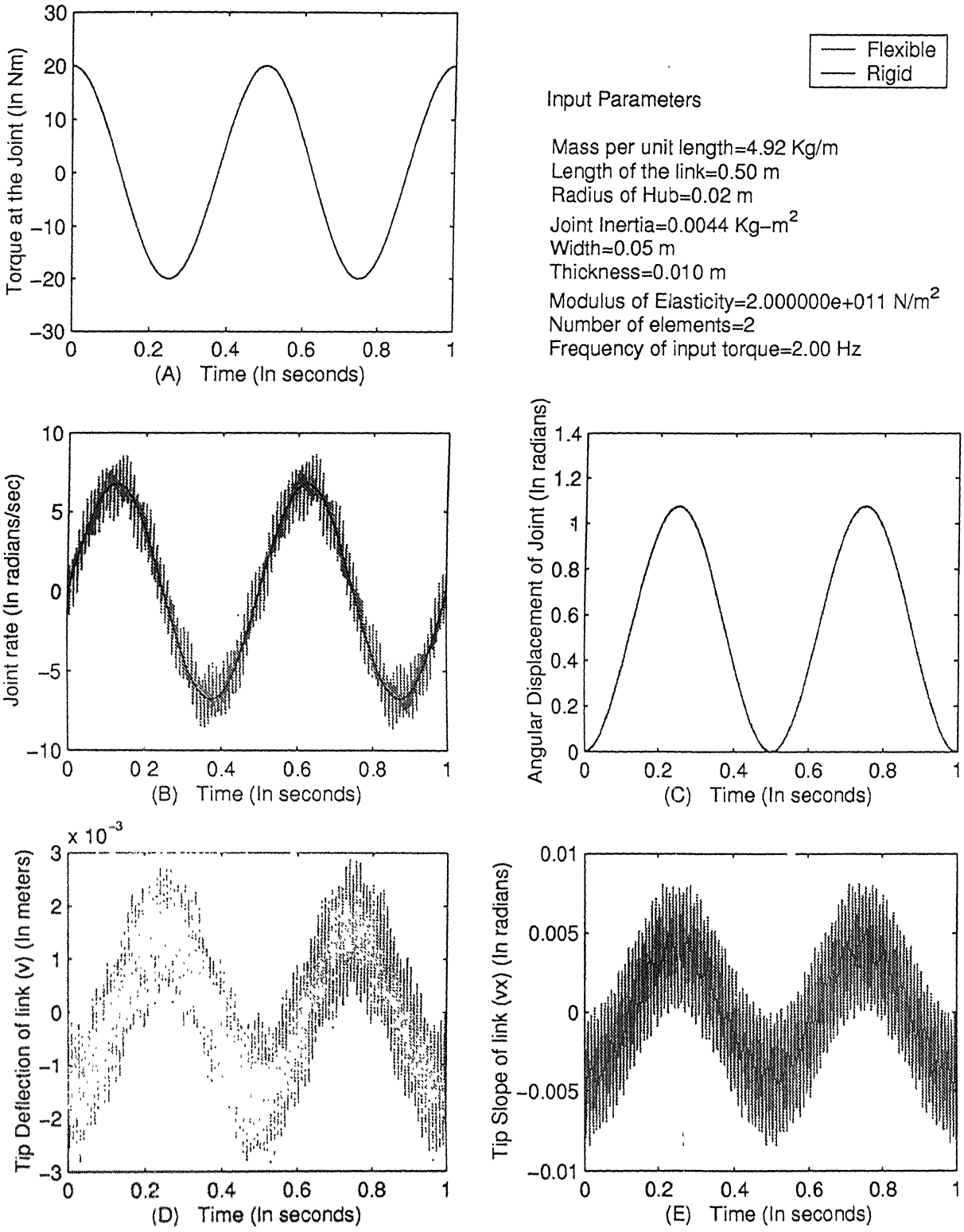

Figure 3.13: Time response of manipulator having Link length=0.5 meters

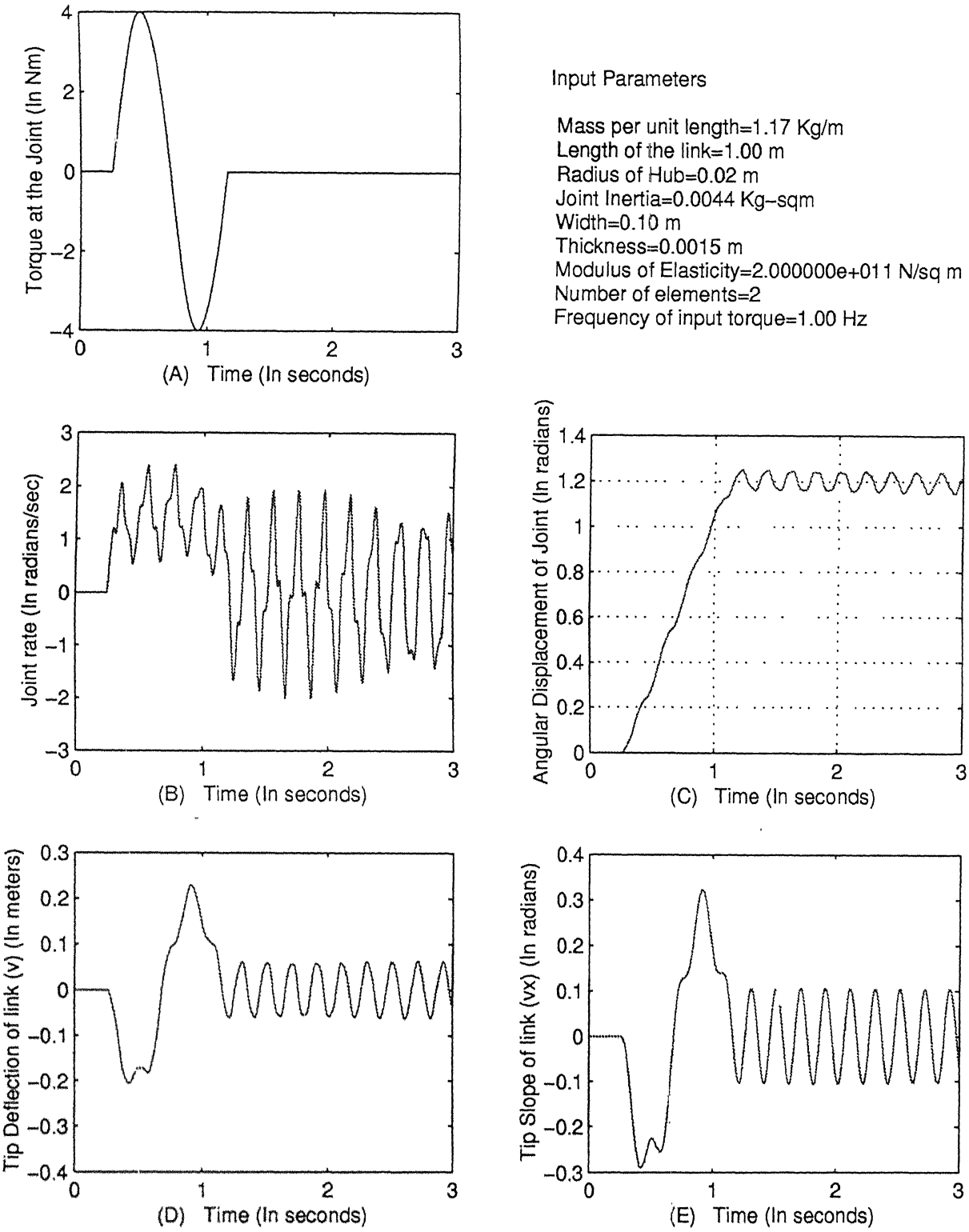

Figure 3.14: Time response of manipulator without damping

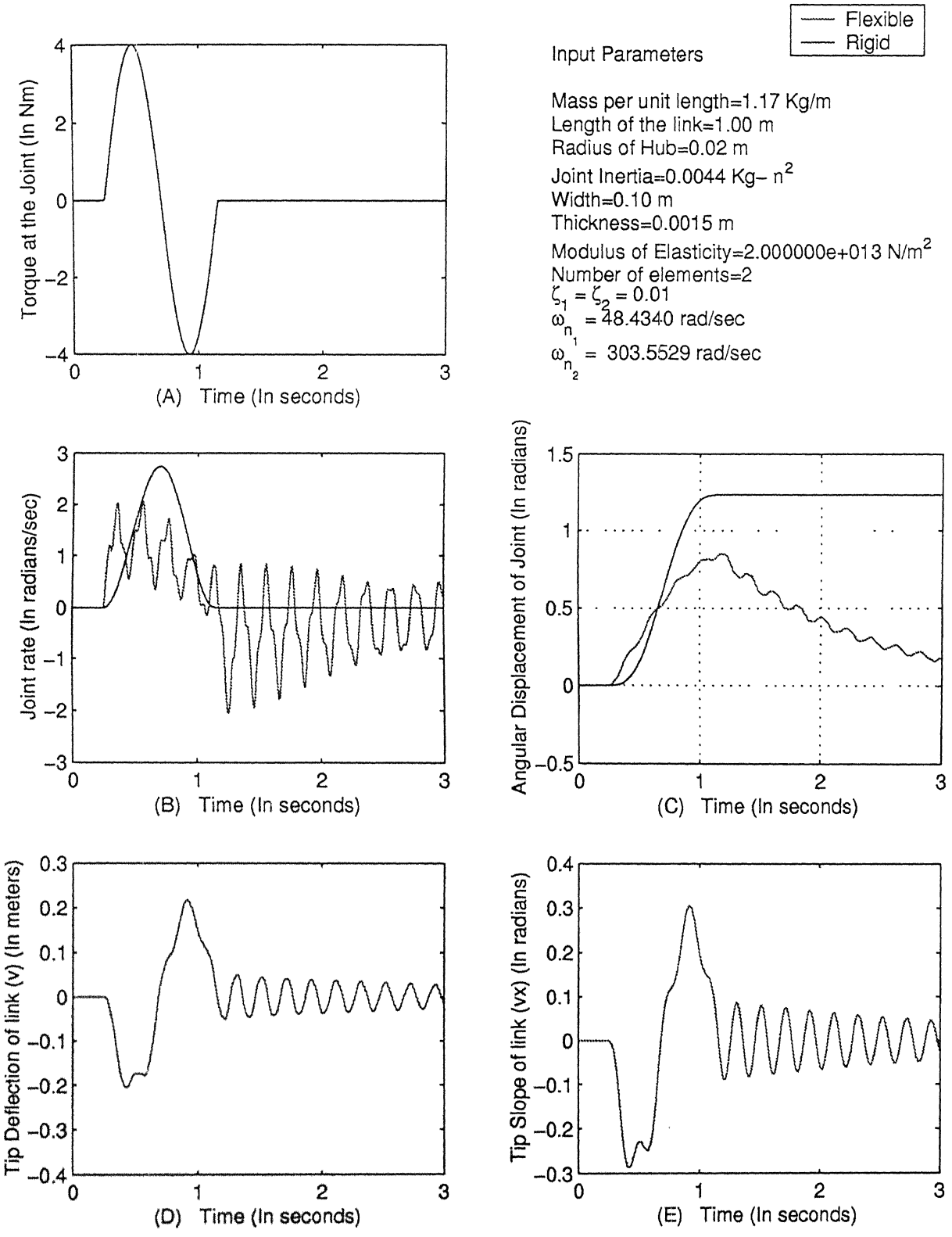

Figure 3.15: Time response of manipulator with damping including the damping of joint motion

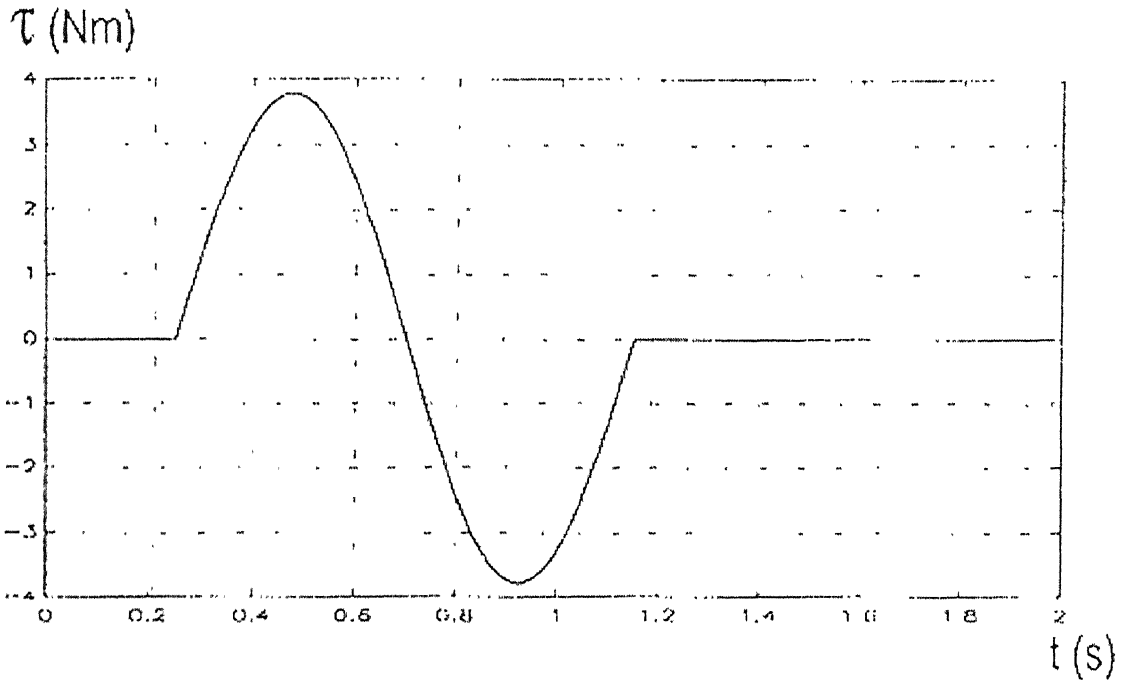

Fig. 6 Input torque profile

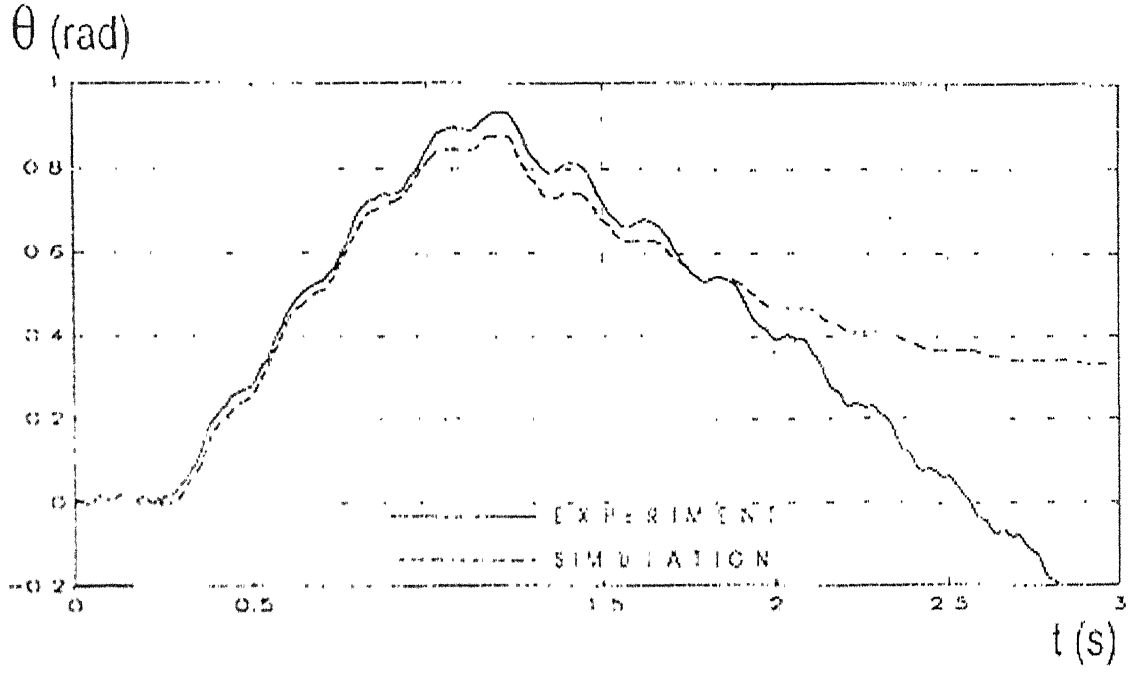

Fig. 7 Joint angle

Figure 3.16: Time response result from an earlier work (Petric 1995) with identical parameters as in figure 3.15

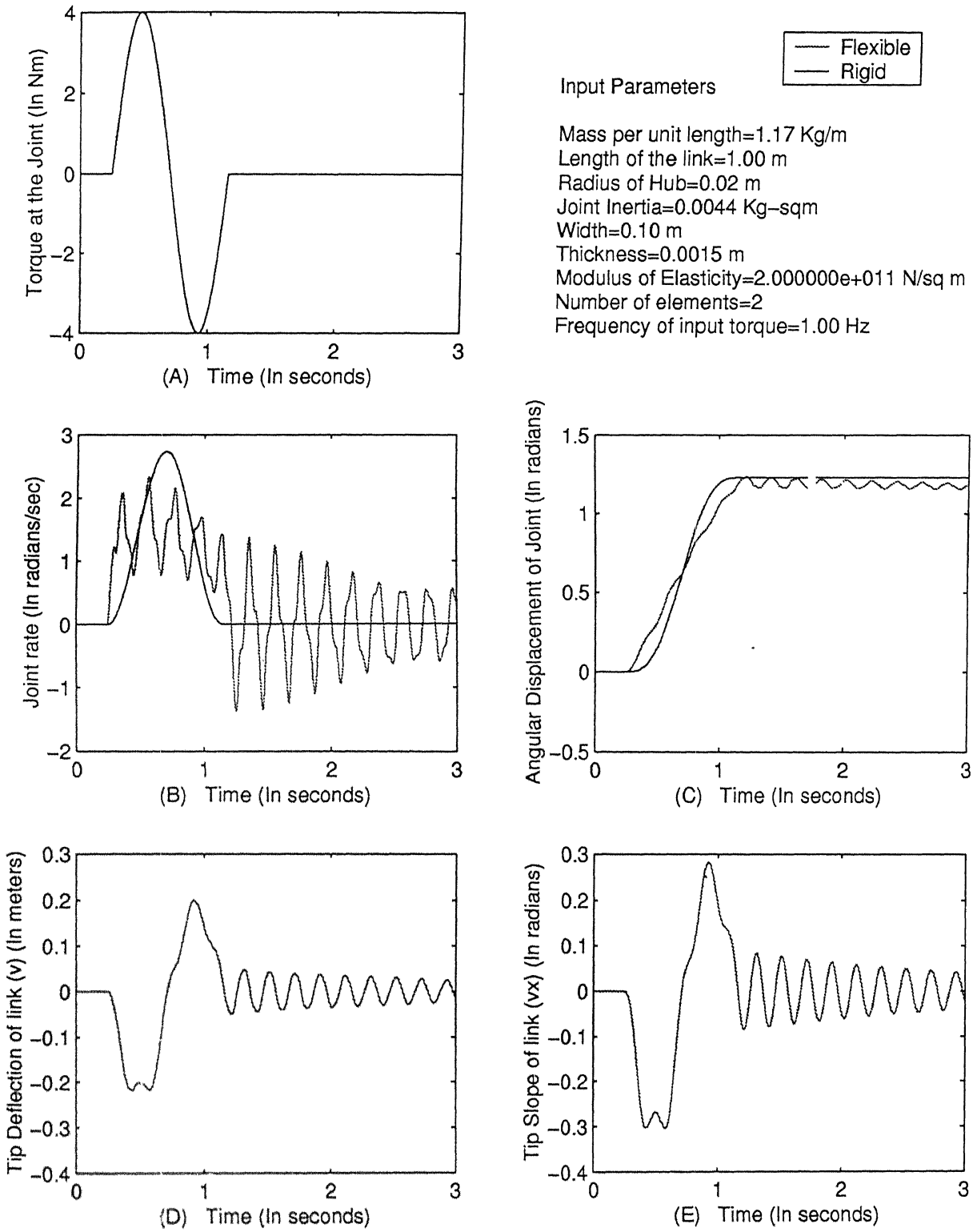

Figure 3.17: Time response of manipulator with damping and no damping of joint motion

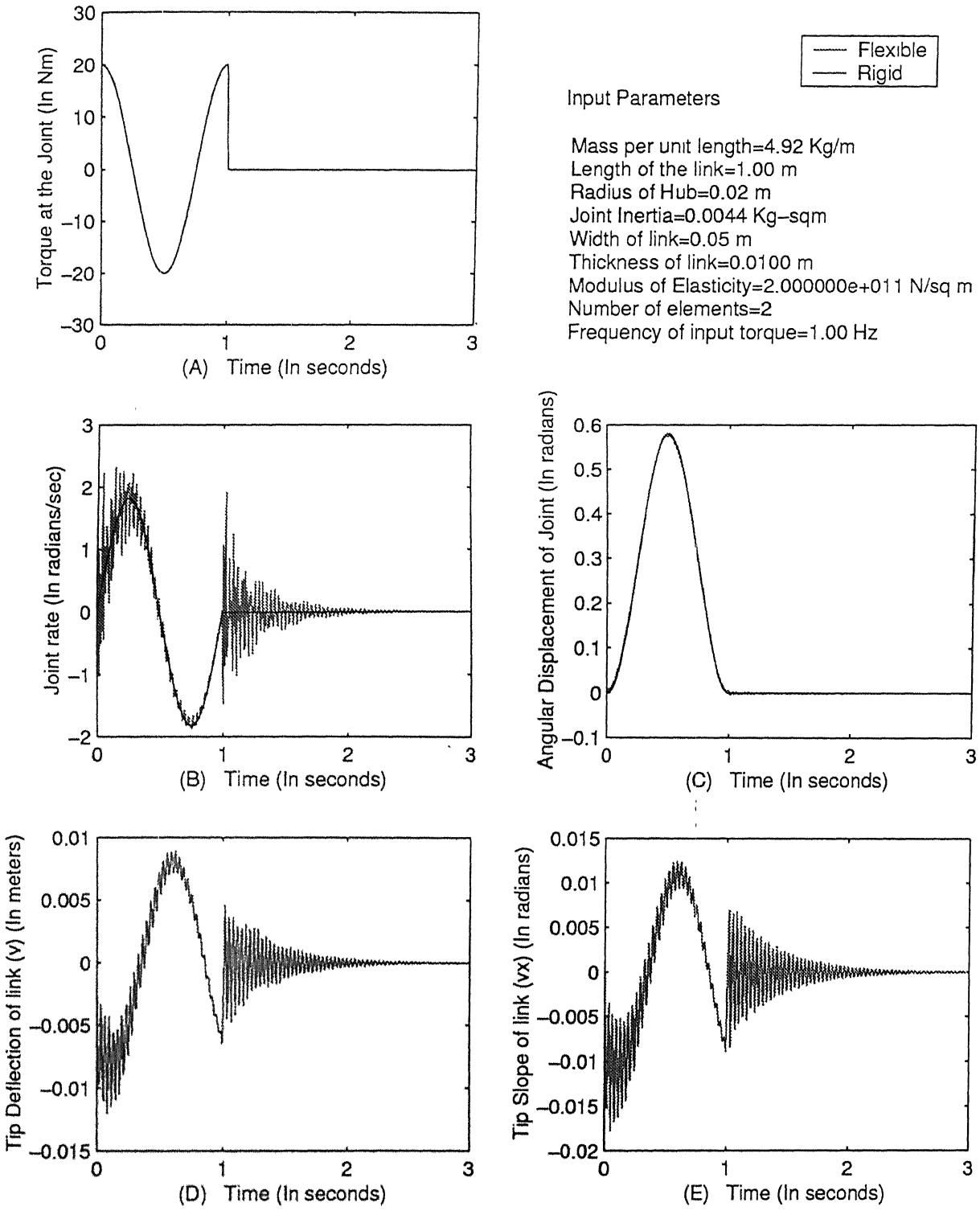

Figure 3.18: Time response of manipulator with damping and no damping of joint motion

Chapter 4

Dynamic Model Derivation and Simulation of Two-Link Manipulator

In this chapter, first the closed form undamped dynamic equations of motion are derived for two-link rigid and flexible manipulators from the formulation given in Chapter 2. Later damping is introduced into the model. Proportional and hybrid dampings are considered. Finally numerical simulation of this dynamic system is carried out and various results are discussed.

4.1 Rigid Two-Link Manipulator

In this section, the dynamic equations of motion for a two-link rigid manipulator are derived in matrix form. A two-link revolute joint planer manipulator with flexible arms is shown in Figure 4.1. In the case considered, both the links are of equal length, i e.

$$L_1 = L_2 = L \tag{4.1}$$

With the help of Equations 2.17 and 2.18, we can find the inertia matrix and vector representing coriolis and centrifugal forces. The two terms are calculated in Appendix A and final results are given as:

Inertia term:

$$\mathbf{D} = \begin{bmatrix} \frac{1}{3}M_1L^2 + \frac{4}{3}M_2L^2 + M_2L^2\cos\theta_2 & \frac{1}{3}M_2L^2 + \frac{1}{2}M_2L^2\cos\theta_2 \\ \frac{1}{3}M_2L^2 + \frac{1}{2}M_2L^2\cos\theta_2 & \frac{1}{3}M_2L^2 \end{bmatrix} \tag{4.2}$$

Coriolis and Centrifugal terms:

$$\mathbf{h}(\theta,\dot{\theta}) = \begin{bmatrix} -\frac{1}{2}M_2L^2\sin\theta_2\dot{\theta_2}^2 - M_2L^2\sin\theta_2\dot{\theta_1}\dot{\theta_2} \\ \frac{1}{2}M_2L^2\sin\theta_2\dot{\theta_1}^2 \end{bmatrix} \tag{4.3}$$

where θ_1 and θ_2 are the joint angles.

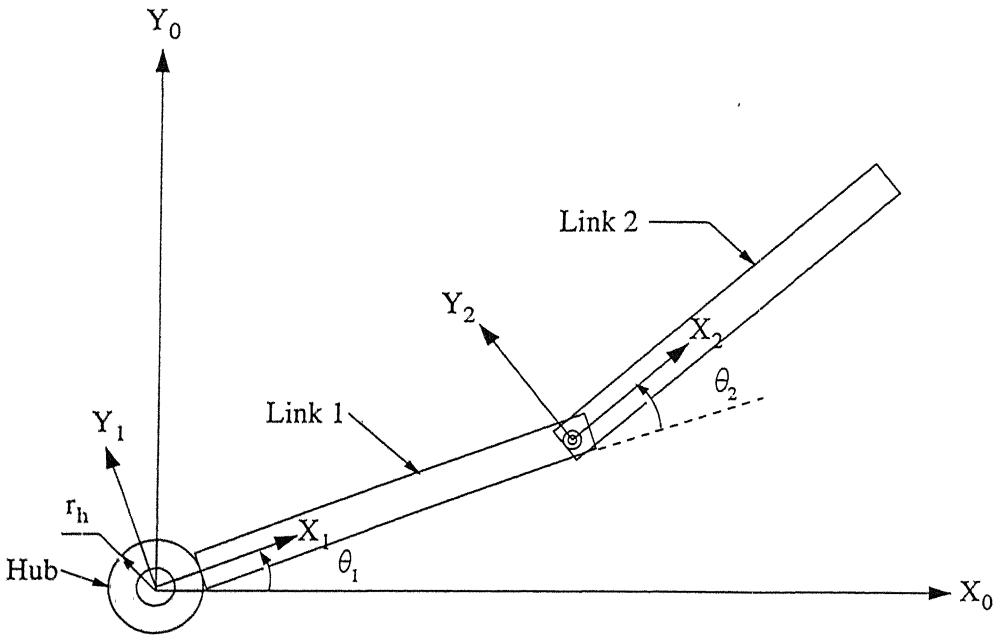

Figure 4.1: A schematic of a Two-link manipulator

Substituting in Equation 2.16, final dynamic equation is given as:

$$\begin{bmatrix} \frac{1}{3}M_1L^2 + \frac{4}{3}M_2L^2 + M_2L^2\cos\theta_2 & \frac{1}{3}M_2L^2 + \frac{1}{2}M_2L^2\cos\theta_2 \\ \frac{1}{3}M_2L^2 + \frac{1}{2}M_2L^2\cos\theta_2 & \frac{1}{3}M_2L^2 \end{bmatrix} \begin{bmatrix} \ddot{\theta_1} \\ \ddot{\theta_2} \end{bmatrix} + \\ + \begin{bmatrix} -\frac{1}{2}M_2L^2\sin\theta_2\dot{\theta_2}^2 - M_2L^2\sin\theta_2\dot{\theta_1}\dot{\theta_2} \\ \frac{1}{2}M_2L^2\sin\theta_2\dot{\theta_1}^2 \end{bmatrix} = \begin{bmatrix} \tau_1 \\ \tau_2 \end{bmatrix} \tag{4.4}$$

where τ_1 and τ_2 are external torques applied at joint 1 and joint 2 respectively.

4.2 Flexible Two-Link manipulator

The dynamic equations of motion for a two-link flexible manipulator are derived using finite element discretization model as developed in Chapter 2. Lagrangian formulation is used for deriving the equations of motion. Numerical results of simulation of this system are presented in Section 4.3 and the effect of damping is shown.

4.2.1 Calculation of Elemental Kinetic Energy

Link-1

We define the joint and link coordinate system according to Section 2.2.3. Therefore the position vector of any material point(s) along the neutral axis of link-1 can be expressed with respect to base coordinate system (X_0, Y_0) as :

$$\mathbf{r}_1^0 = \mathbf{p}_1^0 + \mathcal{R}_1^0\mathbf{r}_1^1 \tag{4.5}$$

Here $\mathbf{p}_1^0$ is a null vector (as joint 1 is at the origin of base coordinate system) and $\mathcal{R}_1^0$ is given by

$$\mathcal{R}_1^0 = \begin{bmatrix} \cos\theta_1 & -\sin\theta_1 \\ -\sin\theta_1 & \cos\theta_1 \end{bmatrix} \tag{4.6}$$

From Figure 2.2, the local position vector $\mathbf{r}_1^1$ is given by:

$$\mathbf{r}_1^1 = \begin{bmatrix} (i-1)l_1 + x_{1,i} + u_{1,i}(x,t) + r_h \\ v_{1,i}(x,t) \end{bmatrix} \tag{4.7}$$

where

$u_{1,i}(x,t)$: elongation deformation along X_1-axis at a distance x and at time t in the ith element of link expressed in coordinate frame of link 1

$v_{1,i}(x,t)$: flexureal transverse deflection along Y_1-axis with reference to neutral axis at a distance x and at time t in the ith element of link expressed in coordinate frame of link 1

and $u_{1,i}(x,t)$ and $v_{1,i}(x,t)$ are given as

$$\begin{bmatrix} u_{1,i}(x,t) \\ v_{1,i}(x,t) \end{bmatrix} = \begin{bmatrix} F_1(x) & 0 & 0 & F_2(x) & 0 & 0 \\ 0 & H_1(x) & H_2(x) & 0 & H_3(x) & H_4(x) \end{bmatrix} \mathbf{q}_{f_{1,i}}(t) \tag{4.8}$$

and

$$\mathbf{q}_{f_{1,i}}(t) = \begin{bmatrix} u_{1,i}(t) & v_{1,i}(t) & vx_{1,i}(t) & u_{1,i+1}(t) & v_{1,i+1}(t) & vx_{1,i+1}(t) \end{bmatrix}^T$$

Where

$u_{1,i}(t)$: axial deformation along X_1-axis at ith node of link 1

$v_{1,i}(t)$: flexural transverse deflection along Y_1-axis at ith node of link 1

$vx_{1,i}(t)$: flexural slope along Y_1-axis at ith node of link 1

Various shape functions are given as in Equation 2.28.

Substituting in Equation 2.29, the expression for kinetic energy due to inertia of joint 1 is given by:

$$T_{joint_1} = \frac{1}{2} I_{h_1} \dot{\theta_1}^2 \tag{4.9}$$

where I_{h_1} is the joint inertia of joint 1.

Now general expression for kinetic energy of the ith element of link 1

$$T_{link_{1,i}} = \frac{1}{2} \int_0^{l_1} m_1 \left(\frac{d\mathbf{r}_1^0}{dt}\right)^T \left(\frac{d\mathbf{r}_1^0}{dt}\right) dx_{1,i} \tag{4.10}$$

we can also write:

$$\begin{aligned} \frac{d\mathbf{r}_1^0}{dt} &= \frac{\partial \mathbf{r}_1^0}{\partial \mathbf{q}_{1,i}} \frac{\partial \mathbf{q}_{1,i}}{\partial t} \\ &= \begin{bmatrix} \frac{\partial \mathbf{r}_1^0}{\partial \theta_1} & \frac{\partial \mathbf{r}_1^0}{\partial u_{1,i}} & \frac{\partial \mathbf{r}_1^0}{\partial v_{1,i}} & \frac{\partial \mathbf{r}_1^0}{\partial vx_{1,i}} & \frac{\partial \mathbf{r}_1^0}{\partial u_{1,i+1}} & \frac{\partial \mathbf{r}_1^0}{\partial v_{1,i+1}} & \frac{\partial \mathbf{r}_1^0}{\partial vx_{1,i+1}} \end{bmatrix} \dot{\mathbf{q}}_{1,i} \end{aligned} \tag{4.11}$$

Where elemental degrees of freedom vector is given by

$$\mathbf{q}_{1,i}(t) = \begin{bmatrix} \theta_1 & u_{1,i}(t) & v_{1,i}(t) & vx_{1,i}(t) & u_{1,i+1}(t) & v_{1,i+1}(t) & vx_{1,i+1}(t) \end{bmatrix}^T$$

From Equation 4.10 and Equation 4.11 the kinetic energy of *ith* element is found and written in the following form

$$T_{link_{1,i}} = \frac{1}{2}\dot{\mathbf{q}}_{1,i}^T \mathbf{M}_{1,i} \dot{\mathbf{q}}_{1,i} \tag{4.12}$$

Where $\mathbf{M}_{1,i}$ is a symmetric 7 x 7 size elemental mass matrix of the following form:

$$\mathbf{M}_{1,i} = \begin{bmatrix} \mathbf{M}_{1,i}(1,1) & \mathbf{M}_{1,i}(1,2) & \dots & \mathbf{M}_{1,i}(1,7) \\ \mathbf{M}_{1,i}(2,1) & & & \\ \vdots & & [\mathbf{P}_{1,i}]_{6x6} & \\ \mathbf{M}_{1,i}(7,1) & & & \end{bmatrix}_{7x7} \tag{4.13}$$

Elements of the above mass matrix are calculated as

$$\mathbf{M}_{1,i}(j,k) = \int_0^{l_1} m_1 \left(\frac{\partial \mathbf{r}_1^0}{\partial \mathbf{q}_{1,i,j}}\right)^T \left(\frac{\partial \mathbf{r}_1^0}{\partial \mathbf{q}_{1,i,k}}\right) dx_{1,i} \tag{4.14}$$

Where $\mathbf{q}_{1,i,j}$ is the jth element of vector $\mathbf{q}_{1,i}$.

After integration all the matrix elements are derived and given in final form in Appendix B.

Similarly to calculate the elemental Kinetic energy of link 2, we can write the position vector of any material point(s) along the neutral axis of link 2 with respect to base coordinate system (X_0, Y_0) as :

$$\mathbf{r}_2^0 = \mathbf{p}_2^0 + \mathcal{R}_2^0 \mathbf{r}_2^2 \tag{4.15}$$

Where

$$\mathbf{p}_2^0 = \mathbf{p}_1^0 + \mathcal{R}_2^1 \mathbf{p}_2^1 \tag{4.16}$$

$$= \mathcal{R}_2^1 \begin{bmatrix} L_1 + u_{1,tip} \\ v_{1,tip} \end{bmatrix} \tag{4.17}$$

and $\mathcal{R}_2^0$ is given by

$$\mathcal{R}_2^0 = \mathcal{R}_1^0 \mathcal{R}_2^1 \tag{4.18}$$

$$= \mathcal{R}_1^0 \begin{bmatrix} \cos\hat{\theta}_2 & -\sin\hat{\theta}_2 \\ -\sin\hat{\theta}_2 & \cos\hat{\theta}_2 \end{bmatrix} \tag{4.19}$$

where

$$\hat{\theta}_2 = \theta_2 + vx_{1,tip}$$

From Figure 4.2, local position vector $\mathbf{r}_2^2$ is given by:

$$\mathbf{r}_2^2 = \begin{bmatrix} (i-1)l_2 + x_{2,i} + u_{2,i}(x,t) \\ v_{2,i}(x,t) \end{bmatrix} \tag{4.20}$$

where

$u_{2,i}(x,t)$: elongation deformation along X_2-axis at a distance x and at time t in the ith element of link expressed in coordinate frame of link 2

$v_{2,i}(x,t)$: flexural transverse deflection along Y_2-axis with reference to neutral axis at a distance x and at time t in the *ith* element of link expressed in coordinate frame of link 2

and $u_{2,i}(x,t)$ and $v_{2,i}(x,t)$ are given as

$$\begin{bmatrix} u_{2,i}(x,t) \\ v_{2,i}(x,t) \end{bmatrix} = \begin{bmatrix} F_1(x) & 0 & 0 & F_2(x) & 0 & 0 \\ 0 & H_1(x) & H_2(x) & 0 & H_3(x) & H_4(x) \end{bmatrix} \mathbf{q}_{f_{2,i}}(t) \tag{4.21}$$

and

$$\mathbf{q}_{f_{2,i}}(t) = \begin{bmatrix} u_{2,i}(t) & v_{2,i}(t) & vx_{2,i}(t) & u_{2,i+1}(t) & v_{2,i+1}(t) & vx_{2,i+1}(t) \end{bmatrix}^T \tag{4.22}$$

Where

$u_{2,i}(t)$: axial deformation along X_1-axis at *ith* node of link 2

$v_{2,i}(t)$: flexural transverse deflection along Y_1-axis at *ith* node of link 2

$vx_{2,i}(t)$: flexural slope along Y_1-axis at *ith* node of link 2

Various shape functions are given as in Equation 2.28.

Now general expression for kinetic energy of the *ith* element of link 2

$$T_{link_{2,i}} = \frac{1}{2}\int_0^{l_2} m_2 \left(\frac{d\mathbf{r}_2^0}{dt}\right)^T \left(\frac{d\mathbf{r}_2^0}{dt}\right) dx_{2,i} \tag{4.23}$$

We can also write:

$$\begin{aligned} \frac{d\mathbf{r}_2^0}{dt} &= \frac{\partial \mathbf{r}_2^0}{\partial \mathbf{q}_{2,i}} \frac{\partial \mathbf{q}_{2,i}}{\partial t} \\ &= \begin{bmatrix} \frac{\partial \mathbf{r}_2^0}{\partial \theta_1} & \frac{\partial \mathbf{r}_2^0}{\partial u_{1,tip}} & \frac{\partial \mathbf{r}_2^0}{\partial v_{1,tip}} & \frac{\partial \mathbf{r}_2^0}{\partial vx_{1,tip}} & \frac{\partial \mathbf{r}_2^0}{\partial \theta_2} & \frac{\partial \mathbf{r}_2^0}{\partial u_{2,i}} & \cdots \\ & & \cdots & \frac{\partial \mathbf{r}_2^0}{\partial v_{2,i}} & \frac{\partial \mathbf{r}_2^0}{\partial vx_{2,i}} & \frac{\partial \mathbf{r}_2^0}{\partial u_{2,i+1}} & \frac{\partial \mathbf{r}_2^0}{\partial v_{2,i+1}} & \frac{\partial \mathbf{r}_2^0}{\partial vx_{2,i+1}} \end{bmatrix} \dot{\mathbf{q}}_{2,i} \end{aligned} \tag{4.24}$$

Where elemental degrees of freedom vector is given by

$$\mathbf{q}_{2,i}(t) = \begin{bmatrix} \theta_1 & u_{1,tip} & v_{1,tip} & vx_{1,tip} & \theta_2 & u_{2,i} & v_{2,i} & vx_{2,i} & u_{2,i+1} & v_{2,i+1} & vx_{2,i+1} \end{bmatrix}^T$$

From Equation 4.23 and Equation 4.24 the kinetic energy of *ith* element is found and written in the following form:

$$T_{link_{2,i}} = \frac{1}{2}\dot{\mathbf{q}}_{2,i}^T \mathbf{M}_{2,i} \dot{\mathbf{q}}_{2,i} \tag{4.25}$$

Where $\mathbf{M}_{2,i}$ is a symmetric 11 x 11 size elemental mass matrix of following form

$$\mathbf{M}_{2,i} = \begin{bmatrix} \mathbf{M}_{2,i}(1,1) & \cdots & \mathbf{M}_{2,i}(1,5) & \cdots & \mathbf{M}_{1,i}(1,11) \\ \vdots & & \vdots & & \vdots \\ \vdots & & \mathbf{M}_{2,i}(5,5) & \cdots & \mathbf{M}_{2,i}(5,11) \\ \vdots & & \vdots & [\mathbf{P}_{2,i}]_{6x6} & \\ \mathbf{M}_{2,i}(11,1) & \cdots & \mathbf{M}_{2,i}(11,5) & & \end{bmatrix}_{11x11} \tag{4.26}$$

And elements of the above mass matrix are calculated as

$$\mathrm{M}_{2,i}(j,k) = \int_0^{l_2} m_2 \left(\frac{\partial \mathbf{r}_2^0}{\partial \mathbf{q}_{2,i,j}}\right)^T \left(\frac{\partial \mathbf{r}_2^0}{\partial \mathbf{q}_{2,i,k}}\right) dx_{2,i} \tag{4.27}$$

Where $\mathbf{q}_{2,i,j}$ is the jth element of vector $\mathbf{q}_{2,i}$.

After integration all the matrix elements are derived and given in final form in Appendix B.

4.2.2 Calculation of Elemental Potential Energy

Link-1

The elastic potential energy of flexible link 1 is due to axial and transverse deformation of link. Elemental potential energy due to axial deformation is given by:

$$V_{a_{1,i}} = \frac{1}{2}\int_0^{l_1} E_1 A_1 \left(\frac{\partial u_{1,i}(x,t)}{\partial x_{1,i}}\right)^2 dx_{1,i} \tag{4.28}$$

where E_1 and A_1 are Young's modulus of elasticity and area of cross-section for link 1 and $u_{1,i}$ is given by

$$u_{1,i}(x,t) = \begin{bmatrix} F_1(x) & F_2(x) \end{bmatrix} \begin{bmatrix} u_{1,i} \\ u_{1,i+1} \end{bmatrix} \tag{4.29}$$

From Equation 4.28 and Equation 4.29, $V_{a_{1,i}}$ is written as:

$$V_{a_{1,i}} = \frac{1}{2} \begin{bmatrix} u_{1,i} & u_{1,i+1} \end{bmatrix} \mathrm{K}_{a_{1,i}} \begin{bmatrix} u_{1,i} \\ u_{1,i+1} \end{bmatrix} \tag{4.30}$$

where

$$\begin{aligned} \mathrm{K}_{a_{1,i}} &= \int_0^{l_1} E_1 A_1 \begin{bmatrix} \frac{1}{l_1^2} & -\frac{1}{l_1^2} \\ -\frac{1}{l_1^2} & \frac{1}{l_1^2} \end{bmatrix} dx_{1,i} \\ &= \frac{E_1 A_1}{l_1} \begin{bmatrix} 1 & -1 \\ -1 & 1 \end{bmatrix} \end{aligned} \tag{4.31}$$

Elemental potential energy due to transverse deformation is given by:

$$V_{t_{1,i}} = \frac{1}{2}\int_0^{l_1} E_1 I_1 \left(\frac{\partial^2 v_{1,i}(x,t)}{\partial x_{1,i}^2}\right)^2 dx_{1,i} \tag{4.32}$$

where I_1 is area moment of inertia of link about neutral axis and $v_{1,i}$ is given by

$$v_{1,i}(x,t) = \begin{bmatrix} H_1(x) & H_2(x) & H_3(x) & H_4(x) \end{bmatrix} \begin{bmatrix} v_{1,i} \\ vx_{1,i} \\ v_{1,i+1} \\ vx_{1,i-1} \end{bmatrix} \tag{4.33}$$

From Equation 4.32 and Equation 4.33, $V_{1,i}$ can be written as

$$V_{1,i} = \frac{1}{2}\begin{bmatrix} v_{1,i} & vx_{1,i} & v_{1,i+1} & vx_{1,i+1} \end{bmatrix} \mathrm{K}_{1,i} \begin{bmatrix} v_{1,i} \\ vx_{1,i} \\ v_{1,i+1} \\ vx_{1,i+1} \end{bmatrix} \tag{4.34}$$

where

$$\mathrm{K}_{1,i} = \frac{E_1 I_1}{l_1^3} \begin{bmatrix} 12 & 6l_1 & -12 & 6l_1 \\ 6l_1 & 4l_1^2 & -6l_1 & 2l_1^2 \\ -12 & 6l_1 & 12 & -6l_1 \\ 6l_1 & 2l_1^2 & -6l_1 & 4l_1^2 \end{bmatrix} \tag{4.35}$$

Therefore total potential energy of link due to axial and transverse deformation can be written in matrix form as:

$$V_{1,i} = \frac{1}{2}\mathrm{q}_{f_{1,i}}^T \mathrm{K}_{1,i} \mathrm{q}_{f_{1,i}} \tag{4.36}$$

where combined stiffness matrix $K_{1,i}$ is given by:

$$\mathrm{K}_{1,i} = \frac{E_1}{l_1} \begin{bmatrix} A_1 & 0 & 0 & -A_1 & 0 & 0 \\ 0 & \frac{12I_1}{l_1^2} & \frac{6I_1}{l_1} & 0 & -\frac{12I_1}{l_1^2} & \frac{6I_1}{l_1} \\ 0 & \frac{6I_1}{l_1} & 4I_1 & 0 & -\frac{6I_1}{l_1} & 2I_1 \\ -A_1 & 0 & 0 & A_1 & 0 & 0 \\ 0 & -\frac{12I_1}{l_1^2} & -\frac{6I_1}{l_1} & 0 & \frac{12I_1}{l_1} & -\frac{6I_1}{l_1} \\ 0 & \frac{6I_1}{l_1} & 2I_1 & 0 & -\frac{6I_1}{l_1} & 4I_1 \end{bmatrix} \tag{4.37}$$

Link-2

Similar to link 1, the total potential energy of link 2 due to axial and transverse deformation can be written in matrix form as:

$$V_{2,i} = \frac{1}{2}\mathrm{q}_{f_{2,i}}^T \mathrm{K}_{2,i} \mathrm{q}_{f_{2,i}} \tag{4.38}$$

where combined stiffness matrix $K_{2,i}$ is given by:

$$\mathrm{K}_{2,i} = \frac{E_2}{l_2} \begin{bmatrix} A_2 & 0 & 0 & -A_2 & 0 & 0 \\ 0 & \frac{12I_2}{l_2^2} & \frac{6I_2}{l_2} & 0 & -\frac{12I_2}{l_2^2} & \frac{6I_2}{l_2} \\ 0 & \frac{6I_2}{l_2} & 4I_2 & 0 & -\frac{6I_2}{l_2} & 2I_2 \\ -A_2 & 0 & 0 & A_2 & 0 & 0 \\ 0 & -\frac{12I_2}{l_2^2} & -\frac{6I_2}{l_2} & 0 & \frac{12I_2}{l_2} & -\frac{6I_2}{l_2} \\ 0 & \frac{6I_2}{l_2} & 2I_2 & 0 & -\frac{6I_2}{l_2} & 4I_2 \end{bmatrix} \tag{4.39}$$

where

E_2 : Young's modulus of elasticity for link 2

A_2 : Area of cross-section for link 2

I_2 : Area moment of inertia of link 2 about neutral axis

4.2.3 Assembly Procedure

The total kinetic and potential energies are calculated by summing the elemental kinetic and potential energies which involves the assembling of various vectors and matrices. If n_1 and n_2 be the number of elements into which link 1 and link 2 are discretized respectively then,

Kinetic Energy

Kinetic energy of the jth link, $T^*_{link_j}$ is given by

$$\begin{aligned} T^*_{link_j} &= \sum_{i=1}^{n_j} \frac{1}{2} \dot{\mathbf{q}}^T_{j,i} \mathbf{M}^*_{j,i} \dot{\mathbf{q}}_{j,i} \\ &= \frac{1}{2} \dot{\mathbf{q}}^T_j \mathbf{M}^*_{link_j} \dot{\mathbf{q}}_j \end{aligned} \tag{4.40}$$

Here $\mathbf{M}^*_{j,i}$ is found by dropping out the terms containing second power of flexible degrees of freedom (i.e. the terms containing $\mathbf{q}^T_{f_{j,i}} \mathbf{P}_{j,i} \mathbf{q}_{f_{j,i}}$) from actual elemental mass matrix $\mathbf{M}_{j,i}$. These dropped out terms are assembled separately for convenience in applying the Lagrange's equation in the next step. Thus the reduced mass matrix $\mathbf{M}^*_{link_j}$ of size $[3(n_j + 1) + 1]$ x $[3(n_j + 1) + 1]$ is obtained by assembling the elemental mass matrices $\mathbf{M}^*_{j,i}$.

$\mathbf{q}_j$ is the generalized variable vector for the jth link and $\mathbf{q}_{f_j}$ is its sub-vector which consists of flexible motion variables of jth the link. These are given by:

Link-1

$$\mathbf{q}_1 = \left[\begin{array}{ccccccccc} \theta_1 & u_{1,1} & v_{1,1} & vx_{1,1} & \cdots & u_{1,n_1+1} & v_{1,n_1+1} & vx_{1,n_1+1} \end{array} \right]^T_{3(n_1+1)+1} \tag{4.41}$$

$$\mathbf{q}_{f_1} = \left[\begin{array}{ccccccccc} u_{1,1} & v_{1,1} & vx_{1,1} & \cdots & u_{1,n_1+1} & v_{1,n_1+1} & vx_{1,n_1+1} \end{array} \right]^T_{3(n_1+1)} \tag{4.42}$$

Link-2

$$\mathbf{q}_2 = \left[\begin{array}{ccccccccccccc} \theta_1 & u_{1,tip} & v_{1,tip} & vx_{1,tip} & \theta_2 & u_{2,1} & v_{2,1} & vx_{2,1} & \cdots & u_{2,n_2+1} & v_{1,n_2+1} & vx_{1,n_2+1} \end{array} \right]^T_{3(n_2+1)+5} \tag{4.43}$$

$$\mathbf{q}_{f_2} = \left[\begin{array}{ccccccccc} u_{2,1} & v_{2,1} & vx_{2,1} & \cdots & u_{2,n_2+1} & v_{2,n_2+1} & vx_{2,n_2+1} \end{array} \right]^T_{3(n_2+1)} \tag{4.44}$$

After finding the kinetic energy for each link, the total kinetic energy of manipulator links T_{links} is found by summation, i.e.

$$\begin{aligned} T_{links} &= \sum_{j=1}^{2} \frac{1}{2} \dot{\mathbf{q}}_{\mathbf{j}}{}^T \mathbf{M}^*_{link_j} \dot{\mathbf{q}}_j \\ &= \frac{1}{2} \dot{\mathbf{q}}^T \mathbf{M}^*_{links} \dot{\mathbf{q}} \end{aligned} \tag{4.45}$$

Here $\mathbf{q}$ is the generalized variable vector for the manipulator and is given by

$$\mathbf{q}_2 = \begin{bmatrix} \theta_1 & u_{1,1} & v_{1,1} & vx_{1,1} & \dots & u_{1,tip} & v_{1,tip} & vx_{1,tip} & \dots & & \\ & \dots & \theta_2 & u_{2,1} & v_{2,1} & vx_{2,1} & \dots & u_{2,n_2+1} & v_{1,n_2+1} & vx_{1,n_2+1} \end{bmatrix}^T_{3(n_1+n_2+2)+}$$

$\mathbf{M}^*_{links}$ is reduced mass matrix of size $[3(n_1 + n_2 + 2) + 2]$ x $[3(n_1 + n_2 + 2) + 2]$ and is found by assembling the mass matrices for the two links. The left out terms (i.e. the terms containing $\mathbf{q}^T_{f_{1,i}}\mathbf{P}_{1,i}\mathbf{q}_{f_{1,i}}$ and $\mathbf{q}^T_{f_{2,i}}\mathbf{P}_{2,i}\mathbf{q}_{f_{2,i}}$) are assembled for each link separately in the following manner:

$$\mathbf{q}^T_{f_j}\mathbf{P}_j\mathbf{q}_{f_j} = \sum_{i=1}^{n_j} \mathbf{q}^T_{f_{j,i}}\mathbf{P}_{j,i}\mathbf{q}_{f_{j,i}} \tag{4.46}$$

We can write the contribution of all these terms in the total kinetic energy as:

From link-1

$$S_1 = \mathbf{q}^T_{f_1}\mathbf{P}_1\mathbf{q}_{f_1}\dot{\theta_1}^2 \tag{4.47}$$

From link-2

$$S_2 = \mathbf{q}^T_{f_2}\mathbf{P}_2\mathbf{q}_{f_2}(\dot{\theta_2}^2 + 2\dot{\theta_1}\dot{vx}_{n_1+1} + 2\dot{\theta_1}\dot{\theta_2} + \dot{vx}^2_{n_1+1} + 2\dot{\theta_2}\dot{vx}_{n_1+1} + \dot{\theta_2}^2) \tag{4.48}$$

Hence total kinetic energy of the manipulator links is given as:

$$T_{link} = \frac{1}{2}\left(\dot{\mathbf{q}}^T\mathbf{M}^*_{links}\dot{\mathbf{q}} + S_1 + S_2\right) \tag{4.49}$$

From Equation 4.9 and Equation 4.49 the total kinetic energy of manipulator T is found as:

$$\begin{aligned} T &= T_{link} + T_{joint} \\ &= \frac{1}{2}\left(\dot{\mathbf{q}}^T\mathbf{M}^*_{links}\dot{\mathbf{q}} + S_1 + S_2\right) + \frac{1}{2}I_{h_1}\dot{\theta_1}^2 \\ &= \frac{1}{2}\left(\dot{\mathbf{q}}^T\mathbf{M}^*\dot{\mathbf{q}} + S_1 + S_2\right) \end{aligned} \tag{4.50}$$

Potential Energy

Potential energy of the jth link, V_j is given by

$$\begin{aligned} V_j &= \sum_{i=1}^{n_j} \frac{1}{2}\mathbf{q}^T_{f_{j,i}}\mathbf{K}_{j,i}\mathbf{q}_{f_{j,i}} \\ &= \frac{1}{2}\mathbf{q}^T_{f_j}\mathbf{K}^*_j\mathbf{q}_{f_j} \end{aligned} \tag{4.51}$$

Here $\mathbf{q}_{f_1}$ and $\mathbf{q}_{f_2}$ are given by Equation 4.42 and Equation 4.44. $\mathbf{K}^*_j$ is the stiffness matrix of size $3(n_j + 1)$ x $3(n_j + 1)$ for jth link. We define $\mathbf{K}_j$, which is obtained by adding a zero

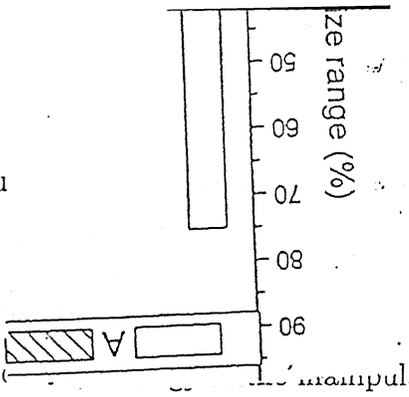

row and colu

$$\begin{bmatrix} & & 0 & \dots & 0 \\ & & \vdots & \mathbf{K}_j^* & \\ & & 0 & & \end{bmatrix} \tag{4.52}$$

Thus total p[illegible] manipulator is rewritten as:

$$V_j = \frac{1}{2}\mathbf{q}_j^T \mathbf{K}_j \mathbf{q}_j \tag{4.53}$$

Therefore total potential energy of the manipulator is given by:

$$\begin{aligned} V &= \sum_{j=1}^{2} \frac{1}{2}\mathbf{q}_j^T \mathbf{K}_j \mathbf{q}_j \\ &= \frac{1}{2}\mathbf{q}^T \mathbf{K} \mathbf{q} \end{aligned} \tag{4.54}$$

where $\mathbf{K}$ is the global stiffness matrix of size $[3(n_1 + n_2 + 2) + 2]$ x $[3(n_2 + n_2 + 2) + 2]$ before application of boundary condition

4.2.4 Boundary Conditions

We assume that link 1 is clamped rigidly with the actuator hub at the joint 1, therefore any displacement at node 1 of this link is constrained. This boundary condition is included into the model by setting the all flexible degrees of freedoms at node 1 to zero, i.e.

$$u_{1,1} = 0, v_{1,1} = 0, vx_{1,1} = 0 \tag{4.55}$$

Same is true for link 2 as here we assume that base end of link 2 is rigidly attached with joint 2, therefore

$$u_{2,1} = 0, v_{2,1} = 0, vx_{2,1} = 0 \tag{4.56}$$

These nodal degrees of freedoms are eliminated from the generalized variable vector $\mathbf{q}$. Thus final $\mathbf{q}$ of size $3(n_1 + n_2) + 2$ is given by:

$$\mathbf{q} = \begin{bmatrix} \theta_1 & u_{1,2} & v_{1,2} & vx_{1,2} & \dots & u_{1,tip} & v_{1,tip} & vx_{1,tip} & \dots & & \\ & & \dots & \theta_2 & u_{2,2} & v_{2,2} & vx_{2,2} & \dots & u_{2,n_2+1} & v_{1,n_2+1} & vx_{1,n_2+1} \end{bmatrix}^T_{3(n_1+n_2)+2}$$

Consequently mass and stiffness matrices are reduced by trimming the corresponding rows and columns.

4.2.5 Application of Lagrange's Equation

The final equations of motions are derived in the matrix form by applying the Lagrange'sequation. From Equations 2.1, 4.50 and 4.54

$$\mathcal{L} = \frac{1}{2}\left(\dot{\mathbf{q}}^T \mathbf{M}^* \dot{\mathbf{q}} + S_1 + S_2 - \mathbf{q}^T \mathbf{K} \mathbf{q}\right) \tag{4.57}$$

To get dynamic equations we first find $\frac{\partial \mathcal{L}}{\partial \mathbf{q}}$ and $\frac{d}{dt}\left(\frac{\partial \mathcal{L}}{\partial \dot{\mathbf{q}}}\right)$. Here again the terms containing the second power of variables (i.e. S_1 and S_2) are considered separately. Now

$$\frac{\partial \mathcal{L}}{\partial \mathbf{q}} = \frac{1}{2}\left(\dot{\mathbf{q}}^T \frac{\partial \mathbf{M}^*}{\partial \mathbf{q}}\dot{\mathbf{q}} - \mathbf{K}\mathbf{q} - \mathbf{q}^T\mathbf{K}\right) \tag{4.58}$$

And

$$\frac{\partial \mathcal{L}}{\partial \dot{\mathbf{q}}} = \frac{1}{2}\left(\mathbf{M}^*\dot{\mathbf{q}} + \dot{\mathbf{q}}^T\mathbf{M}^*\right) \tag{4.59}$$

Therefore

$$\begin{aligned}\frac{d}{dt}\frac{\partial \mathcal{L}}{\partial \dot{\mathbf{q}}} &= \frac{1}{2}\left[\mathbf{M}^*\ddot{\mathbf{q}} + \ddot{\mathbf{q}}^T\mathbf{M}^* + \sum_{k=1}^{3(n_1+n_2)+2}\left(\dot{\mathbf{q}}_k^T\frac{\partial \mathbf{M}^*}{\partial \dot{\mathbf{q}}_k}\dot{\mathbf{q}} + \dot{\mathbf{q}}^T\frac{\partial \mathbf{M}^*}{\partial \dot{\mathbf{q}}_k}\dot{\mathbf{q}}_k\right)\right] \\ &\quad - \left[\mathbf{M}^*\ddot{\mathbf{q}} + \sum_{k=1}^{3(n_1+n_2)+2}\left(\dot{\mathbf{q}}_k^T\frac{\partial \mathbf{M}^*}{\partial \dot{\mathbf{q}}_k}\dot{\mathbf{q}}\right)\right]\end{aligned} \tag{4.60}$$

Left-out terms (S_1 and S_2) are considering in the following manner:

From equation 4.47,

$$S_1 = \mathbf{q}_{f_1}^T\mathbf{P}_1\mathbf{q}_{f_1}\dot{\theta}_1^2$$

$$\begin{aligned}\frac{1}{2}\left[\frac{d}{dt}\begin{pmatrix}\partial S_1\\ \partial \dot{\mathbf{q}}\end{pmatrix} \quad \frac{\partial S_1}{\partial \mathbf{q}}\right] &= \frac{1}{2}\left[\frac{d}{dt}\left(\frac{\partial}{\partial \dot{\mathbf{q}}}\left(\mathbf{q}_{f_1}^T\mathbf{P}_1\mathbf{q}_{f_1}\dot{\theta}_1^2\right)\right) - \frac{\partial}{\partial \mathbf{q}}\left(\mathbf{q}_{f_1}^T\mathbf{P}_1\mathbf{q}_{f_1}\dot{\theta}_1^2\right)\right] \\ &= \begin{bmatrix}\mathbf{q}_{f_1}^T\mathbf{P}_1\mathbf{q}_{f_1} & 0 & \dots & 0 & 0 & 0 & \dots & 0\end{bmatrix}^T\ddot{\theta}_1^2 + \\ &+ \begin{bmatrix}2\mathbf{q}_{f_1}^T\mathbf{P}_1\dot{\mathbf{q}}_{f_1} & 0 & \dots & 0 & 0 & 0 & \dots & 0\end{bmatrix}^T\dot{\theta}_1 - \\ &\begin{bmatrix}0 & \left[\mathbf{P}_1\mathbf{q}_{f_1}\right]^T & 0 & \dots & 0\end{bmatrix}^T\dot{\theta}_1^2\end{aligned} \tag{4.61}$$

Similarly the expression for $\frac{1}{2}\left[\frac{d}{dt}\left(\frac{\partial S_2}{\partial \dot{\mathbf{q}}}\right) - \frac{\partial S_2}{\partial \mathbf{q}}\right]$ is found out which is given in Appendix C.

Now the terms containing the second derivative of general variables (i.e. terms containing $\ddot{\theta}_1$, $\ddot{x}_{n_1,1}$ or $\ddot{\theta}_2$ in right hand side of Equation 4.61 and Equation C.1 to Equation C.6) are assembled with the inertia term $\mathbf{M}^*\ddot{\mathbf{q}}$, to get the final inertia term in the form of $\mathbf{M}\ddot{\mathbf{q}}$, where $\mathbf{M}$ is the global mass matrix.

Rest of the terms (i.e. terms containing up-to first derivative of variables in Equation 4.61 and C.1 to equation C.6) are assembled (for both links) to get the vector $\mathbf{f}(\dot{\mathbf{q}}, \mathbf{q})$ of nonlinear terms.

Now from the Equations 2.1, 4.58 and 4.60 the dynamic equations in the matrix form are given as:

$$\mathbf{M}\ddot{\mathbf{q}} + \sum_{k=1}^{3(n_1+n_2)+2}\left(\dot{\mathbf{q}}_k^T\frac{\partial \mathbf{M}^*}{\partial \mathbf{q}_k}\dot{\mathbf{q}}\right) - \frac{1}{2}\dot{\mathbf{q}}^T\frac{\partial \mathbf{M}^*}{\partial \mathbf{q}}\dot{\mathbf{q}} - \mathbf{K}\mathbf{q} + \mathbf{f} = \mathbf{Q} \tag{4.62}$$

Let

$$\mathbf{F} = \sum_{k=1}^{3(n_1+n_2)+2} \left(\dot{\mathbf{q}}_k^T \frac{\partial \mathbf{M}^*}{\partial \mathbf{q}_k} \dot{\mathbf{q}} \right) - \frac{1}{2} \dot{\mathbf{q}}^T \frac{\partial \mathbf{M}^*}{\partial \mathbf{q}} \dot{\mathbf{q}} + \mathbf{fc} \tag{4.63}$$

We get the final equation in the form as:

$$\mathbf{M}\ddot{\mathbf{q}} + \mathbf{F}(\dot{\mathbf{q}}, \mathbf{q}) + \mathbf{K}\mathbf{q} = \mathbf{Q} \tag{4.64}$$

where $\mathbf{M}$ is the mass matrix, $\mathbf{F}$ the vector consisting of cetrifugal and coriolis forces, $\mathbf{K}$ the stiffness matrix and $\mathbf{Q}$ the force vector. $\mathbf{q}$ is the genralized degrees of freedom vector.

Now defining a state vector $\mathbf{z} = \begin{bmatrix} \mathbf{q} & \dot{\mathbf{q}} \end{bmatrix}^T$, Equation 4.64 can be re-written in the form:

$$\dot{\mathbf{z}} = \begin{bmatrix} \dot{\mathbf{q}} \\ \mathbf{M}^{-1}[\mathbf{Q} - \mathbf{F} - \mathbf{K}\mathbf{q}] \end{bmatrix} \tag{4.65}$$

The above equation gives a system of first order differential equations which can be integrated to get the time response of the system.

4.2.6 Damping Matrix

From Equation 2.39, Viscous damping matrix can be found by the following relation:

$$\mathbf{C} = \alpha\mathbf{M} + \beta\mathbf{K} \tag{4.66}$$

where the constants α and β are given by:

$$\alpha = \frac{2\omega_{n_1}\omega_{n_2}(\omega_{n_2}\zeta_1 - \omega_{n_1}\zeta_2)}{\omega_{n_2}^2 - \omega_{n_1}^2} \tag{4.67}$$

$$\beta = \frac{2(\omega_{n_2}\zeta_2 - \omega_{n_1}\zeta_1)}{\omega_{n_2}^2 - \omega_{n_1}^2} \tag{4.68}$$

where ω_{n_1} and ω_{n_2} and are the first and second undamped natural frequencies and ζ_1 and ζ_2 are respective damping factors. In the current work, values of both ζ_1 and ζ_2 are equal to 0.01. After finding the damping matrix $\mathbf{C}$ the modified final equation of motion is written as:

$$\mathbf{M}\ddot{\mathbf{q}} + \mathbf{C}\dot{\mathbf{q}} + \mathbf{F}(\mathbf{q}, \dot{\mathbf{q}}) + \mathbf{K}\mathbf{q} = \mathbf{Q} \tag{4.69}$$

4.2.7 Hybrid Damping

Various material damping properties of the hybrid damped links are given in Table 3.1. It is noted that usually this damping is highly dependent on the strain. From Equation 2.45 average elemental strain in ith element of the jth link may be written in matrix form as:

$$\varepsilon_{j,i} = \frac{1}{l_j}\left[(u_{j,i+1} - u_{j,i}) + \frac{y}{l_j}(vx_{j,i+1} - vx_{j,i})\right] \tag{4.70}$$

Next, the strain value calculated, may be used to determine the loss factor for passive layer (η_p) by using the strain vs damping data (Bhattacharya 2000). The loss factors for host layer (η_h) and magnetostrictive layer (η_m) are kept constant and equal to 0.001.

Once we find the loss factor values, the equivalent values of $E.1$ and EI for total link thickness are calculated with the help of Equations 2.46 to 2.50. Hence elemental stiffness matrix given by Equation 1.37 is modified into the following form to get elemental stiffness matrix of link j for passive damped system.

$$\mathrm{K}_{p_{ij}} \begin{bmatrix} \frac{(E.1)_j}{l_j} & 0 & 0 & -\frac{(E.1)_j}{l_j} & 0 & 0 \\ 0 & \frac{12(EI)_j}{l_j^3} & \frac{6(EI)_j}{l_j^2} & 0 & -\frac{12(EI)_j}{l_j^3} & \frac{6(EI)_j}{l_j^2} \\ 0 & \frac{6(EI)_j}{l_j^3} & \frac{4(EI)_j}{l_j} & 0 & -\frac{6(EI)_j}{l_j} & \frac{2(EI)_j}{l_j} \\ -\frac{(E.1)_j}{l_j} & 0 & 0 & \frac{(E.1)_j}{l_j} & 0 & 0 \\ 0 & -\frac{12(EI)_j}{l_j^3} & -\frac{6(EI)_j}{l_j^2} & 0 & \frac{12(EI)_j}{l_j^3} & -\frac{6(EI)_j}{l_j^2} \\ 0 & \frac{6(EI)_j}{l_j^2} & \frac{2(EI)_j}{l_j} & 0 & -\frac{6(EI)_j}{l_j^2} & \frac{4(EI)_j}{l_j} \end{bmatrix} \tag{4.71}$$

Calculation of Active Damping

Elemental active damping matrix is calculated from Equation 2.51 and assembled to get the global active damping matrix.

Thus calculated values of K_p and C_a are included into the model which gives the following dynamic equation for hybrid damped system.

$$\mathrm{M}\ddot{\mathrm{q}} + \mathrm{C}_a\dot{\mathrm{q}} + \mathrm{F}(\mathrm{q}, \dot{\mathrm{q}}) + \mathrm{K}_p\mathrm{q} = \mathrm{Q} \tag{4.72}$$

4.3 Results And Discussion

For a two-link manipulator the numerical simulations are carried out by developing a MATLAB code and "ode45" routine is used to numerically integrate the system of first order differential equations (see Equation 4.65). The physical properties of manipulator are given in Table 4.1. Later to study the effect of variation of these parameters, results are presented for different values of these parameters which are given in corresponding figures. The time responses for flexible as well as rigid manipulator are discussed together and a comparison has been done. In all the cases (except in Figure 4.6 and 4.7) the manipulator is considered to be in stretched-out position i.e. initial angular displacement at each joint is zero. As done in case of single link manipulator, angular displacement, joint rate, tip deflection and tip slope are studied for each link with respect to the variation in type, frequency and actuation point of input torque, material properties of links and slenderness ratio of links.

Physical system parameters	Value
Mass per unit of length of links (m)	7.39 kg/m
Length of links (L)	1.0 m
Hub radius at joint 1 (r_h)	0.02 m
Hub Inertia (I_h)	0.0041 kgm^2
Width of links (w)	50 mm
Thickness of links (t)	15 mm
Modulus of elasticity (E)	200 GPa

Table 1.1: Physical system parameters for two-link mainipulator

1. **Time Response Under Different Types of Input Torque**

Time response under three types of input torque namely sine wave, cosine wave and square wave of equal amplitudes and frequencies, are shown in Figure 4.2-4.3, Figure 4.4-4.5 and Figure 4.8-4.9 respectively. In each case time response for two complete cycles of input torque is studied.

The given torque is applied at the joint 1 and no torque is applied at joint 2. In terms of variation of angular displacement and joint rate, the link 1 follows the basic behaviour shown by the single link manipulator (as discussed in Section 3.3) under respective input torque. In the absence of any torque at joint 2, the variation of joint variable at this joint is in the reverse direction to that for joint 1. The effect of link 2 on the dynamics of link 1 is notable particularly for sine and square wave input torque, with the decrease in the amplitude of variation of joint rate (for both links) for the second cycle (see Figure 4.2B and Figure 4.8B). This is due to the fact that with the uniform increase (in negative direction) in θ_2, the dominance of coriolis and centrifugal forces increase which leads to lower angular acceleration. The effect of flexibility is observed in the form of increasing difference between the angular displacement and joint rate variation for both links (see Figure 4.2 and Figure 4.8).

The variation of tip deflection and tip slope suggests that both the links start to deflect in a direction opposite to the direction of rotation of respective link i.e. link 1 deflects in the negative direction and link 2 deflects in positive direction at the application of input torque. However in the case of torques with non-zero initial value (i.e. cosine and square wave input torque) a small initial deflection towards the direction of rotation is noticed which dies down within a very short time (see Figure 4.5A,C and Figure 4.9A,C). This glitch is attributed to the coriolis force effect of link 2 on the tip of the link 1 which dominates the inertia force of link 2 on the tip of link 1 during this small time interval. However, as the magnitude of angular displacement of link 2 increases the force at the tip of link 1 increases, which results in a deflection

in negative direction. This is evident from the absence of any glitch for the case when initial θ_2 is -90^0 as shown in Figure 4.7A,C.

2. **Variation in Time Response With Respect to Change in Input Torque-Frequency**

Time responses under cosine wave input torque of equal amplitude and with frequency equal to 1 Hz, 2 Hz, 4 Hz and 8 Hz are shown in Figure 4.10-4.11, Figure 4.4-4.5, Figure 4.12-4.13 and Figure 4.14-4.15respectively.

It is observed that for the increasing frequencies, the variation of angular displacement at each joint decreases as with lower time period, each link gets lesser time to rotate in one particular direction. Now since θ_2 is restricted to a smaller value for the higher frequencies, the effect of the link 2 on the dynamics of link 1 is less. Therefore for each high frequency case, both the links tend to maintain the amplitude of variation of joint rate as well as of angular displacement for the second cycle, which earlier showed a decreasing behaviour at low frequencies. The joint variables for flexible manipulator follows the rigid manipulator more closely at higher frequency. However the vibratory nature in the joint rate, due to flexural vibrations in the flexible links, is more and more visible for higher frequency cases. This causes the angular displacement of flexible manipulator to deviate at the peaks at higher frequencies. Tip deflection and tip slope vary similarly for different frequency cases.

3. **Performance of Link Materials Having Different Modulus of Elasticity and Density**

Time responses under cosine wave input torque of equal amplitude for the manipulators having links made up of Aluminium, Steel and CFRP are shown in Figure 4.16-4.17, Figure 4.4-4.5 and Figure 4.18-4.19 respectively.

It is observed that the Aluminium and CFRP links manipulator with their low mass densities show high angular displacements and joint rates because of their low inertia. Also, since link 2 is allowed to rotate to larger values of θ_2, the effect of link 2 on the dynamics of link 1 increases and in both these cases the variation of joint rates at both joints shows decreasing amplitude for second torque cycle (see Figure 4.16B,C and Figure 4.18B,C). With this angular displacement variations are no longer sinusoidal as during the second input torque cycle link 2 rotates to such an extent (θ_2 is close to the a value -90^0) (see Figure 4.16E and Figure 4.18E) such that the effect of torque is in the reverse direction and links continue to rotate in same direction during second torque cycle.

The effect of variation of modulus of elasticity is observed in the variation of maximum tip deflection values. The values of tip deflection and tip slope are highest for Aluminium links due to their high flexibility i.e. less modulus of elasticity.

4. **Variation in Time Response With Respect to Change in Slenderness Ratio (L/T) of Links**

Time response with variation in link lengths equal to 1.5 meters, 1.0 meters and 0.75 meters are are shown in Figure 4.20-4.21, Figure 4.4-4.5 and Figure 4.22-4.23 respectively with thickness of links remain constant.

It is observed that for manipulator having shorter links, the link 2 moves to higher values of angular displacement (Figure 4.22C) which in-turn gives rise to distorted variation of angular displacements at both joints.

However tip deflection and tip slope are maximum for the longer links of manipulator which can be attributed to the cubic relationship of deflection with the length of links.

5. **Time Response Under Actuation At Both Joints**

Apart from the cases discussed so far simulation runs are performed with torque at both the joints. Two cases, with equal torque ($\tau_{1_{max}} = \tau_{2_{max}} = 20Nm$) and unequal torque ($\tau_{1_{max}} = 20Nm$ and $\tau_{2_{max}} = 10Nm$) are shown in Figure 4.24-4.25 and Figure 4.26-4.27 respectively.

It is observed that with the application of an additional torque at joint 2, the direction of angular displacement of links is governed by this torque i.e. now link 2 rotates in positive direction and with the effect of that link 1 moves to negative angular position. Also, for flexible links, the vibrations in the joint rate at joint 2 are drastically increased however the mean position of these vibrations follows the sinusoidal curve of rigid manipulator (see Figure 4.24C and Figure 4.26C). The angular displacement variation pattern at joint 2 is severely distorted due to these vibrations (see Figure 4.24E and Figure 4.26E).

As expected both the links starts to deflect in the negative direction and no initial glitch is observed in tip deflection and tip slope variation. Further the magnitude of tip deflection of link 2 is found to be directly proportional to the torque amplitude at joint 2.

6. Time Response With Proportional Damping

In Figure 4.28-4.29, results for manipulator with physical parameters given in Table 4.1, with propotional damping of links is shown. On comparison with undamped and rigid link response with same input parameters (shown in Figure 4.4-4.5), it is observed that the proportional damping is able to damp out the high frequency mode oscillations in joint rate of joint 2 effectively (see Figure 4.28C). However if we compare the tip deflection and tip slope characterictics in above two cases (see Figure 4.5 and Figure 4.29), it is observed that there is marginal decrease in the magnitude of oscillations at tip of links with elimination of some peaks. Logarithmic decrement in tip slope variation of link 1 is found to be equal to 0.3243. However damping is not able to eliminate link oscillations completely as done in case of single-link manipulator case and therefore a better control strategy is required to eliminate these oscillations.

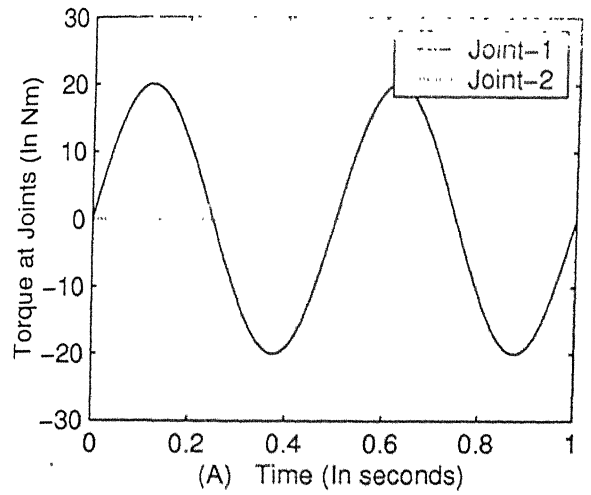

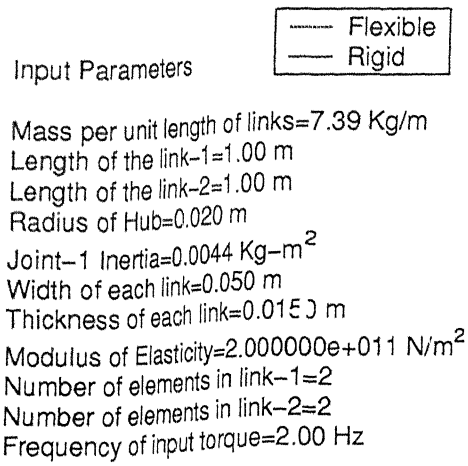

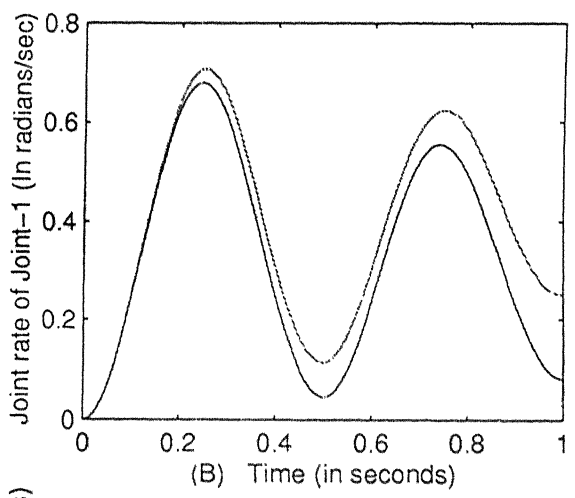

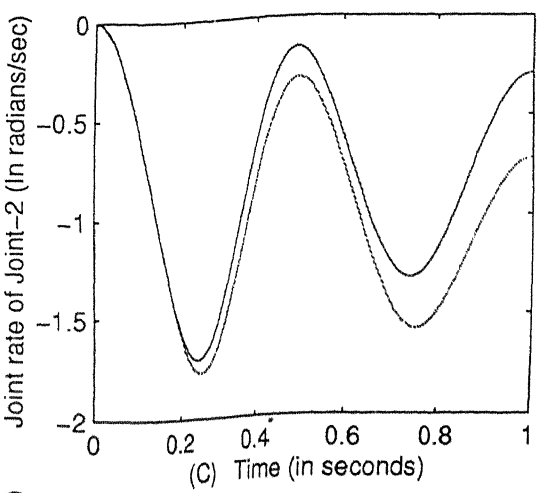

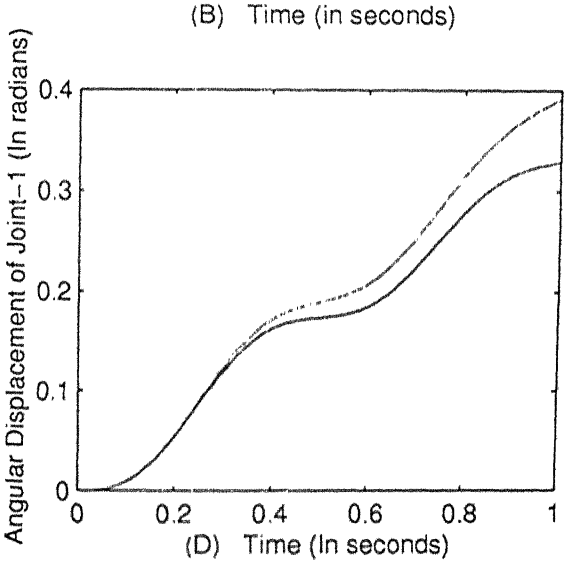

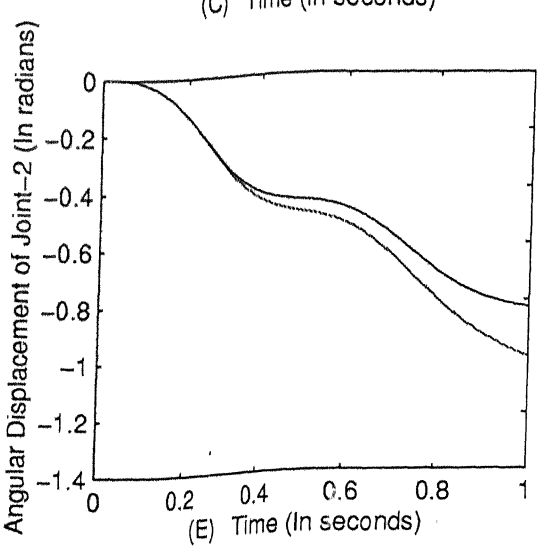

Figure 4.2: Time response under a sine wave input torque

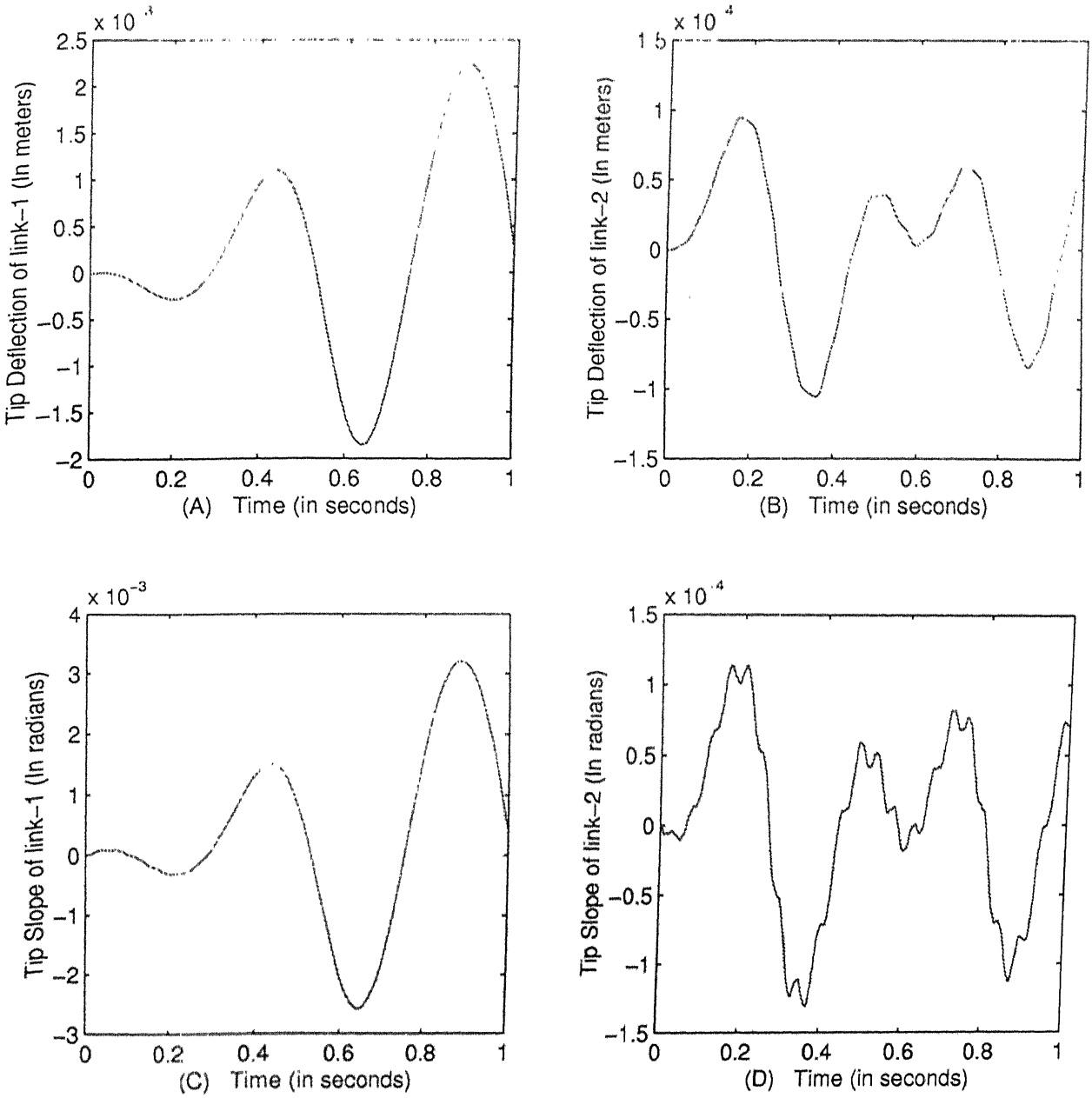

Figure 4.3: Tip deflection and slope variation under a sine wave input torque

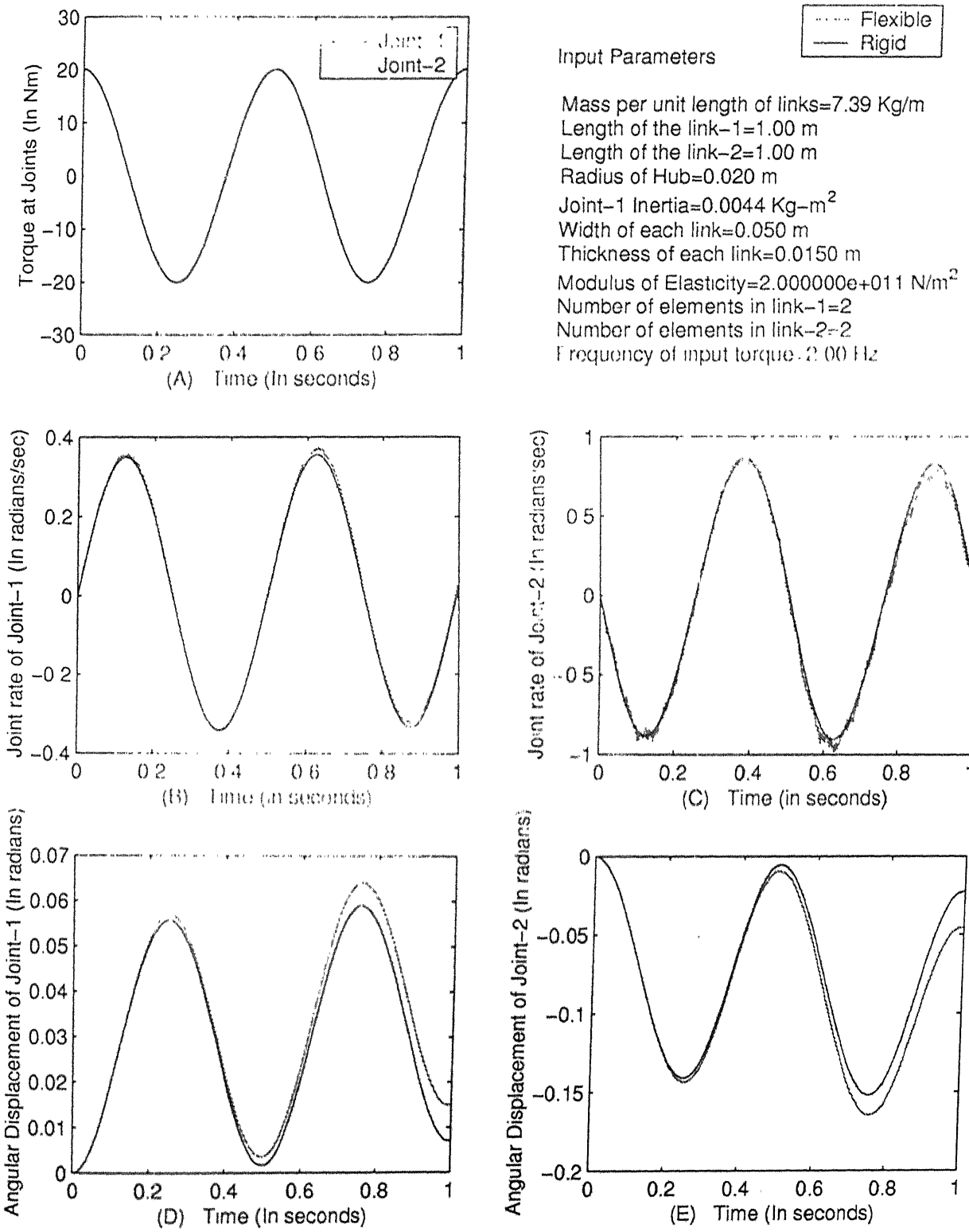

Figure 4.4: Time response under a cosine wave input torque

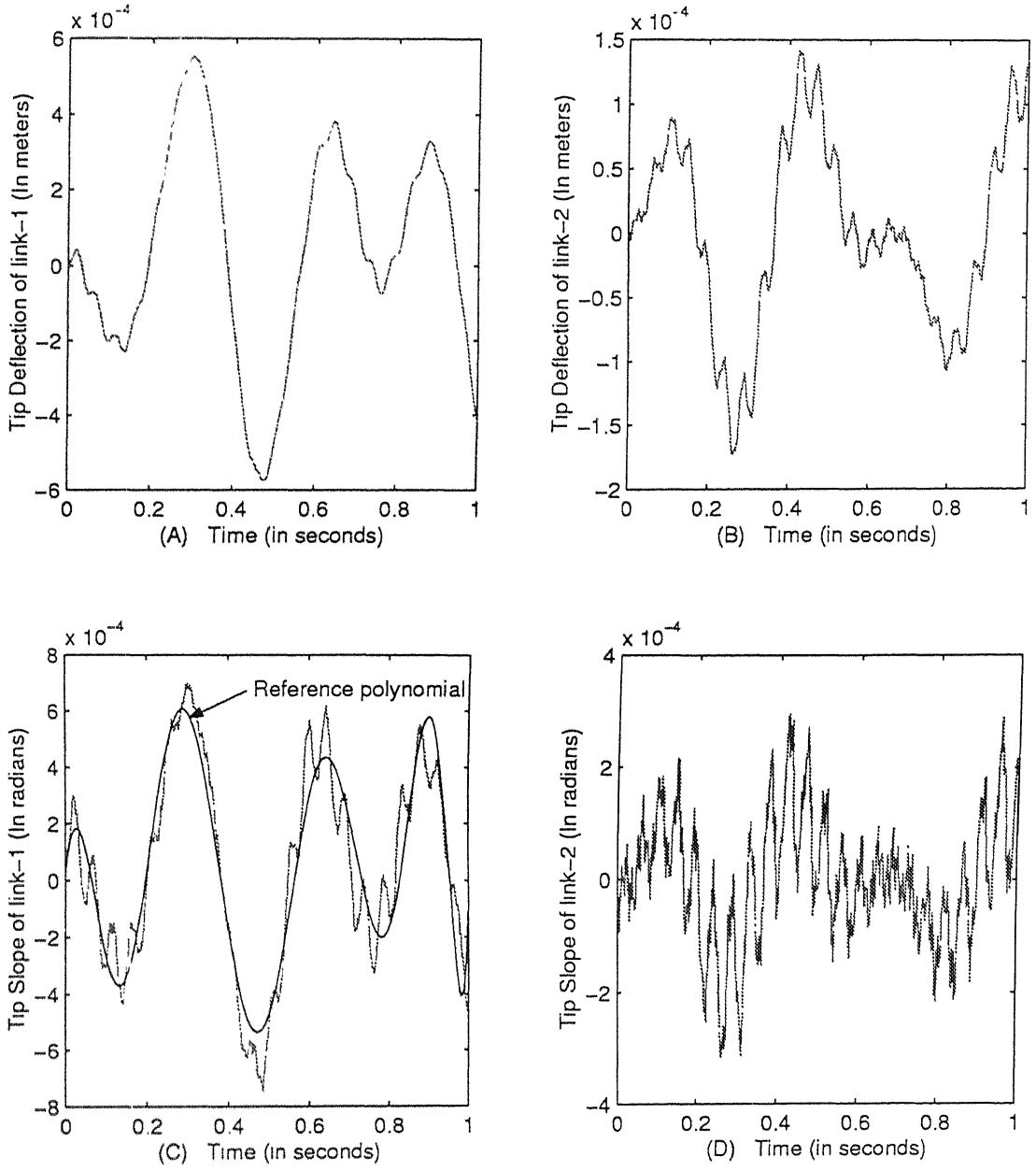

Figure 4.5: Tip deflection and slope variation under a cosine wave input torque

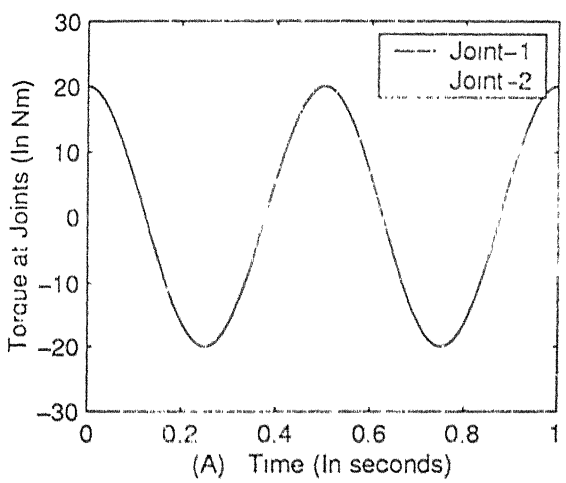

Flexible
Rigid

Input Parameters

Mass per unit length of links=7.39 Kg/m
Length of the link–1=1.00 m
Length of the link–2=1.00 m
Radius of Hub=0 020 m
Joint 1 Inertia=0 0044 Kg-m^2
Width of each link=0 050 m
Thickness of each link 0.0150 m
Modulus of Elasticity=2.000000e+011 N/m^2
Number of elements in link–1=2
Number of elements in link–2=2
Frequency of input torque=1.00 Hz

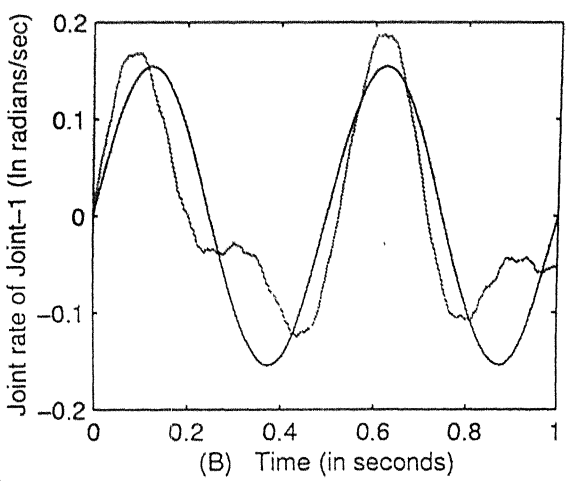

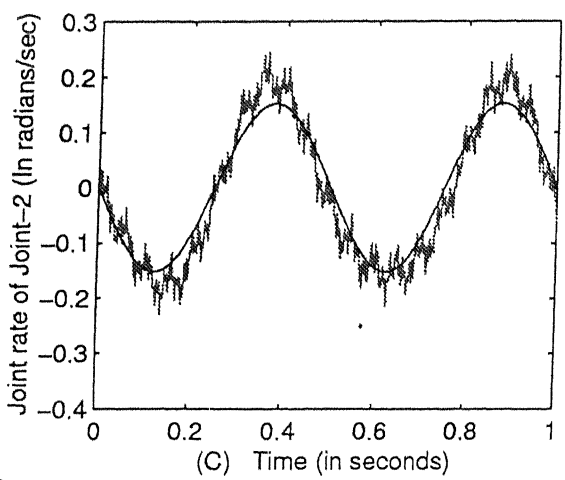

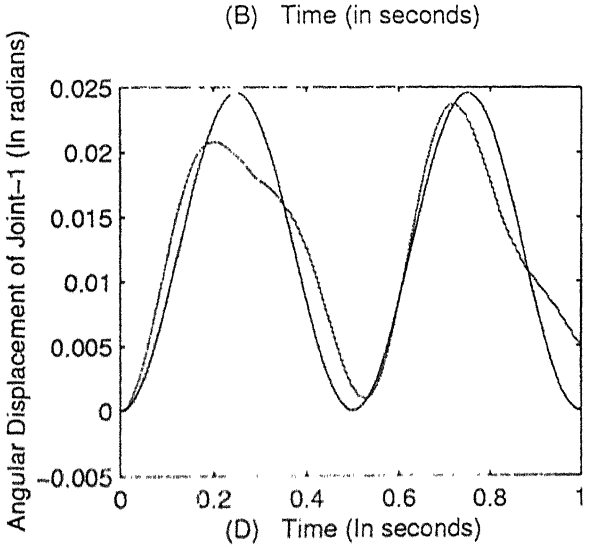

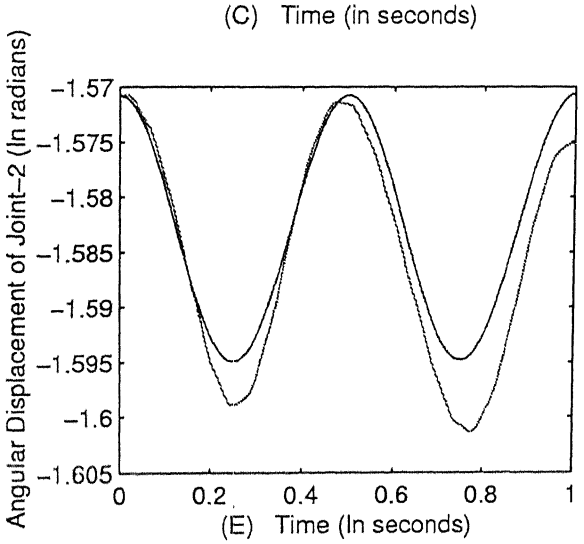

Figure 4.6: Time response with initial $\theta_2 = -90^0$

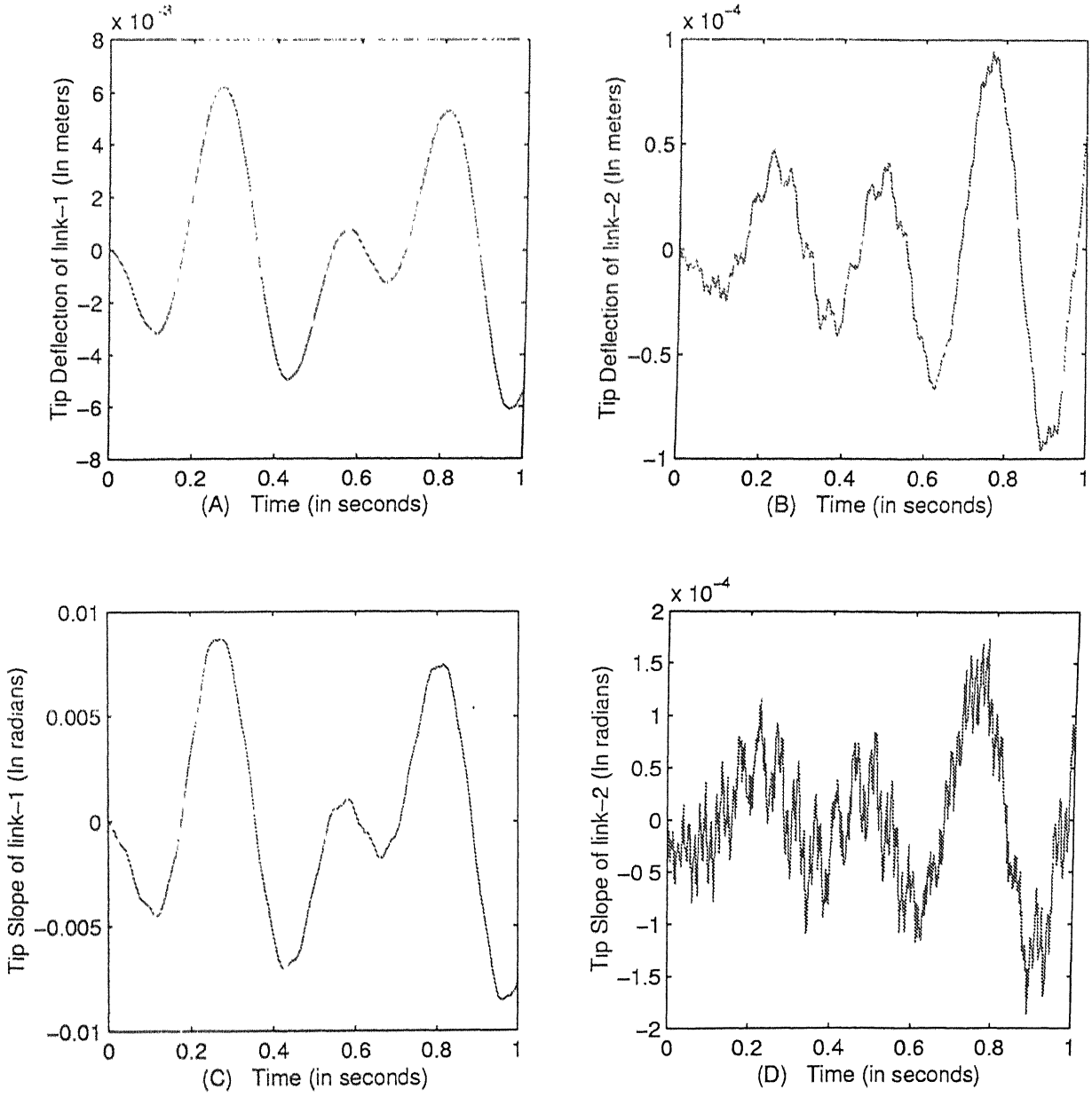

Figure 4.7: Tip deflection and slope variation with initial $\theta_2 = -90^0$

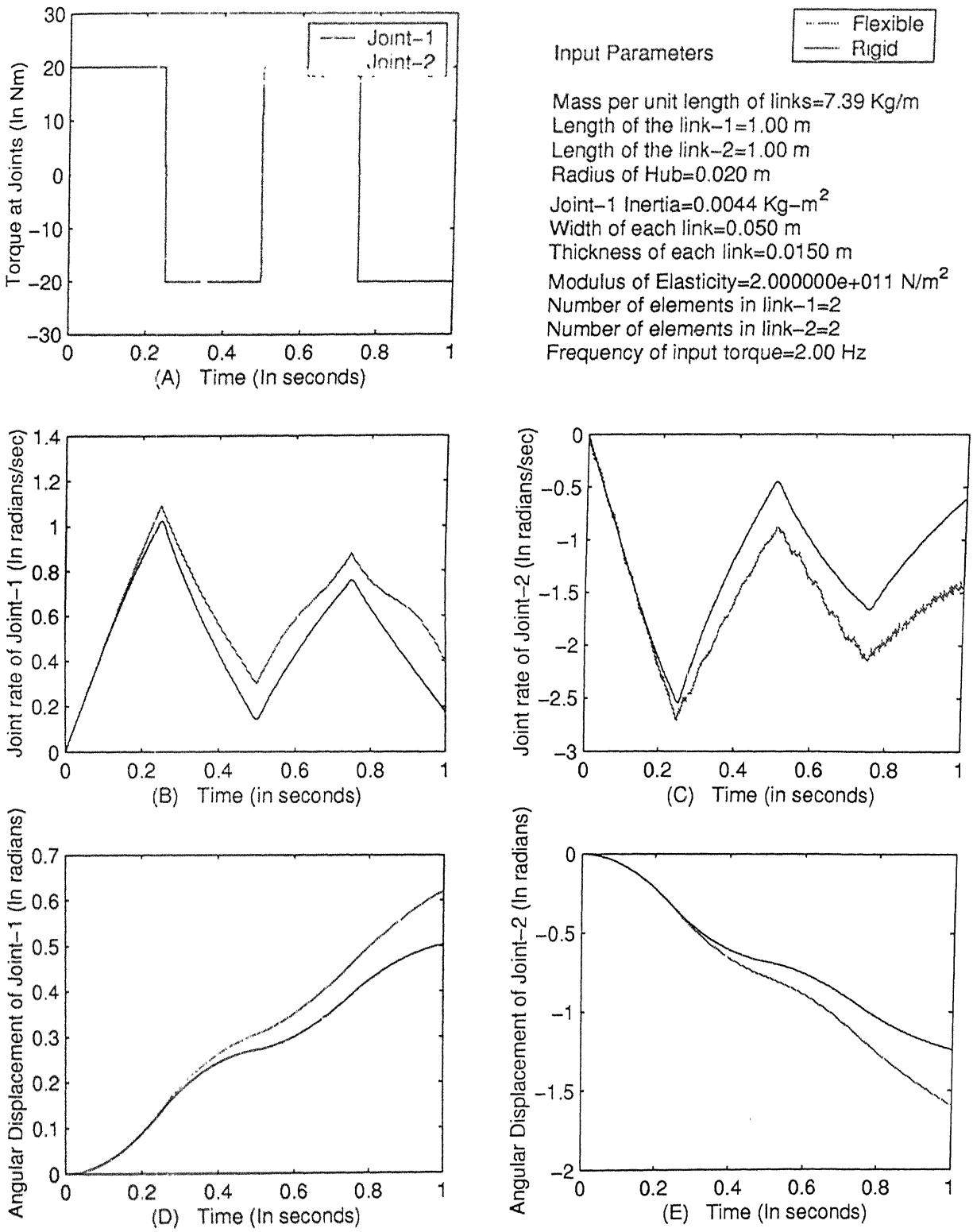

Figure 4.8: Time response under a square wave input torque

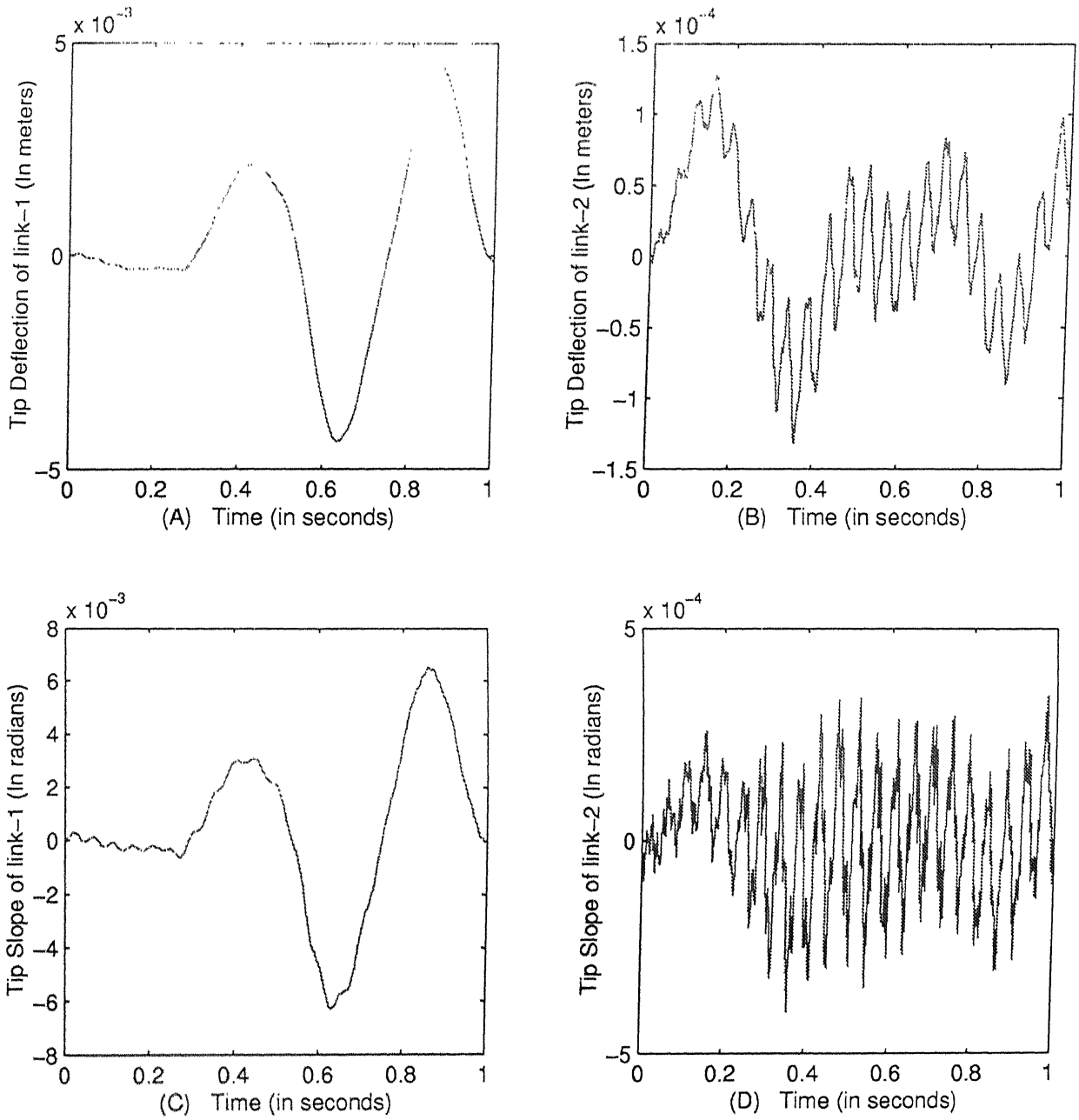

Figure 4.9: Tip deflection and slope variation under a square wave input torque

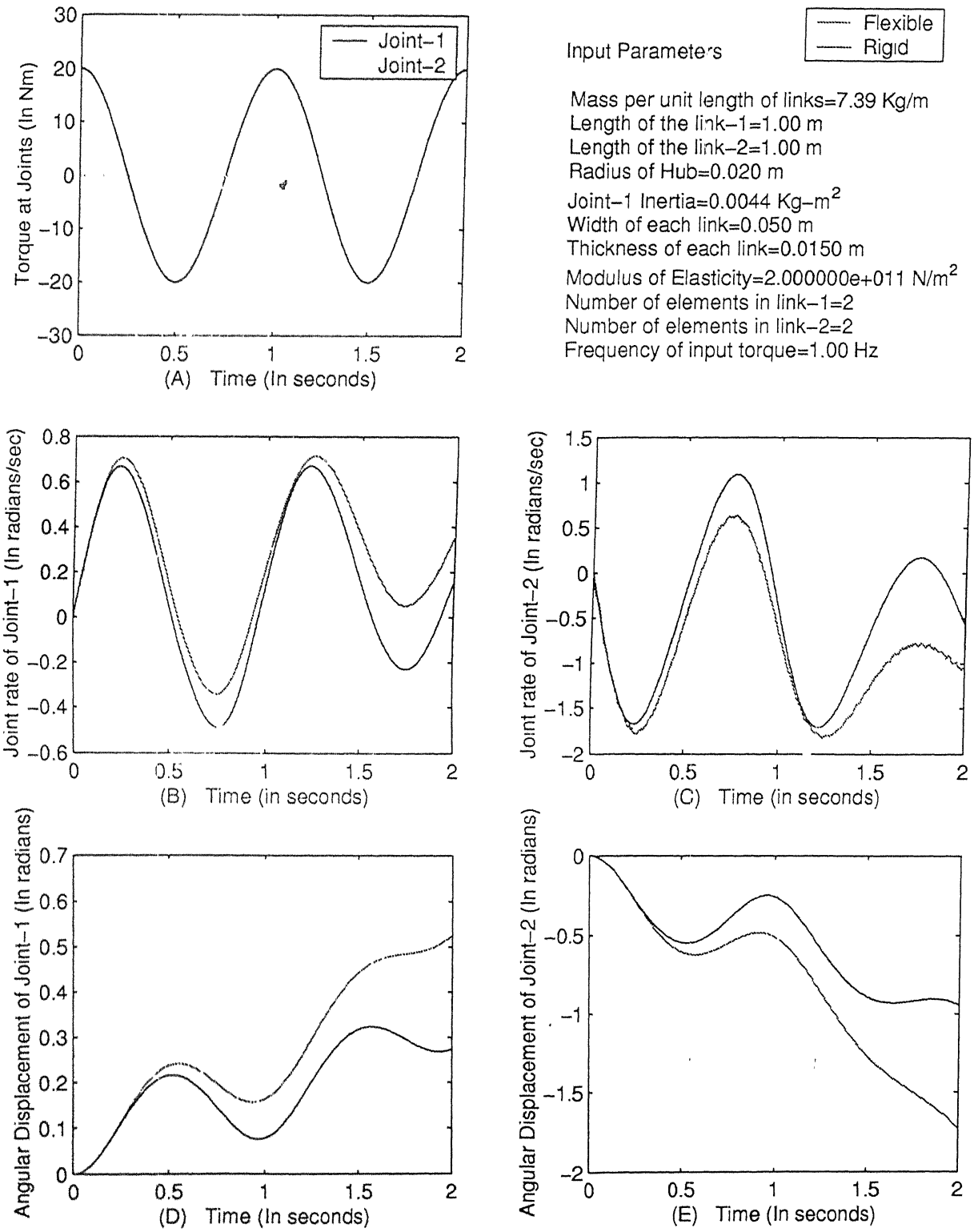

Figure 4.10: Time response under a cosine wave input torque of frequency=1.0 Hz

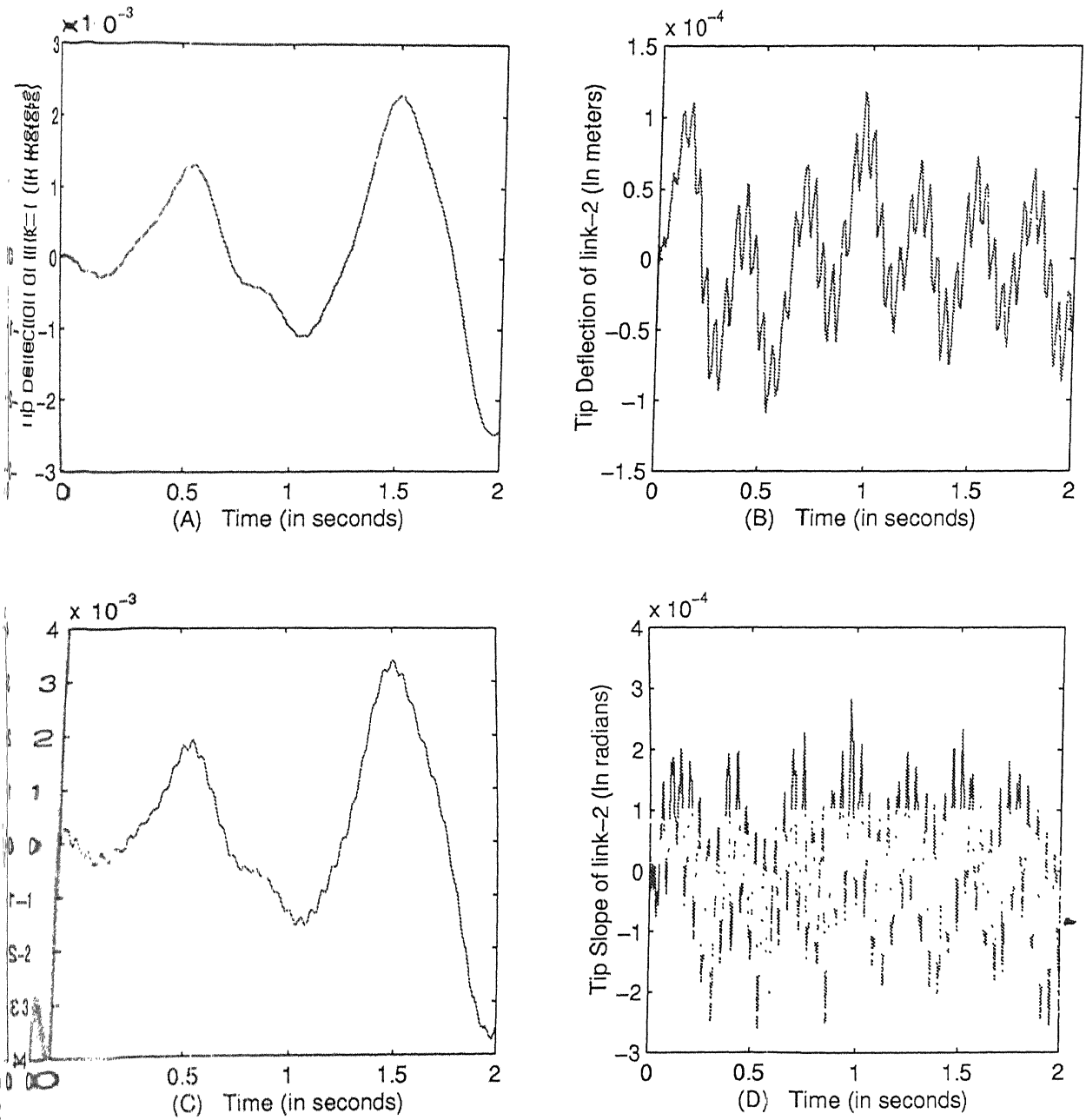

Figure 4.11: Tip deflection and slope variation under a cosine wave input torque of frequency 1.0 Hz

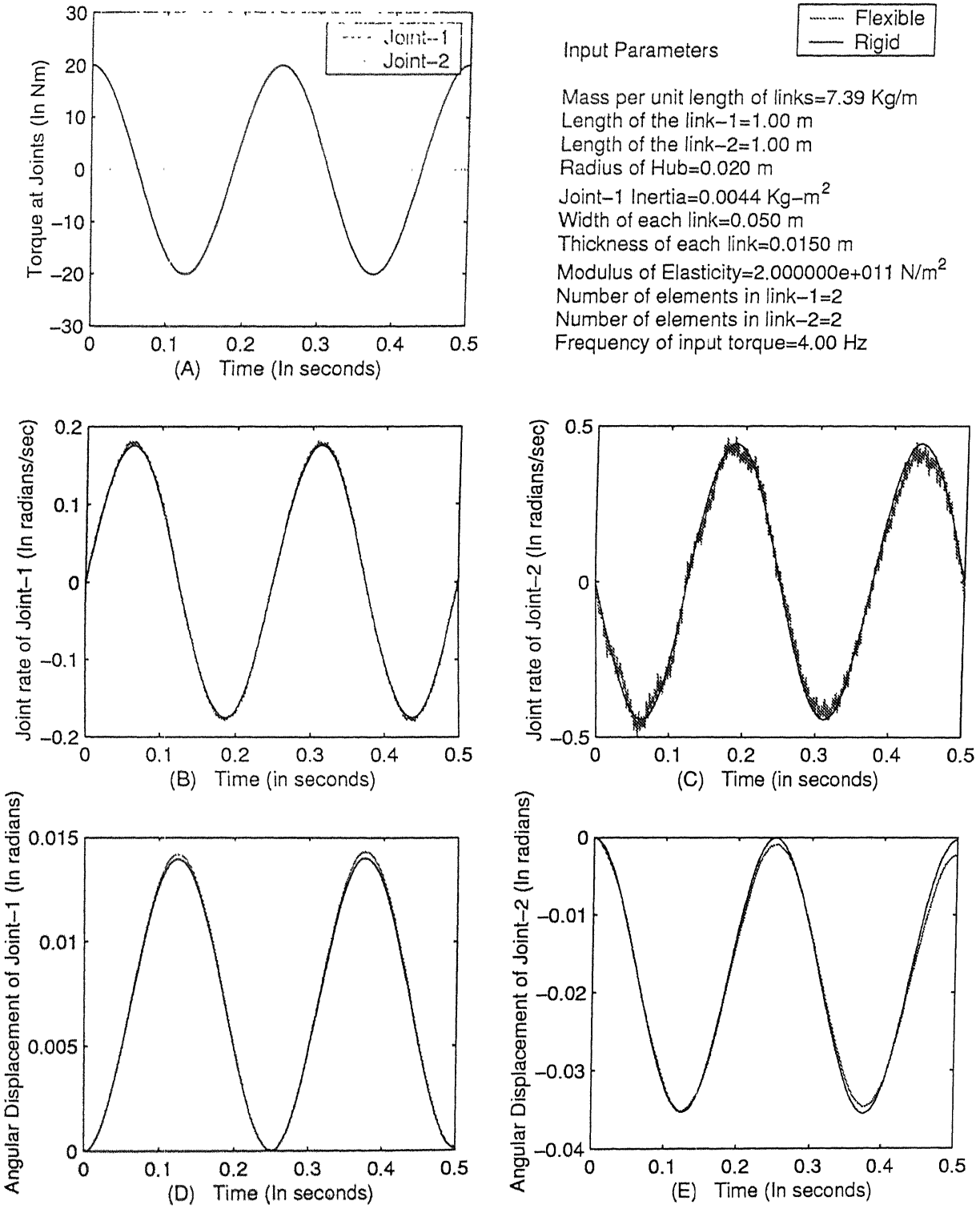

Figure 4.12: Time response under a cosine wave input torque of frequency=4.0 Hz

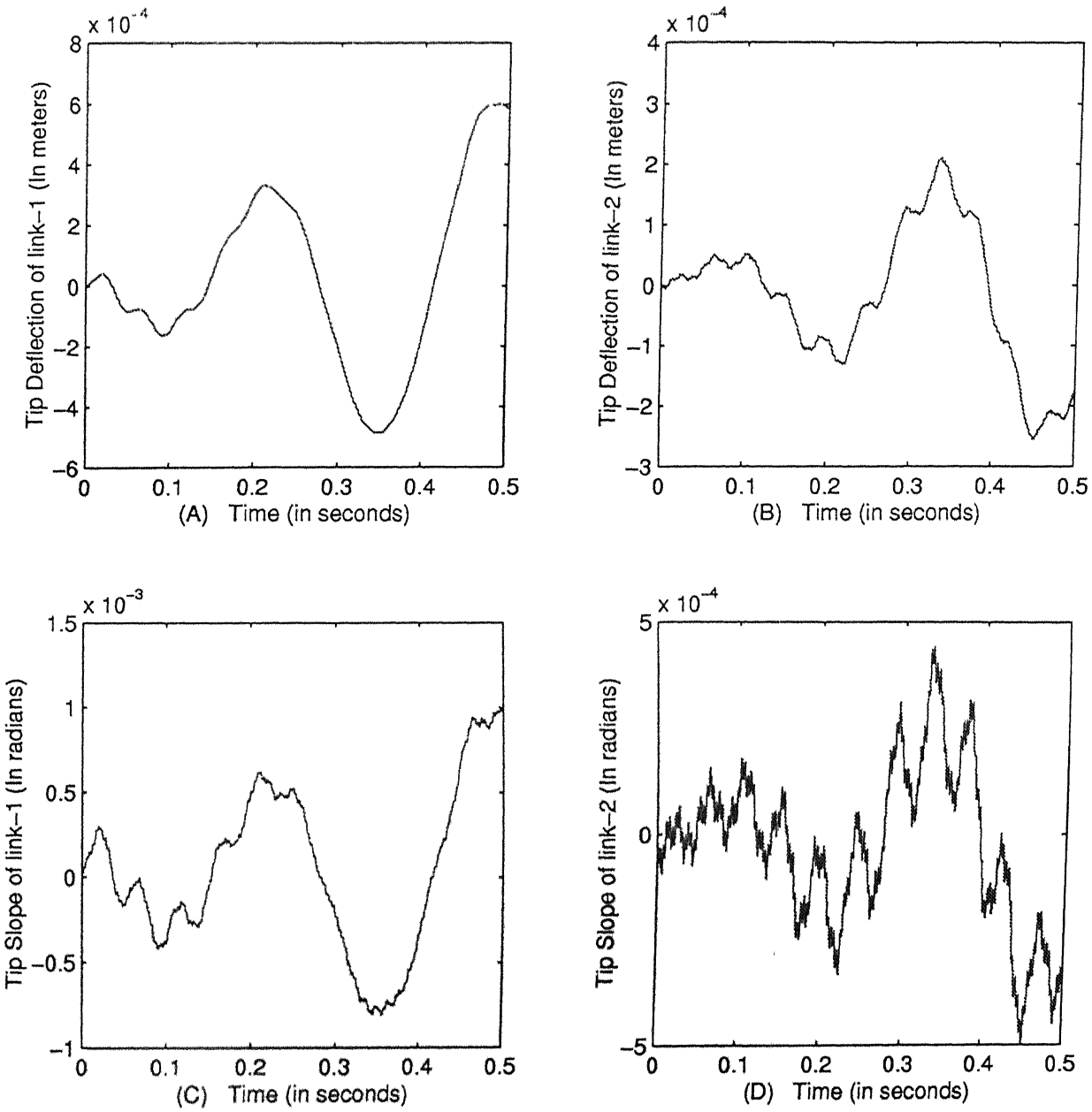

Figure 4.13: Tip deflection and slope variation under a cosine wave input torque of frequency=4.0 Hz

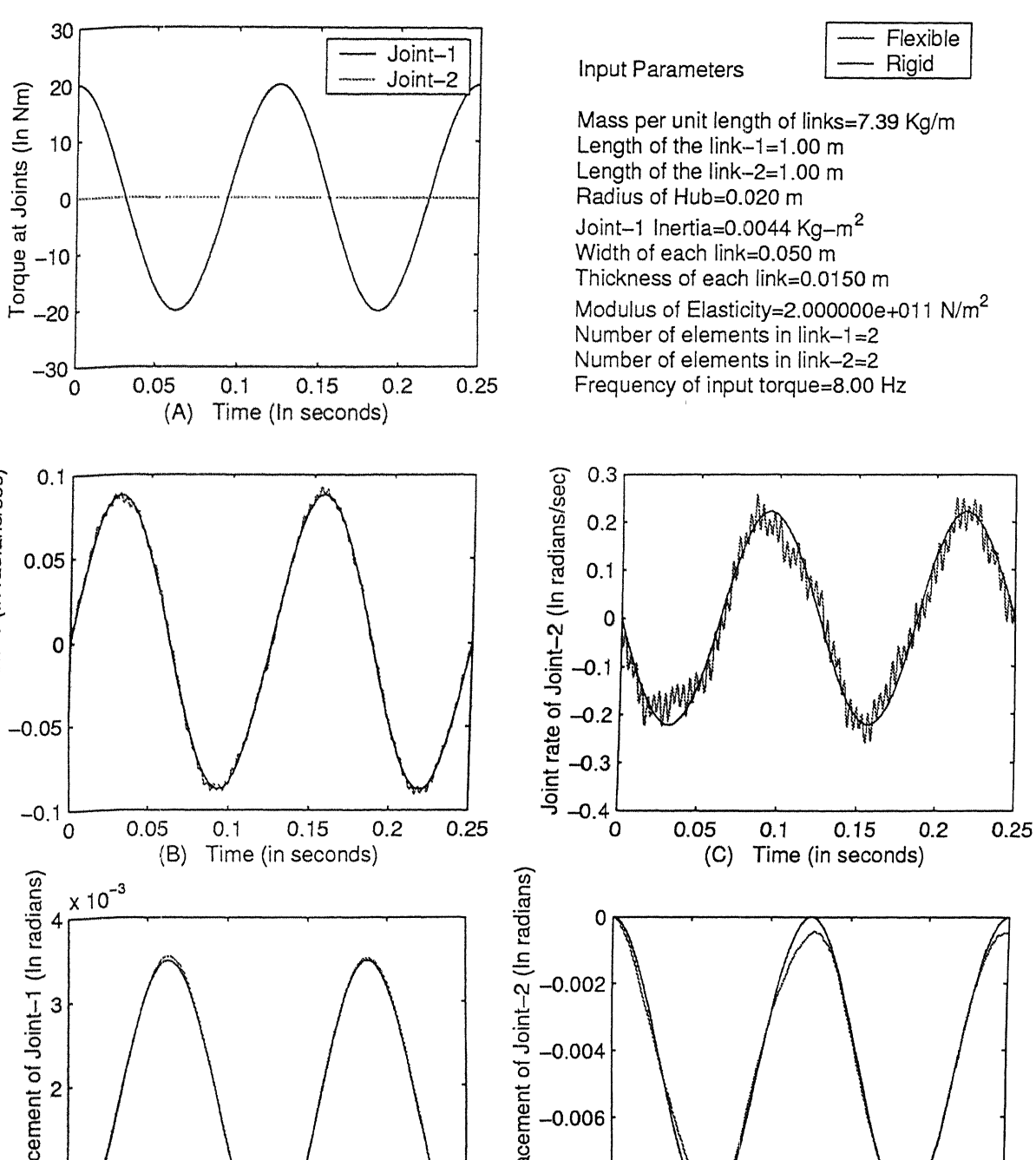

Figure 4.14: Time response under a cosine wave input torque of frequency=8.0 Hz

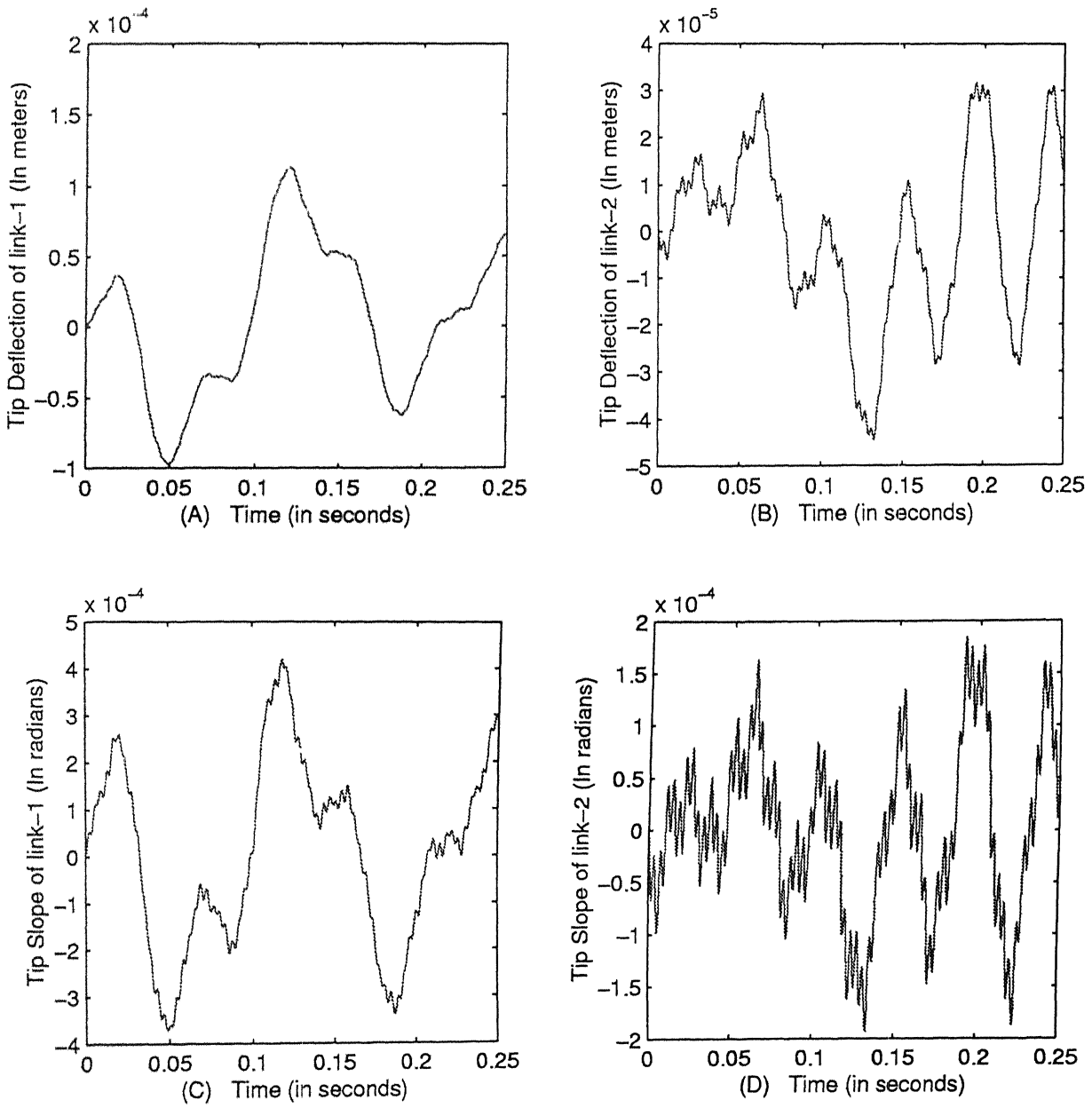

Figure 4.15: Tip deflection and slope variation under a cosine wave input torque of frequency=8.0 Hz

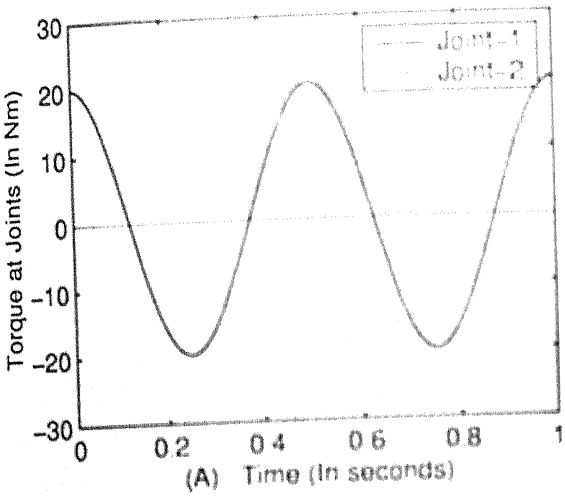

Flexible
Rigid

Input Parameters

Mass per unit length of links=2.02 Kg/m
Length of the link–1=1.00 m
Length of the link–2=1.00 m
Radius of Hub=0.020 m
Joint–1 Inertia=0.0044 Kg–m^2
Width of each link=0.050 m
Thickness of each link=0.0150 m
Modulus of Elasticity=7.000000e+010 N/m^2
Number of elements in link–1=2
Number of elements in link–2=2
Frequency of input torque=2.00 Hz

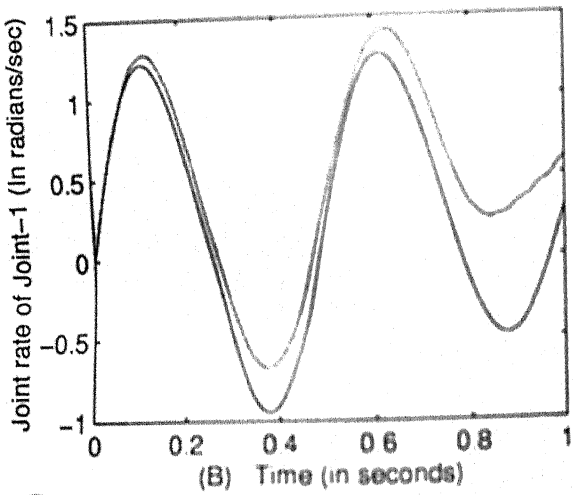

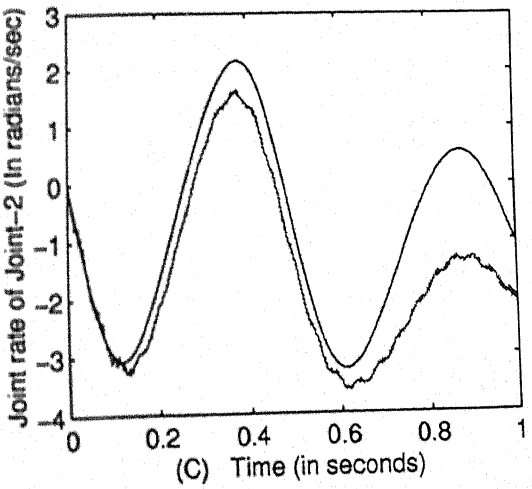

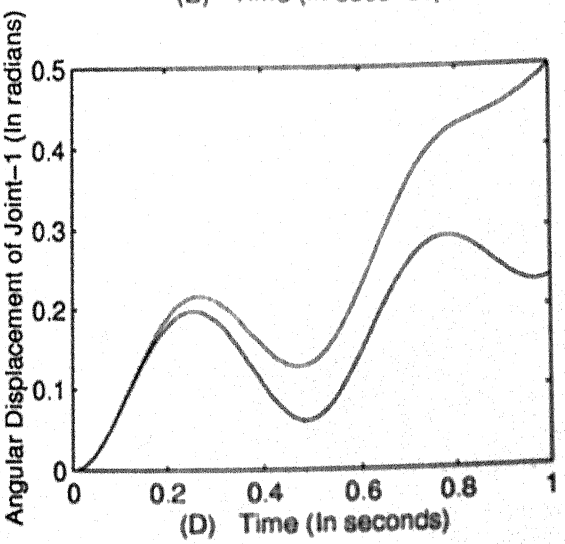

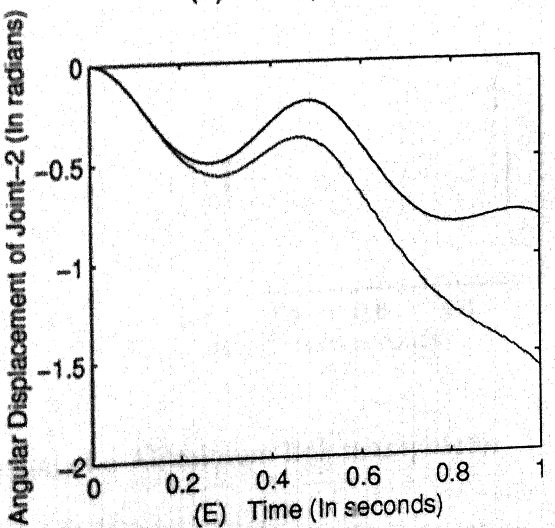

Figure 4.16: Time response of a Aluminium link manipulator

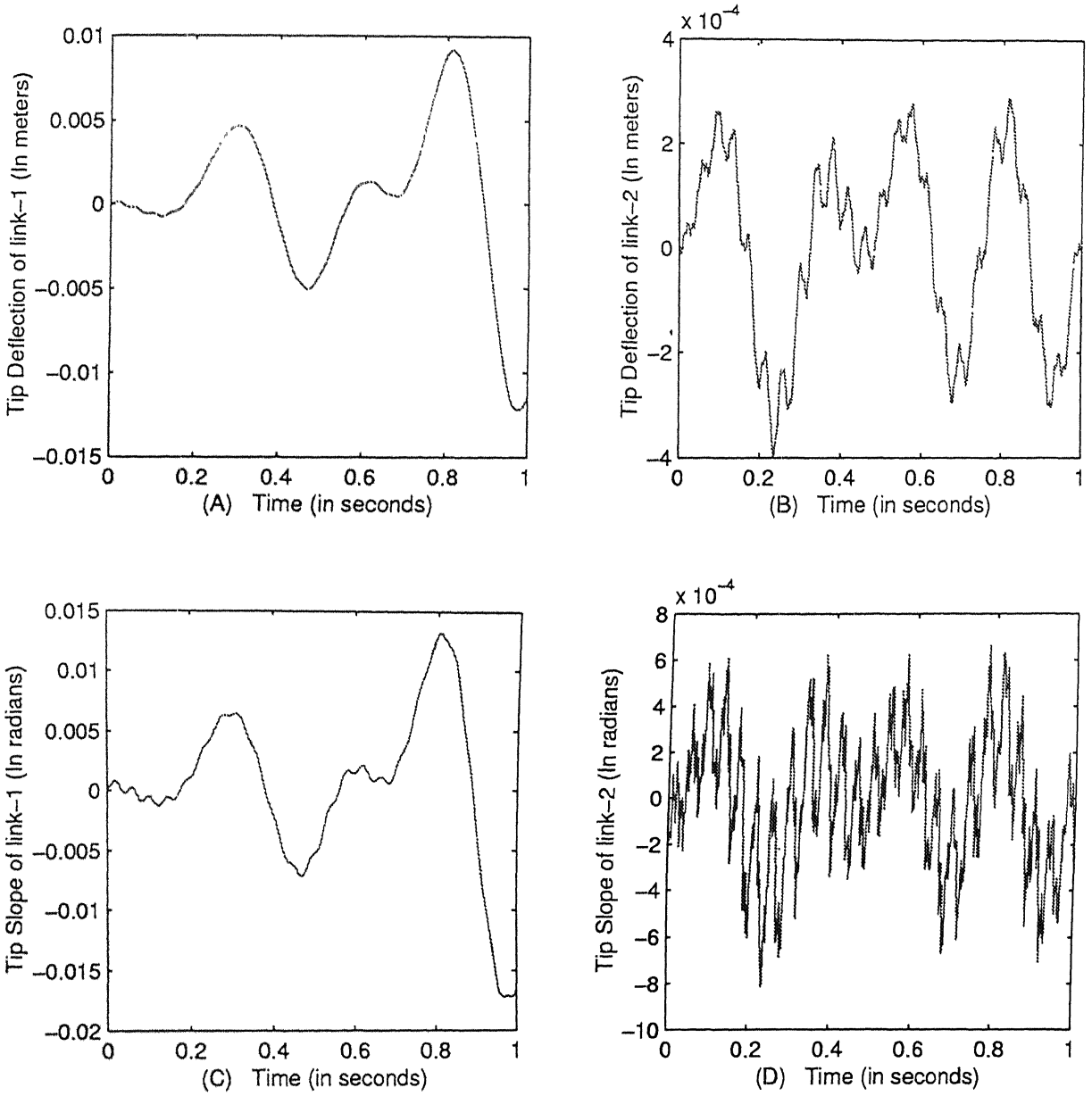

Figure 4.17: Tip deflection and slope variation of a Aluminium link manipulator

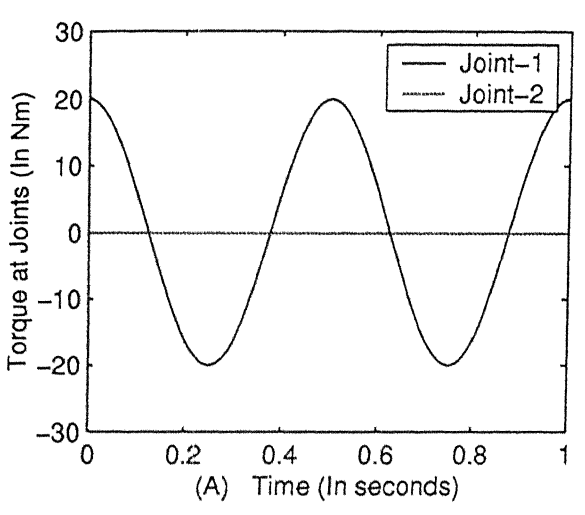

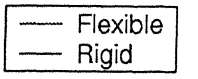

Input Parameters

Mass per unit length of links=1.73 Kg/m
Length of the link–1=1.00 m
Length of the link–2=1.00 m
Radius of Hub=0.020 m
Joint–1 Inertia=0.0044 Kg–m^2
Width of each link=0.050 m
Thickness of each link=0.0150 m
Modulus of Elasticity=3.000000e+011 N/m^2
Number of elements in link–1=2
Number of elements in link–2=2
Frequency of input torque=2.00 Hz

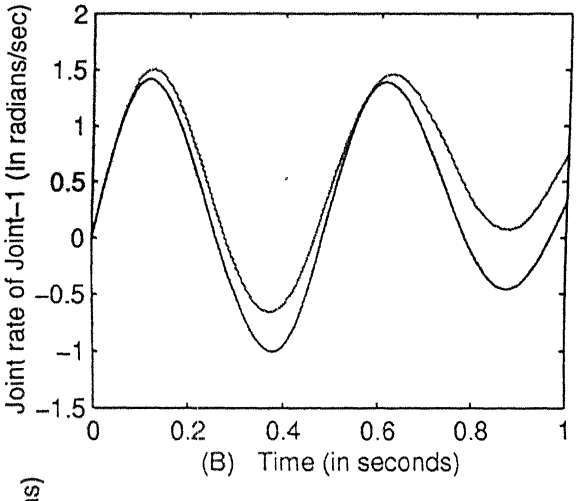

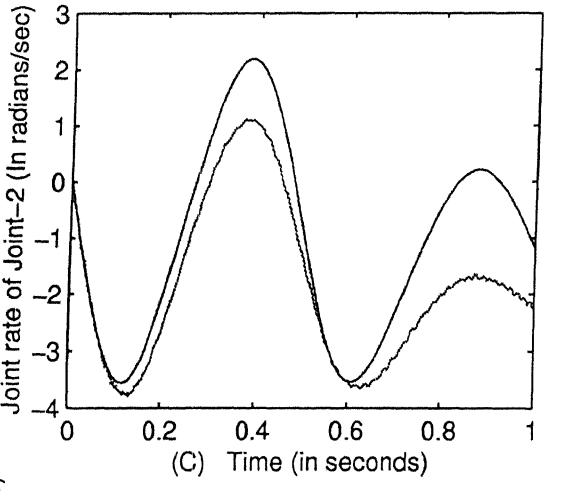

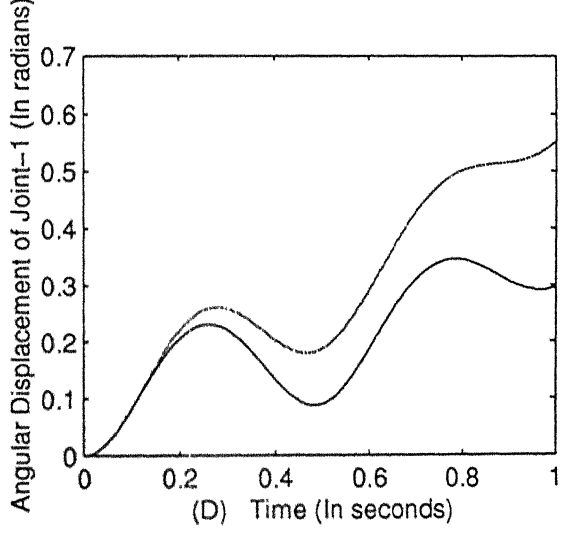

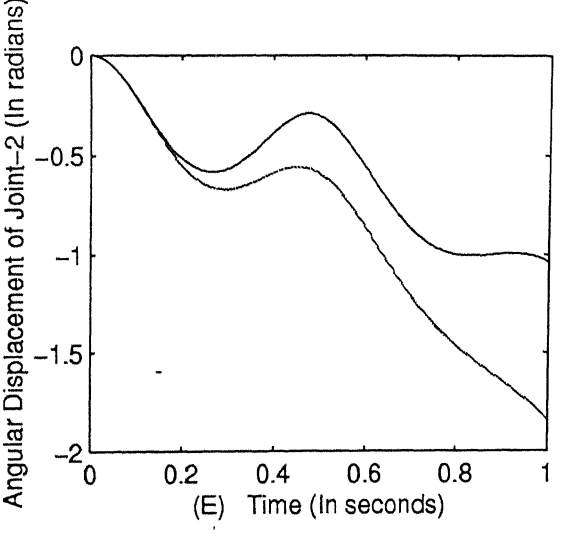

Figure 4.18: Time response of a CFRP link manipulator

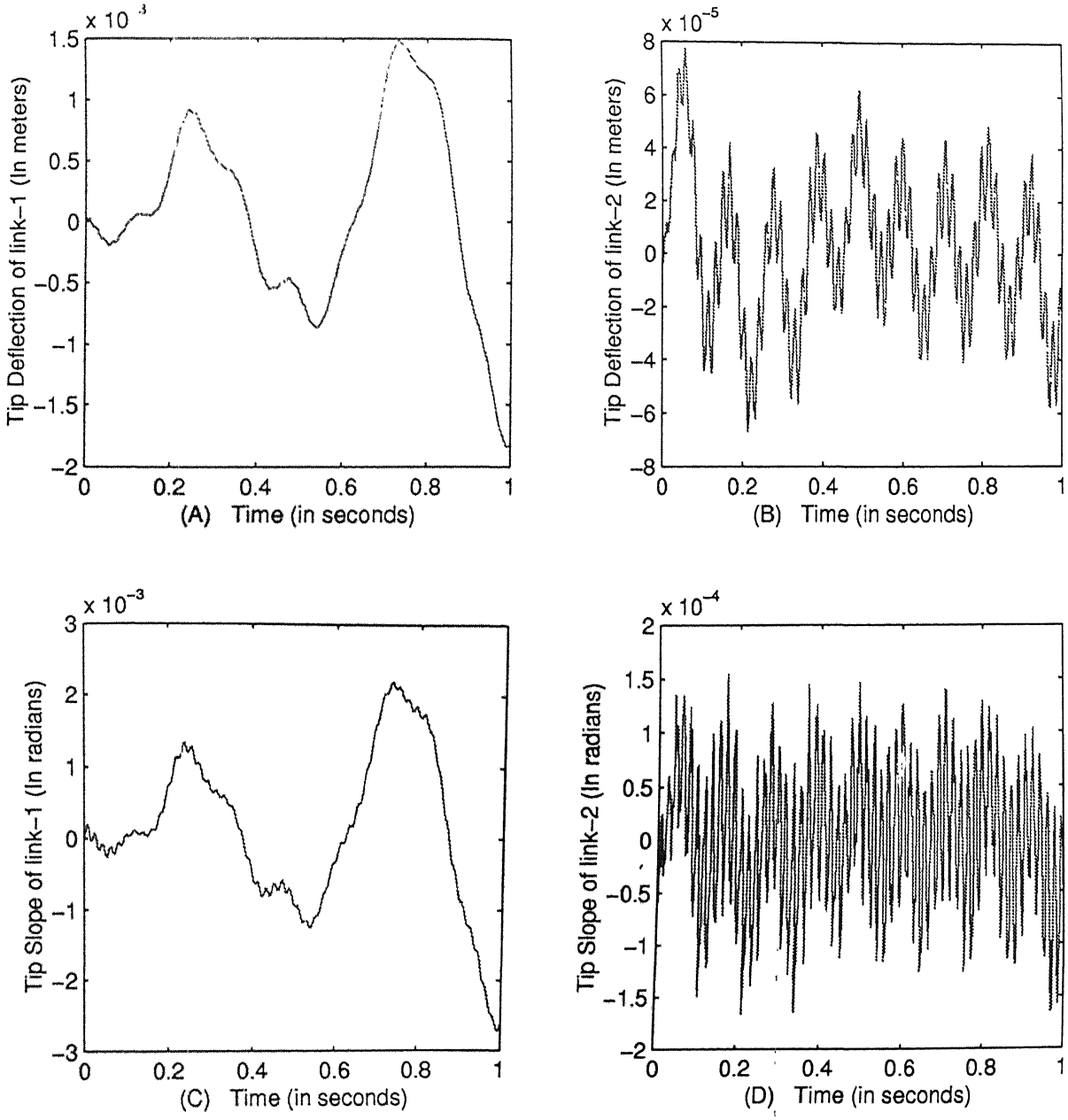

Figure 4.19: Tip deflection and slope variation of a CFRP link manipulator

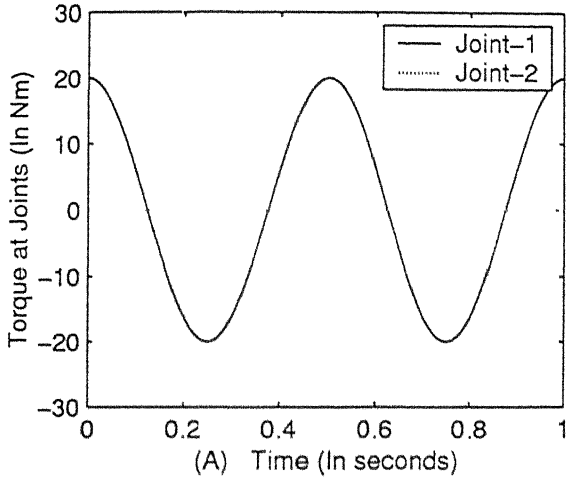

Flexible
Rigid

Input Parameters

Mass per unit length of links=7.39 Kg/m
Length of the link–1=1.50 m
Length of the link–2=1.50 m
Radius of Hub=0.020 m
Joint–1 Inertia=0.0044 Kg–m^2
Width of each link=0.050 m
Thickness of each link=0.0150 m
Modulus of Elasticity=2.000000e+011 N/m^2
Number of elements in link–1=2
Number of elements in link–2=2
Frequency of input torque=2.00 Hz

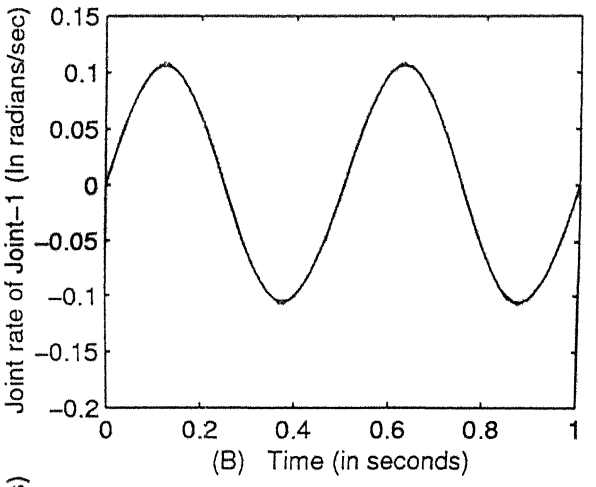

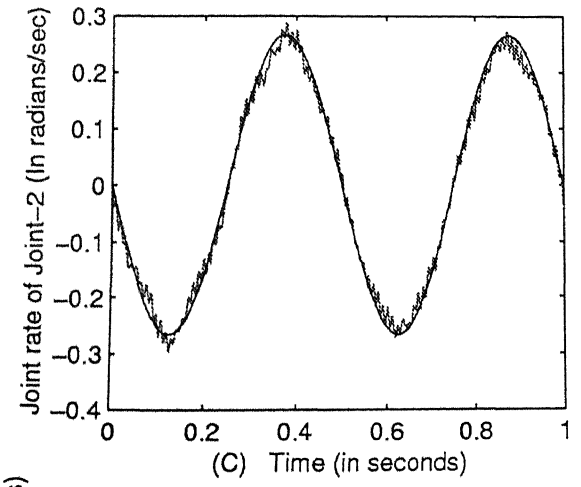

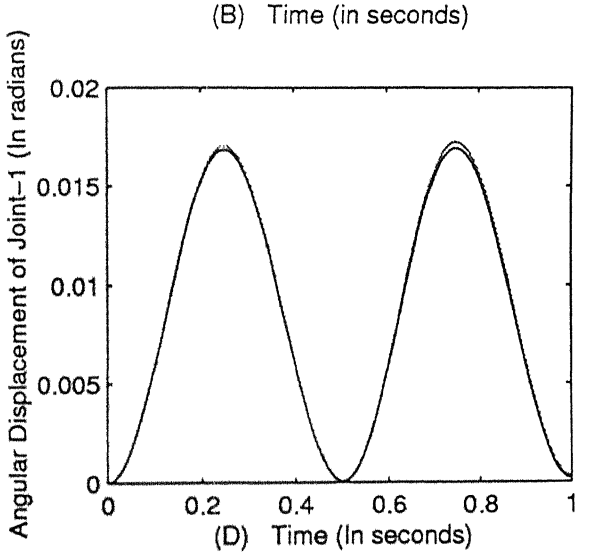

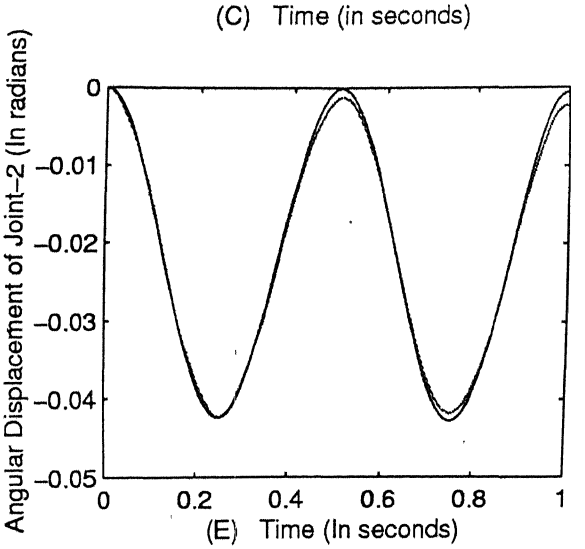

Figure 4.20: Time response of manipulator having link lengths=1.5 meters

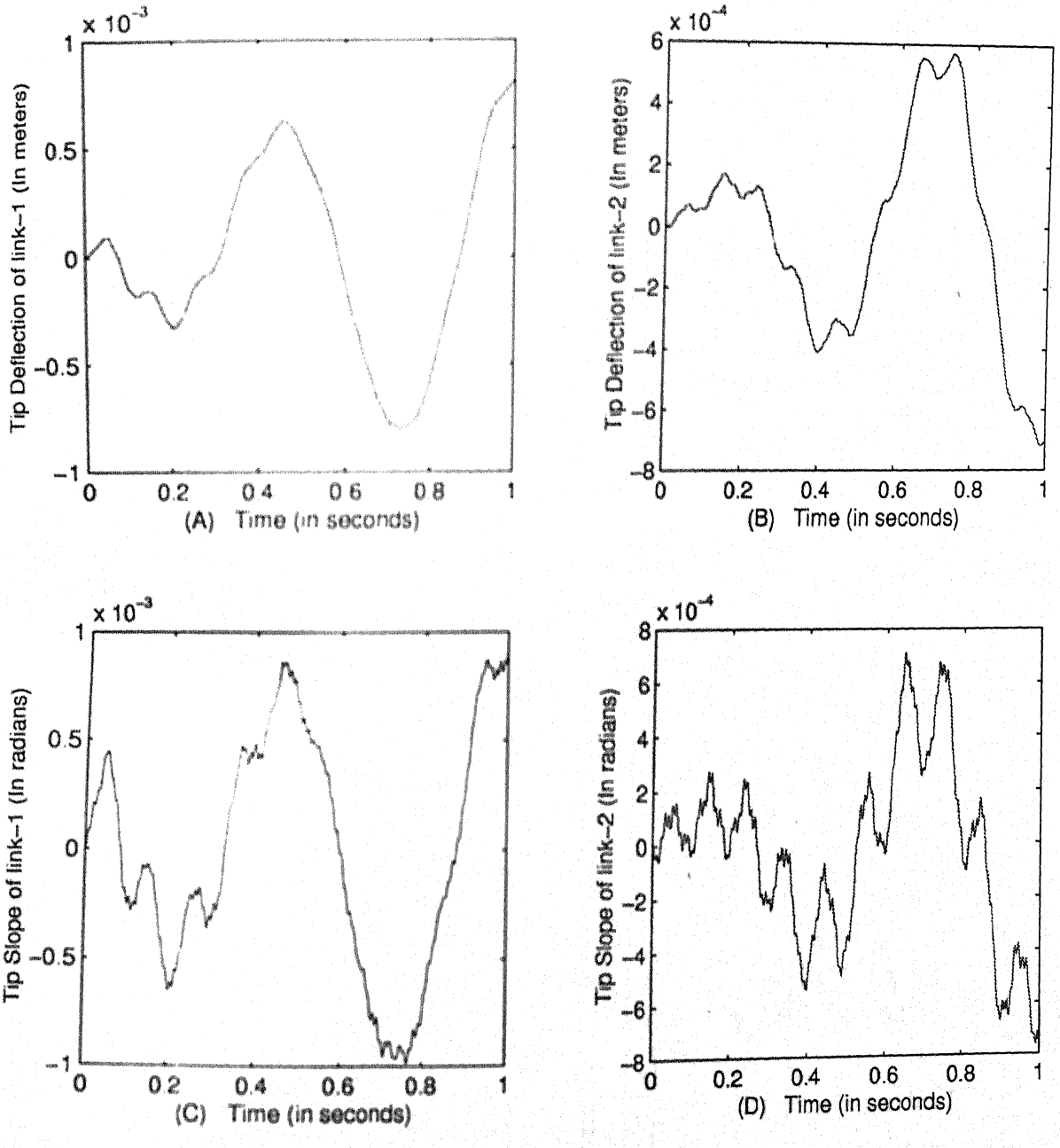

Figure 4.21: Tip deflection and slope variation of manipulator having link lengths=1.5 meters

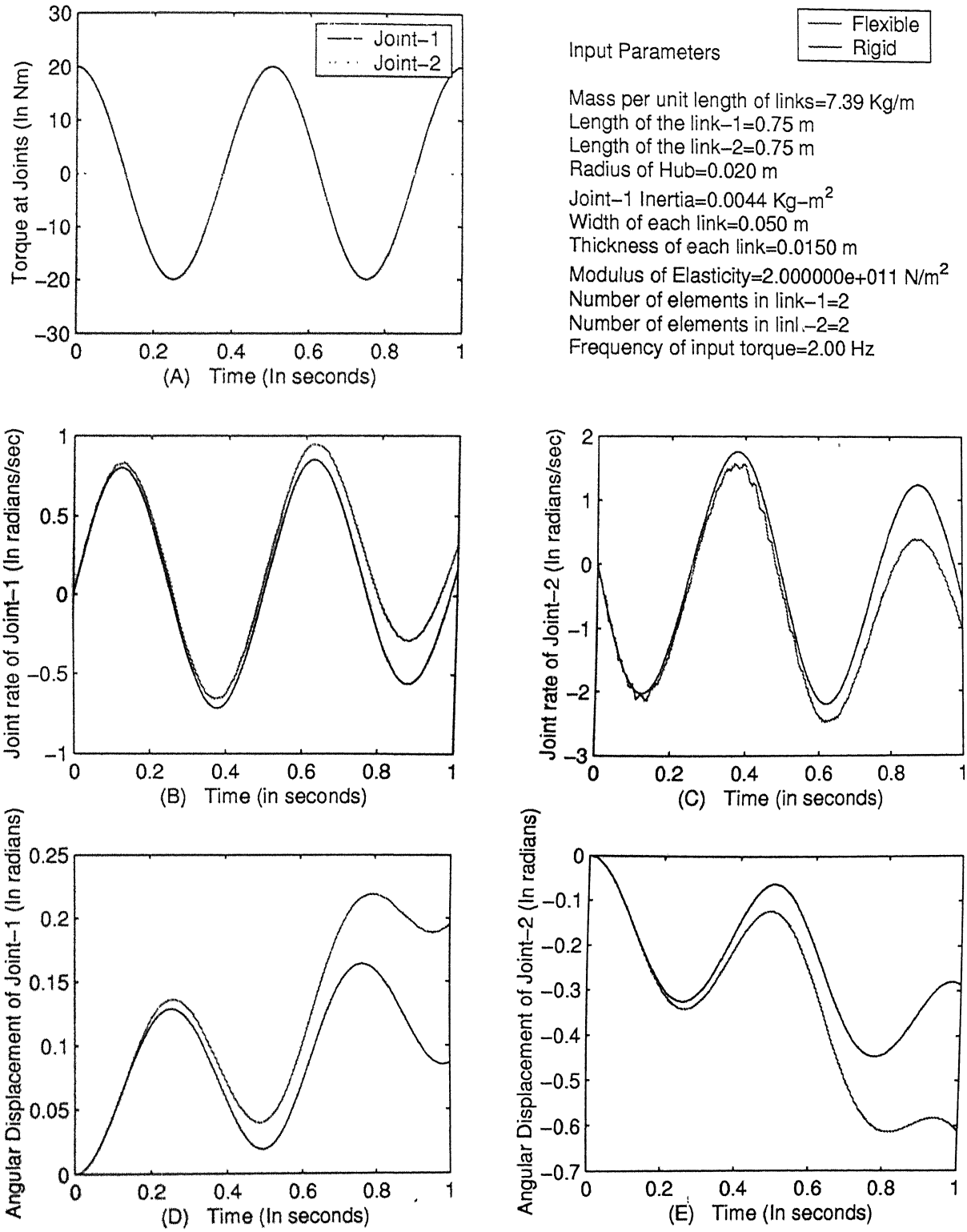

Figure 4.22: Time response of manipulator having link lengths=0.75 meters

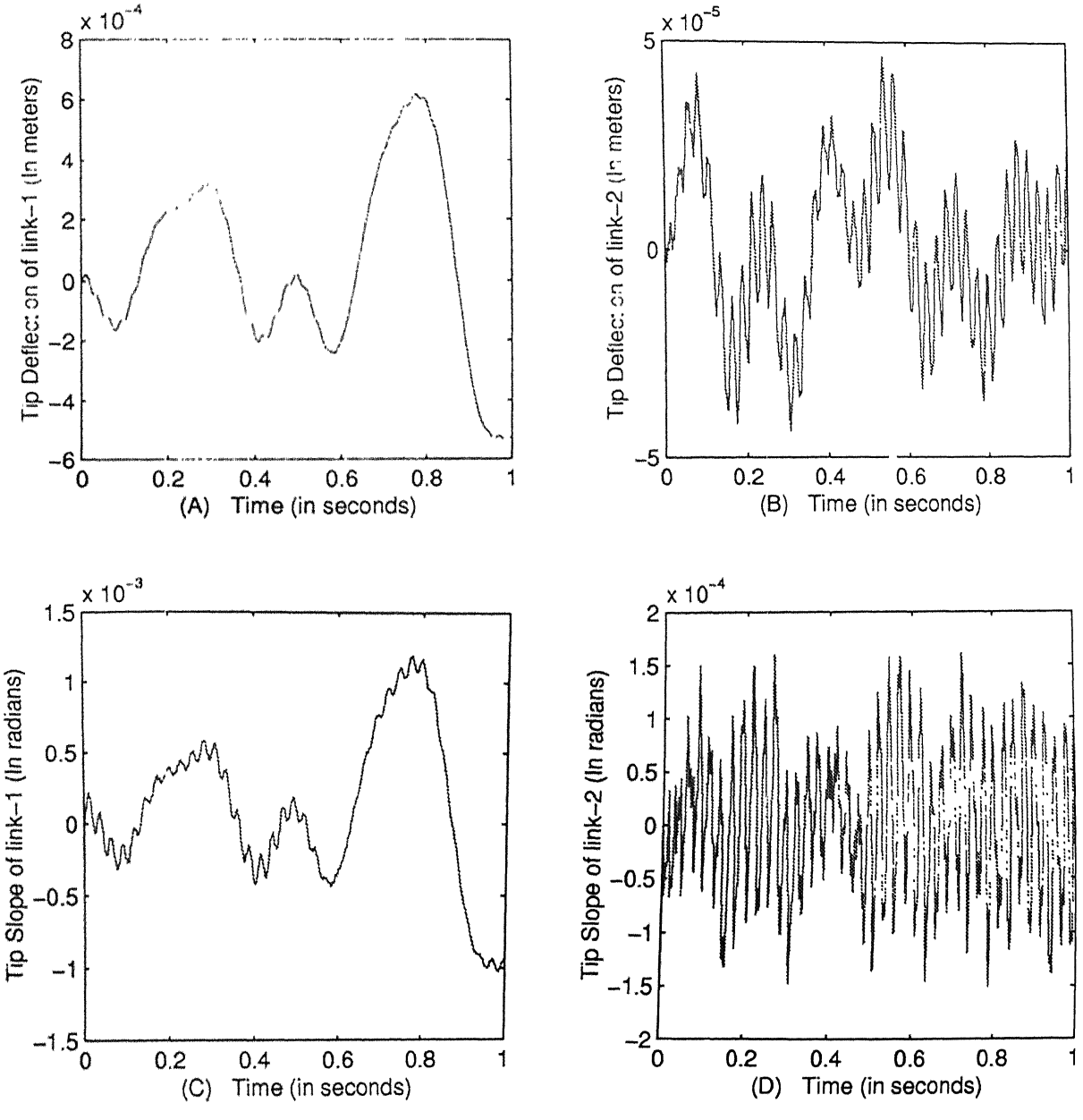

Figure 4.23: Tip deflection and slope variation of manipulator having link lengths=0.75 meters

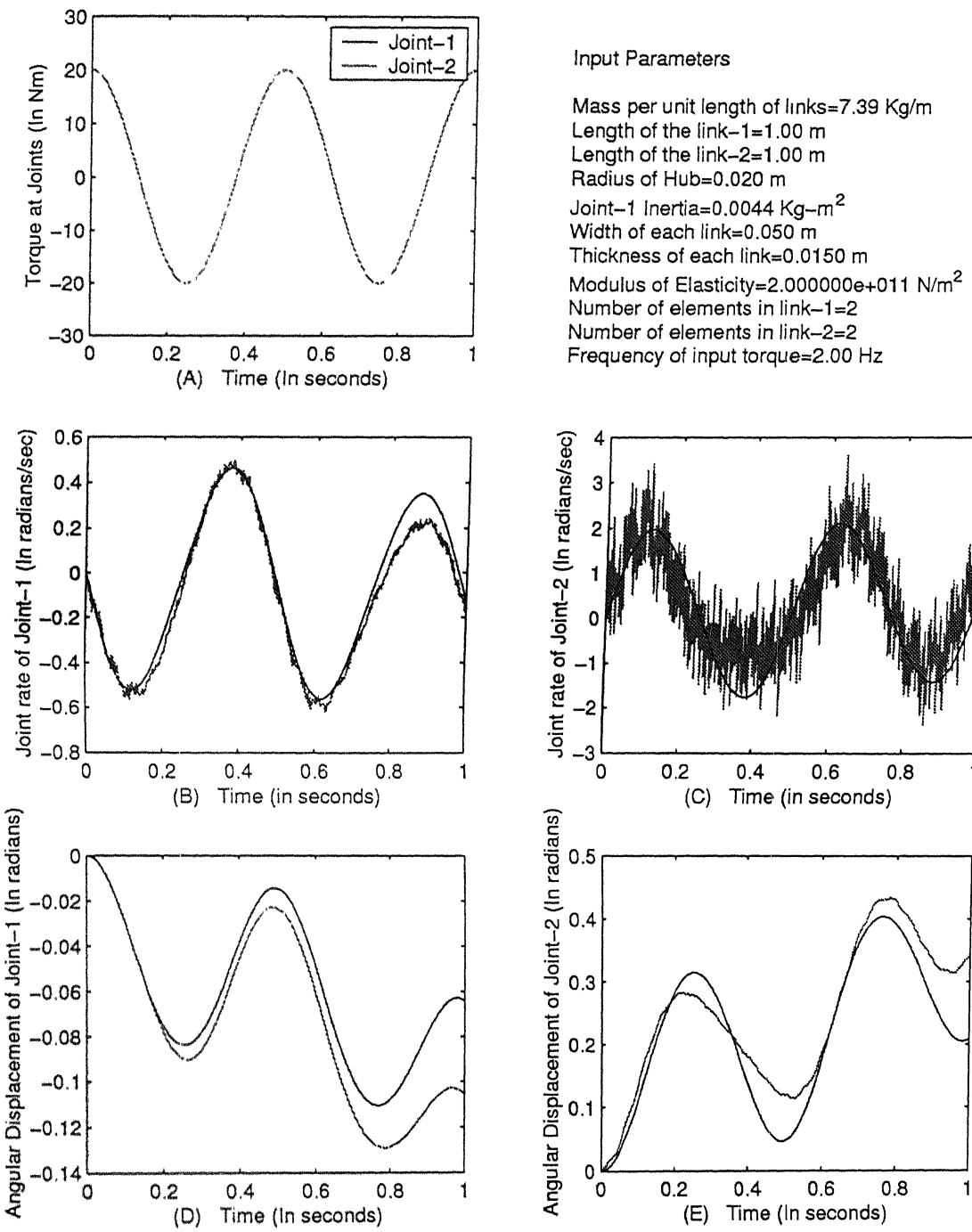

Figure 4.24: Time response of manipulator under action of equal torques at both joints

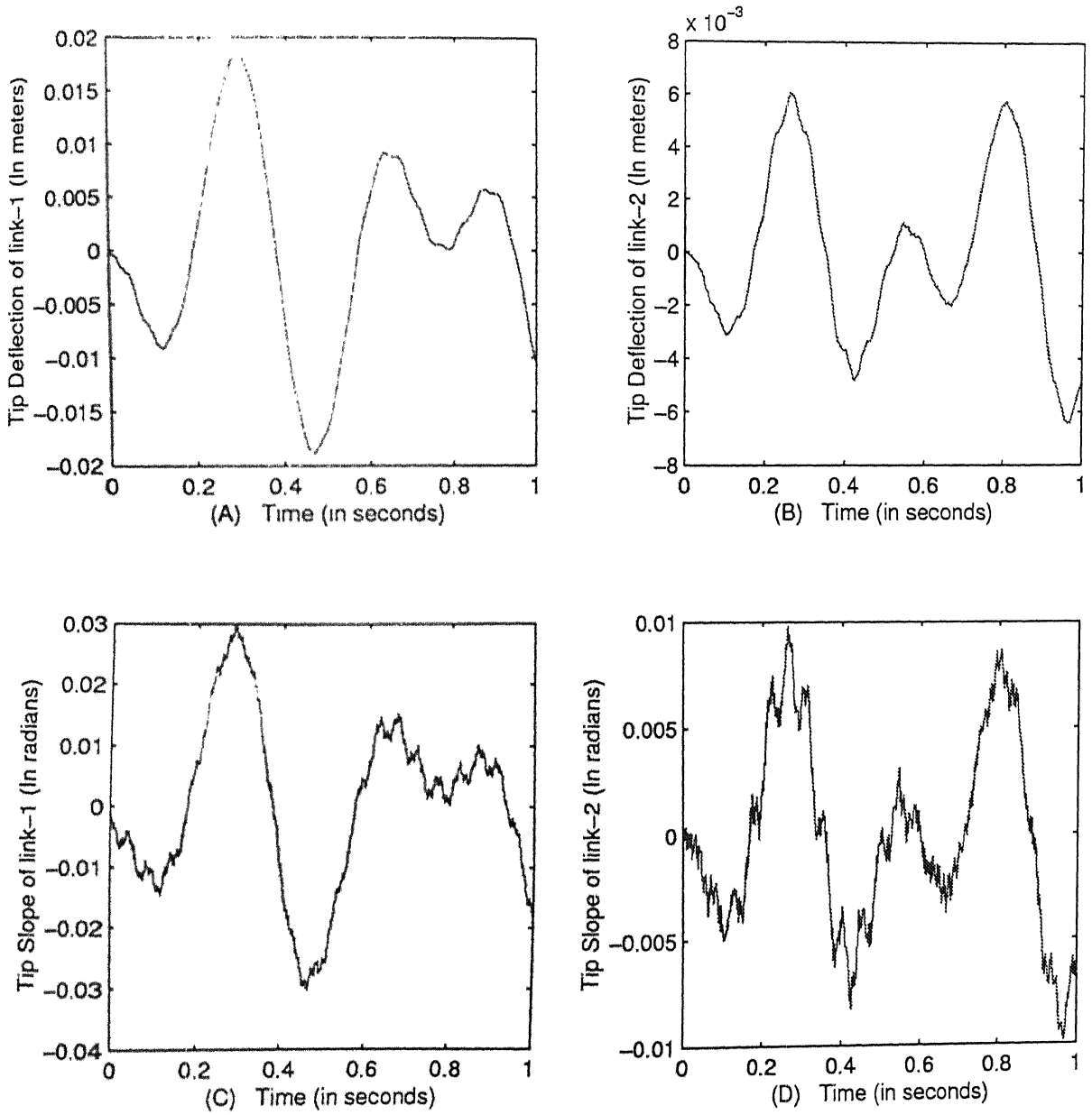

Figure 4.25: Tip deflection and slope variation of manipulator under action of equal torques at both joints

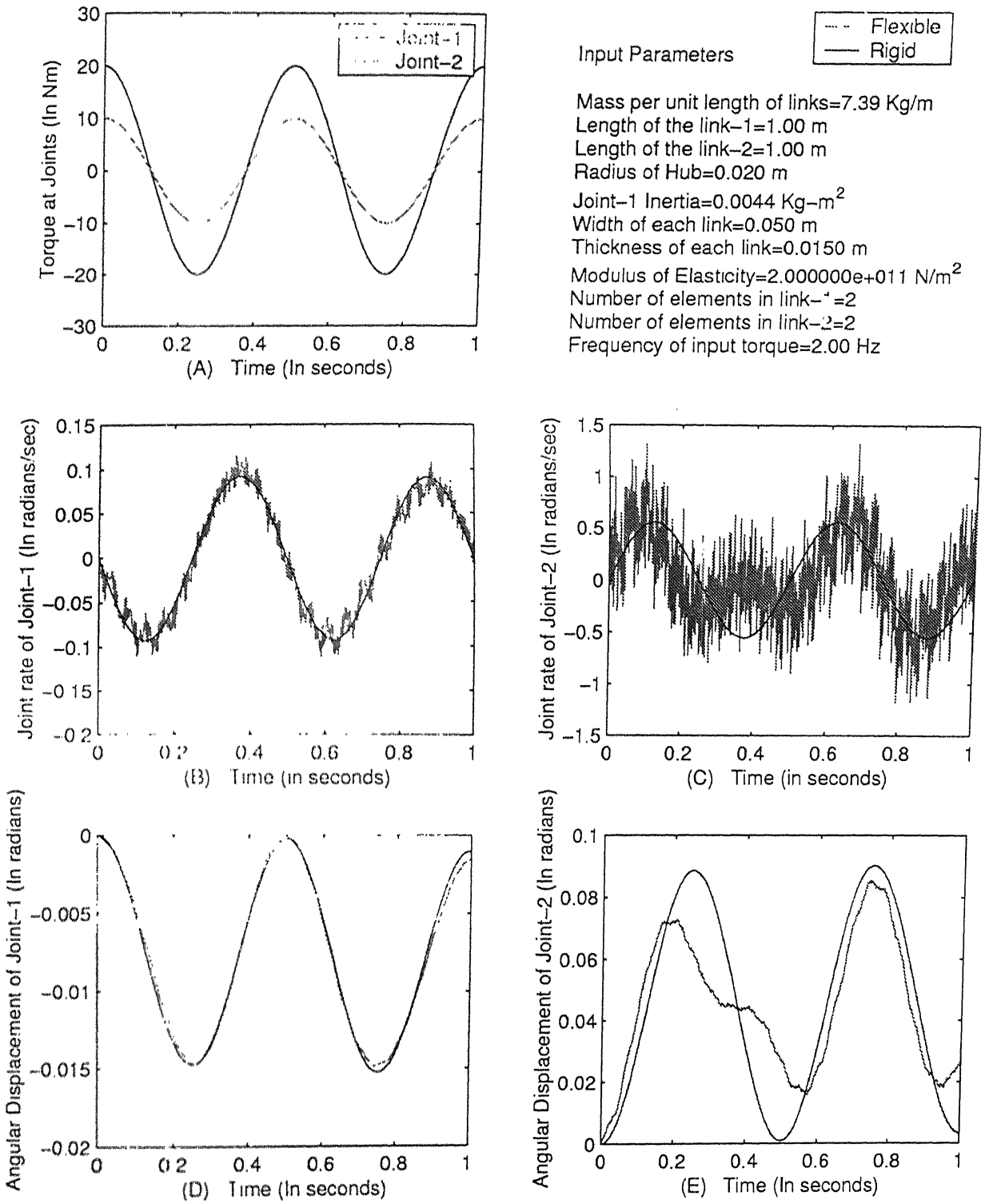

Figure 4.26: Time response of manipulator under action of unequal torques at both joints

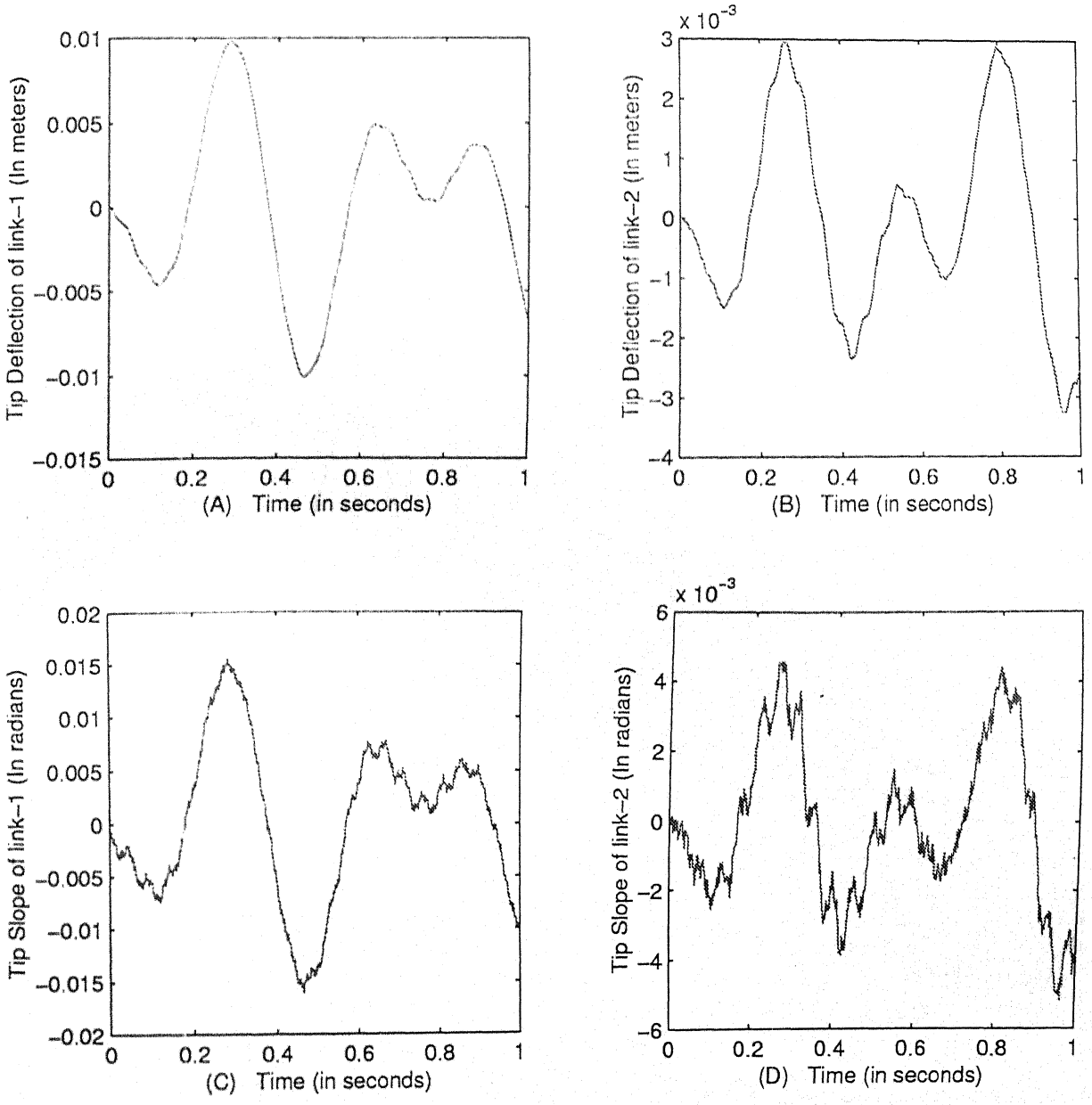

Figure 4.27: Tip deflection and slope variation of manipulator under action of unequal torques at both joints

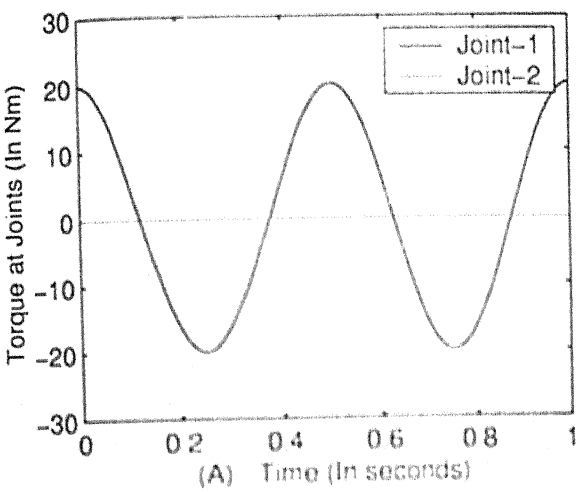

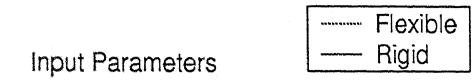

Input Parameters

Mass per unit length of links=7.39 Kg/m
Length of the link–1=1.00 m
Length of the link–2=1.00 m
Radius of Hub=0.020 m
Joint–1 Inertia=0.0044 Kg–m^2
Width of each link=0.050 m
Thickness of each link=0.0150 m
Modulus of Elasticity=2.000000e+011 N/m^2
Number of elements in link–1=2
Number of elements in link–2=2
Frequency of input torque=2.00 Hz

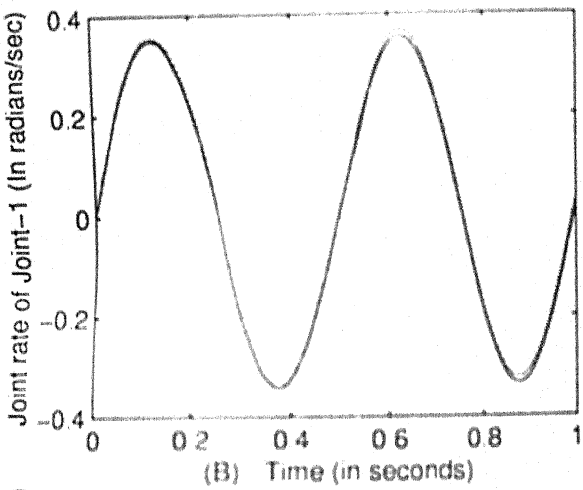

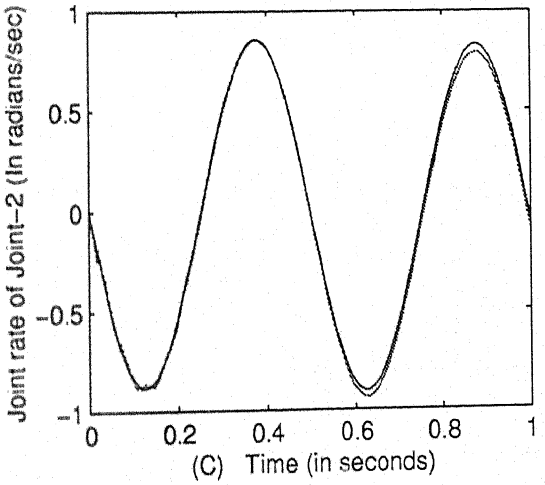

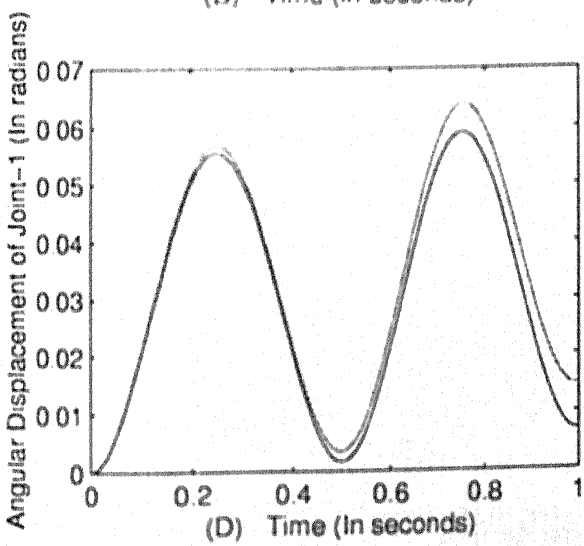

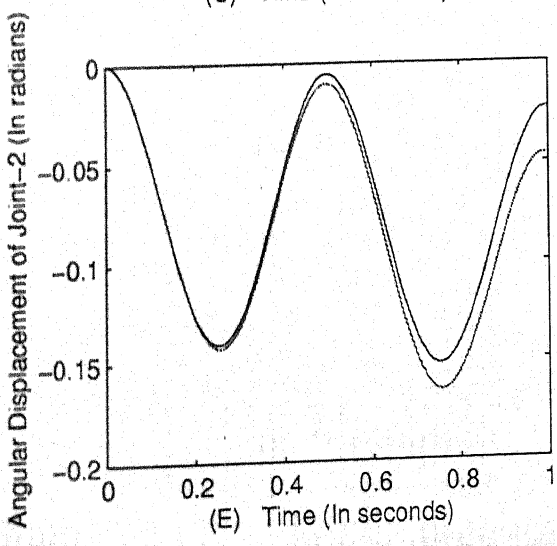

Figure 4.28: Time response of manipulator with proportional damping

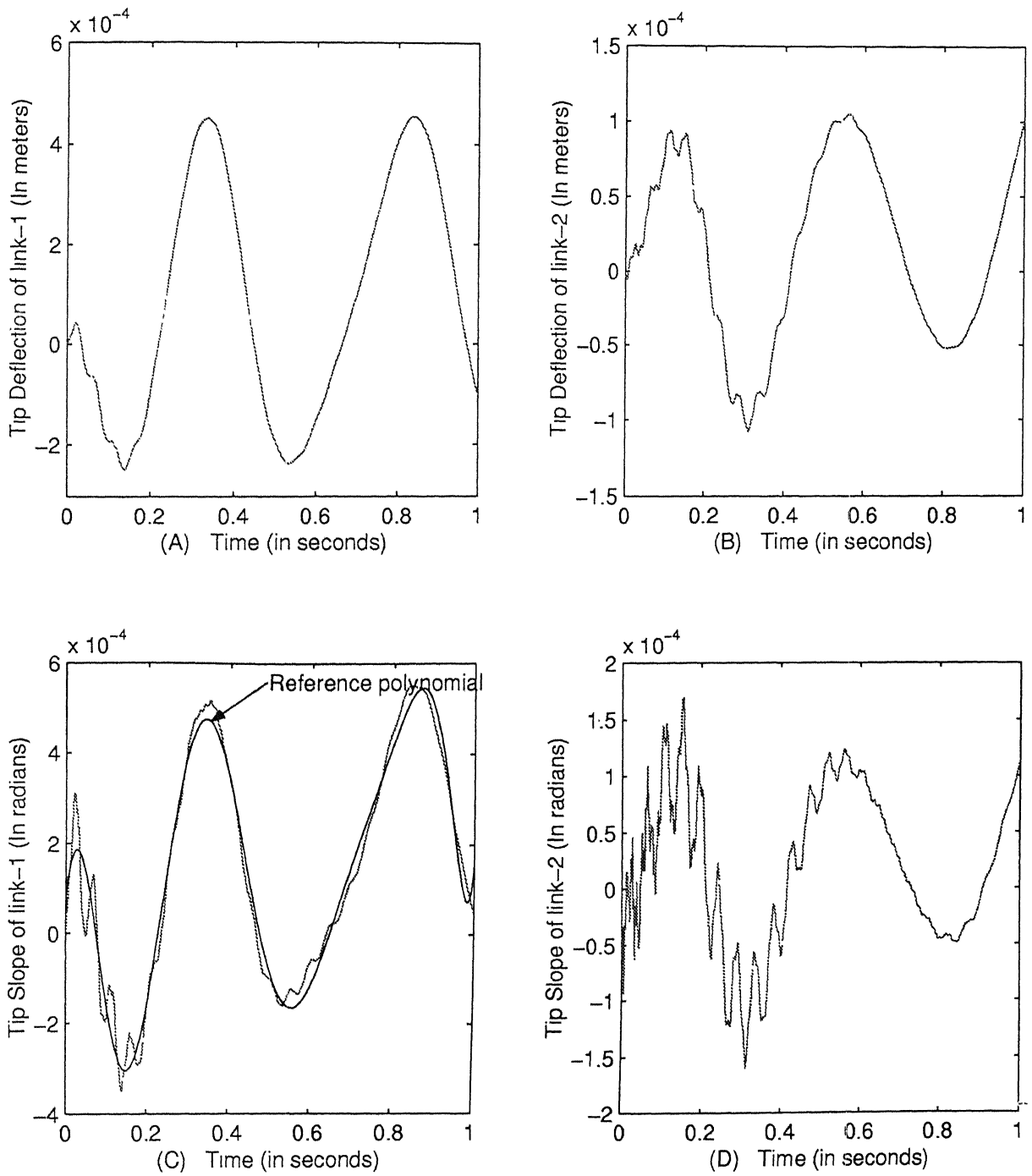

Figure 4.29: Tip deflection and slope variation of manipulator with proportional damping

Chapter 5

Closure

5.1 Summary

This thesis addresses the problem of modelling and control of flexible manipulators. The methods and concepts used in this thesis are of general applicability for all flexible manipulators.

In chapter 1, flexible manipulators are introduced and their need and potential advantages over rigid manipulators are highlighted. Problems associated with modelling and control of flexible manipulators are discussed. In the section of literature survey, available literature addressing these problems are critically examined. Based on this study our thesis problem is defined and main contributions are presented.

In chapter 2, a Generalized Lagrangian approach is used for deriving the dynamic equations of motion for rigid and flexible manipulators. For flexible manipulator, finite element method is used to discretize the continuous system. Proportional damping is modelled in the system. A combined active and passive damping is also proposed and discussed.

In chapter 3, single-link flexible and rigid manipulators are modelled and equations of motion are derived in matrix form. Simulation results with a number of different input parameters are discussed in detail.

In chapter 4, modelling is carried out for two-link flexible and rigid manipulators and their equations of motion are derived in matrix form. Manipulator dynamics is numerically simulated and results with proportional damping are examined.

5.2 Conclusion

For a single-link manipulator the effect of flexibility is visible in the form of oscillations in the variation of angular displacement. These ocsilltions are observed to have the frequency equal to the first natural frequency of link. The study of flexural transverse deflection and slope at the tip of link suggests that tip deflection and slope variations show two modes

of oscillations. A relatively fast mode with frequency equal to the first natural frequency of link is superimposed on a relatively slower oscillatory mode having frequency equal to excitation torque frequency. Other important observations are as follows:

- As shown by results given in Table 3.3, the error ratio in the joint angular displacement at corresponding points increases (error ratio=0.050 at frequency=1 Hz to error ratio=0.98 at frequency=8 Hz) with the frequency of input torque, which suggests that angular displacement variation is severely affected by oscillations at higher frequencies. Tip transverse deflection amplitude remains constant (=1.1) for all considered cases with ferquency varying from 1 Hz to 8 Hz.

- A comparision in the performance of manipulator links made up of Steel, Aluminium and Carbon Fibre Reinforced Plastic (CFRP) laminates is made in Table 3.4 and variation of performance with material properties is shown in Figure 3.11. It is concluded that for the CFRP, which has maximum specific modulus of elasticity (E/ρ = 130.43x10$^6 Nm/kg$), error ratio in angular displacement is least (=0.050), while error ratio increases to 0.167 at E/ρ = 20.31x10$^6 Nm/kg$ for Steel link. Thus CFRP manipulator gives the smoothest variation in angular displacement. Comparision of tip deflection amplitude suggests that it is dependent on the material modulus of elasticity only and is not affected by density of link material. Therefore amplitude of tip deflection is maximum (=3.20) for Aluminium ($E = 70GPa$) while in case of CFRP ($E = 300GPa$) it is least (=0.8). Hence we conclude that specific modulus of elasticity (E/ρ) is a good performance index of flexible maniplator link material.

- Results with different slenderness ratio (keeping the link thickness constant) are presented in Table 3.5. Manipulator having higher link length (=2.0 m) is severely affected by flexibility with error ratio in angular displacement=0.940 and tip deflection amplitude=5.0, while manipulator with shorter link (=0.50 m) performs well with error ratio=0.028 and tip deflection amplitude=0.3.

- Response of a single-link damped manipulator suggests the proportional damping is able to damp-out the undesirable vibrations of a flexible link effectively without affecting the requisite angular displacement. Logarithmaic decrement in the amplitude of tip slope is found to be equal to 0.2231.

In the case of a two-link manipulator, the final equations of motion suggest a highly non-linear dynamics, which is well exhibited in all the simulation results. Similar to single-link manipulator, the flexibility of manipulator links is visible from the oscillations in the variation of angular displacement. Two modes of oscillations are noticed in vibrations of tip deflection and tip slope variation. In results with variation of different parameters like

nature and frequency of input torque, material properties and slenderness ratio of manipulator links, basic similarities were found between single and two-link manipulators, however due to high dependence of two-link manipulator dynamics on the angular displacement at joint 2 (θ_2), the effect of θ_2 is dominant in all the results. A damped model of a two-link manipulator suggests that proportional damping has been able to damp-out the link vibrations effectively. Similar to the single link manipulator the logarithmaic decrement in the amplitude of tip slope of link 1 is found to be equal to 0.3243. However need for a better control strategy is emphasized.

5.3 Suggestions for Future Work

Modelling and control are the two fundamental and critical issues related to the development of flexible manipulators. In this thesis effort is made to tackle some of the problems associated with flexible manipulators. The suggestions for future work are as follows:

1. The work can be extended to the cases with planer manipulators having more than two links on the basis of general scheme given in chapter 2.

2. Similar work for flexible manipultors in 3-D will be of great importance form practical applications point of view.

3. A strategy, to model the manipulators having one or more prismatic joints, can be developed.

4. Inclusion of joint flexibility in the model.

5. Implementation of hybrid damping into the model.

Bibliography

[1] Agarwal D. Bhagwan and Lawerence J. Broutman 1990, "Analysis and performance of fibre composites", *John Wiley and Sons Inc.*.

[2] Al-Badoor D.O. and Almusallam A.A. 1999, "Dynamics of flexible link and flexible joint manipulator carrying a payload with rotary inertia", *Mechanism and Machines Theory*, Vol. 35, pp.785-820.

[3] Balas M.J.1982, "Trends in large space structure control theory: Fondest hopes, wildest dreams"' *IEEE Transactions on Automatic control*, Vol. 27(3), pp.522-535

[4] Bhattacharya B. 1997, "Studies on dynamics and control of smart lamonated composite beams and plates", *Ph.D. Thesis, Department of Mechanical Engineering, Indian Institute of Science, Bangalore*

[5] Bhattacharya B., Vidyashankar B.R., Patsias S. And Tomlinson G.R. 2000, "Active and passive vibration control of flexible structures using a combination of magnetostrictive and ferro-magnetic alloys", *Proceedings of SPIE Fifth European Conference on Smart Structures and Materials*, Vol. 4073, pp.204-214

[6] Book W.J. 1993, "Controlled motion in an elastic world"', *Journal of Systems, Measurement and Control*, Vol. 115(1), pp.252-261.

[7] Boyer Frederic and Coiffet Philippe 1996, "Generalization of Newton-Euler model for flexible manipulators"', *Journal of Robotics Systems*, Vol. 13(1), pp.11-24.

[8] Chedmail P., Aoustin Y. and Chevallereau Ch. 1991. "Modelling and control of flexible manipulators", *International Journal for Numerical Methods in Engineering*, Vol. 32, pp.1595-1619.

[9] Craig John J. 1991, "Introduction to robotics:Mechanics and control", *Addison-Wesley Publishing Co., Inc.*.

[10] Dong Sun, Mills J.K. 1999. "Study on piezoelectric actuatorsin control of a single-link flexible manipulator", *Proceedings of 1999 IEEE international Conference on Robotics and Automation, IEEE, Piscataway, NJ, USA* Vol. 2., pp.849-854.

[11] Fraser Anthony R. and Daniel Ron R. 1991, "Perturbation techniques for flexible manipulators", *Kluwer Academic Publishers.*

[12] Fu K.S., Gonzalez R.C. and Lee C.S.G. 1987. "Robotics: Control, Sensing, Vision and Intelligence", *McGraw-Hill Book Company.*

[13] Gamarra Rosado and Yuhara E.A.O. 1999, "Dynamic modelling and simulation of a flexible robotic manipulator", *Robotica* Vol. 17, pp.523-528.

[14] Ho Cheol Shin and Seung Bok Choi 2001, "Position control of a two-link flexible manipulator featuring piezoelectric actuators and sensors", *Mechatronics*, Vol. 11(6), pp.707-729.

[15] Kim Hyoung-Kyu, Choi Seung-Bok and Thompson Brian S. 2000, "Compliant control of a two-link flexible manipulator featuring piezoelectric actuators", *Mechanism and Machines Theory*, Vol. 36, pp.411-424.

[16] Meirovitch L. 1967. "Elements of vibration analysis", *McGraw-Hill Book Company.*

[17] Petric Jesko 1995, "Mathematical Modelling of the flexible one-link manipulator by finite element method", *International Journal for Engineering Modelling*, Vol. 8, pp.77-84.

[18] Spactor, V.A., and Flashner, H. 1990. "Modeling and Design Implications of Noncollocated Control in Flexible Systems", *ASME Journal of Dynamic Systems, Measurement, and Control* Vol. 112. AC-37(11), pp.1782-1786.

[19] Theodore Rex J. 1995, "Dynamic modelling and control analysis of multi-link flexible manipulator", *Ph.D. Thesis, Department of Mechanical Engineering, Indian Institute of Science, Bangalore.*

[20] Usoro P.B., Nadira R. and Mahil S.S. 1986, "A finite element/Lagrangian approach to modelling lightweight flexible manipulators", *Journal of Dynamic Systems, Measurement and Control*, Vol. 108, pp.198-205.

[21] Wang P.K.C. and Wei Jin-Duo 1987, "Vibrations in a moving flexible arm", *Journal of Sound and vibration*, Vol. 116(1), pp.149-160.

[22] Yan Liu, Meng M. and Wang D. 1999, "Influence of mode truncation and elaongation deformation to a flexible manipulator", *Proceeding of IEEE Canadian Conference on Electrical and Computer Engineering*, Vol. 3, pp.1398-1402.

[23] Yue Shigang, Yu Yue-Qing and Bai Shixian 1997, "Flexible rotor beam element for the manipulators with joint and link flexibility", *Mechanism and Machine Theory*, Vol. 32(2), pp. 209-219.

[24] Zhang Xuping, Yu Yue-Qing 1999, "A new spatial rotor beam element for modeling spatial manipulators with joint and link flexibility", *Mechanism and Machines Theory*, Vol. 35, pp.403-421.

[25] Zienkiewicz O.C. 1986. "The Finite Element Method", *McGraw-Hill Book Company.*

Appendix

Appendix A

Calculation of Inertia Matrix and Vector Representing Coriolis and Centrifugal Forces For Two-Link Rigid Manipulator

A.1 Calculation of Transformation Matrices

(Fu, Gonzalez and Lee 1987)

We assume joint variables= θ_1, θ_2; mass of links= M_1, M_2; length of each link= L. From equation 2.5, the homogeneous transformation matrices are obtained as:

$$\mathcal{R}_1^0 = \begin{bmatrix} \cos\theta_1 & -\sin\theta_1 & L\cos\theta_1 \\ \sin\theta_1 & \cos\theta_1 & L\sin\theta_1 \\ 0 & 0 & 1 \end{bmatrix} \tag{A.1}$$

$$\mathcal{R}_2^1 = \begin{bmatrix} \cos\theta_2 & -\sin\theta_2 & L\cos\theta_2 \\ \sin\theta_2 & \cos\theta_2 & L\sin\theta_2 \\ 0 & 0 & 1 \end{bmatrix} \tag{A.2}$$

$$\mathcal{R}_2^0 = \begin{bmatrix} \cos(\theta_1+\theta_2) & -\sin(\theta_1+\theta_2) & L(\cos(\theta_1+\theta_2)+\cos\theta_1) \\ \sin(\theta_1+\theta_2) & \cos(\theta_1+\theta_2) & L(\sin(\theta_1+\theta_2)+\sin\theta_1) \\ 0 & 0 & 1 \end{bmatrix} \tag{A.3}$$

Therefore we can find:

$$\frac{\partial \mathcal{R}_1^0}{\partial \theta_1} = \begin{bmatrix} -\sin\theta_1 & -\cos\theta_1 & -L\sin\theta_1 \\ \cos\theta_1 & -\sin\theta_1 & L\cos\theta_1 \\ 0 & 0 & 0 \end{bmatrix} \tag{A.4}$$

$$\frac{\partial \mathcal{R}_2^0}{\partial \theta_1} = \begin{bmatrix} -\sin(\theta_1+\theta_2) & -\cos(\theta_1+\theta_2) & -L(\sin(\theta_1+\theta_2)+\sin\theta_1) \\ \cos(\theta_1+\theta_2) & -\sin(\theta_1+\theta_2) & L(\cos(\theta_1+\theta_2)+\cos\theta_1) \\ 0 & 0 & 0 \end{bmatrix} \tag{A.5}$$

$$\frac{\partial \mathcal{R}_2^0}{\partial \theta_2} = \begin{bmatrix} -\sin(\theta_1+\theta_2) & -\cos(\theta_1+\theta_2) & -L\sin(\theta_1+\theta_2) \\ \cos(\theta_1+\theta_2) & -\sin(\theta_1+\theta_2) & L\cos(\theta_1+\theta_2) \\ 0 & 0 & 0 \end{bmatrix} \tag{A.6}$$

A.2 Calculation of Mass Matrix

Using equation 2.10, assuming all the products of inertia are zero, we can derive the pseudo inertia matrix J_j:

$$J_1 = \begin{bmatrix} \frac{1}{3}M_1L^2 & 0 & 0 & \frac{1}{3}M_1L \\ 0 & 0 & 0 & 0 \\ 0 & 0 & 0 & 0 \\ -\frac{1}{3}M_1L^2 & 0 & 0 & M_1 \end{bmatrix} \tag{A.7}$$

$$J_2 = \begin{bmatrix} \frac{1}{3}M_2L^2 & 0 & 0 & \frac{1}{3}M_2L \\ 0 & 0 & 0 & 0 \\ 0 & 0 & 0 & 0 \\ -\frac{1}{3}M_2L^2 & 0 & 0 & M_2 \end{bmatrix} \tag{A.8}$$

Then using equation 2.17, we have

$$D_{11} = Tr\left(\frac{\partial \mathcal{R}_1^0}{\partial \theta_1} J_1 \left(\frac{\partial \mathcal{R}_1^0}{\partial \theta_1}\right)^T\right) + Tr\left(\frac{\partial \mathcal{R}_2^0}{\partial \theta_1} J_2 \left(\frac{\partial \mathcal{R}_2^0}{\partial \theta_1}\right)^T\right)$$

Substituting values of $\frac{\partial \mathcal{R}_1^0}{\partial \theta_1}$ and J_1 from equations A.4 and A.7, we get

$$D_{11} = \frac{1}{3}M_1L^2 + \frac{4}{3}M_2L^2 + M_2L^2\cos\theta_2 \tag{A.9}$$

Similarly,

$$\begin{aligned} D_{12} = D_{21} &= Tr\left(\frac{\partial \mathcal{R}_2^0}{\partial \theta_2} J_2 \left(\frac{\partial \mathcal{R}_2^0}{\partial \theta_1}\right)^T\right) \\ &= \frac{1}{3}M_2L^2 + \frac{1}{2}M_2L^2\cos\theta_2 \end{aligned}$$

And

$$\begin{aligned} D_{22} &= Tr\left(\frac{\partial \mathcal{R}_2^0}{\partial \theta_2} J_2 \left(\frac{\partial \mathcal{R}_2^0}{\partial \theta_2}\right)^T\right) \\ &= \frac{1}{3}M_2L^2 \end{aligned}$$

A.3 Calculation of Vector Representing Coriolis and Centrifugal Forces

For $j = 1$, using equation 2.15, we have

$$\begin{aligned} h_1 &= \sum_{k=1}^{2}\sum_{m=1}^{2} h_{1km}\dot{\theta}_k\dot{\theta}_m \\ &= h_{111}\dot{\theta}_1^2 + h_{112}\dot{\theta}_1\dot{\theta}_2 + h_{121}\dot{\theta}_1\dot{\theta}_2 + h_{122}\dot{\theta}_2^2 \end{aligned} \tag{A.10}$$

Using equation 2.18, we can obtain the value of h_{jkm}, therefore

$$h_1 = -\frac{1}{2}M_2L^2 \sin\theta_2\dot{\theta_2}^2 - M_2L^2 \sin\theta_2\dot{\theta}_1\dot{\theta}_2$$

Similarly, for $j = 2$, we have

$$\begin{aligned} h_2 &= \sum_{k=1}^{2}\sum_{m=1}^{2} h_{2km}\dot{\theta}_k\dot{\theta}_m \\ &= h_{211}\dot{\theta}_1^2 + h_{212}\dot{\theta}_1\dot{\theta}_2 + h_{221}\dot{\theta}_1\dot{\theta}_2 + h_{222}\dot{\theta}_2^2 \\ &= \frac{1}{2}M_2L^2 \sin\theta_2\dot{\theta}_1^2 \end{aligned} \tag{A.11}$$

Appendix B

Mass Matrix Elements of Two-Link Flexible Manipulator

B.1 Mass Matrix Elements of Link 1

Form equation 4.13 the elemental mass matrix of link 1, $\mathbf{M}_{1,i}$ is given in the following form:

$$\mathbf{M}_{1,i} = \begin{bmatrix} \mathbf{M}_{1,i}(1,1) & \mathbf{M}_{1,i}(1,2) & \dots & \mathbf{M}_{1,i}(1,7) \\ \mathbf{M}_{1,i}(2,1) & & & \\ \vdots & & [\mathbf{P}_{1,i}]_{6x6} & \\ \mathbf{M}_{1,i}(7,1) & & & \end{bmatrix}_{7x7}$$

And elements of the above mass matrix of are given as follows:

$$\mathbf{P}_{1,i} = \frac{m_1 l_1}{420} \begin{bmatrix} 140 & 0 & 0 & 70 & 0 & 0 \\ 0 & 156 & 22l_1 & 0 & 54 & -13l_1 \\ 0 & 22l_1 & 4l_1^2 & 0 & 13l_1 & -3l_1^2 \\ 70 & 0 & 0 & 140 & 0 & 0 \\ 0 & 54 & 13l_1 & 0 & 156 & -22l_1 \\ 0 & -13l_1 & -3l_1^2 & 0 & -22l_1 & 4l_1^2 \end{bmatrix} \tag{B.1}$$

$$\mathbf{M}_{1,i}(1,1) = m_1 l_1 \left[l_1^2 \left(i^2 - i + \frac{1}{3} \right) + l_1 r_h (2i-1) + r_h^2 \right] + \mathbf{q}_{f_{1,i}}^T \mathbf{P}_{1,i} \mathbf{q}_{f_{1,i}} + \tag{B.2}$$

$$+ \; 2m \begin{bmatrix} \left(\frac{il_1^2}{2} - \frac{l_1^3}{3} + \frac{r_h l_1}{2} \right) & \left(\frac{il_1^2}{2} - \frac{l_1^3}{6} + \frac{r_h l_1}{2} \right) \end{bmatrix} \begin{bmatrix} u_{1,i} \\ u_{1,i+1} \end{bmatrix} \tag{B.3}$$

$$\mathbf{M}_{1,i}(1,2) = -\frac{m_1 l_1}{20} \begin{bmatrix} 7 & l_1 & 3 & -l_1 \end{bmatrix} \begin{bmatrix} v_{1,i} \\ vx_{1,i} \\ v_{1,i+1} \\ vx_{1,i+1} \end{bmatrix} \tag{B.4}$$

$$\mathbf{M}_{1,i}(1,3) = \frac{m_1 l_1}{20} (10il_1 - 7l_1 + 10r_h) + \frac{m_1 l_1}{20} \begin{bmatrix} -13 & 3 \end{bmatrix} \begin{bmatrix} u_{1,i} \\ u_{1,i+1} \end{bmatrix} \tag{B.5}$$

$$\mathbf{M}_{1,i}(1,4) = \frac{m_1 l_1^2}{60} (5il_1 - 3l_1 + 5r_h) + \frac{m_1 l_1^2}{20} \begin{bmatrix} 1 & 4 \end{bmatrix} \begin{bmatrix} u_{1,i} \\ u_{1,i+1} \end{bmatrix} \tag{B.6}$$

$$\mathbf{M}_{1,i}(1,5) = -\frac{m_1 l_1}{60}\begin{bmatrix} 9 & 2l_1 & 21 & 3l_1 \end{bmatrix}\begin{bmatrix} v_{1,i} \\ vx_{1,i} \\ v_{1,i+1} \\ vx_{1,i+1} \end{bmatrix} \tag{B.7}$$

$$\mathbf{M}_{1,i}(1,6) = \frac{m_1 l_1}{20}(10il_1 - 3l_1 + 10r_h) + \frac{m_1 l_1}{20}\begin{bmatrix} 17 & 7 \end{bmatrix}\begin{bmatrix} u_{1,i} \\ u_{1,i+1} \end{bmatrix} \tag{B.8}$$

$$\mathbf{M}_{1,i}(1,7) = -\frac{m_1 l_1^2}{60}(5il_1 - 2l_1 + 5r_h) + \frac{m_1 l_1^2}{20}\begin{bmatrix} -2 & 3 \end{bmatrix}\begin{bmatrix} u_{1,i} \\ u_{1,i+1} \end{bmatrix} \tag{B.9}$$

B.2 Mass Matrix Elements of Link 2

Form equation 4.26 the elemental mass matrix of link 2, $\mathbf{M}_{2,i}$ is given in the following form:

$$\mathbf{M}_{2,i} = \begin{bmatrix} \mathbf{M}_{2,i}(1,1) & \dots & \mathbf{M}_{2,i}(1,5) & \dots & \mathbf{M}_{1,i}(1,11) \\ \vdots & & \vdots & & \vdots \\ \vdots & & \mathbf{M}_{2,i}(5,5) & \dots & \mathbf{M}_{2,i}(5,11) \\ \vdots & & \vdots & [\mathbf{P}_{2,i}]_{6x6} & \\ \mathbf{M}_{2,i}(11,1) & \dots & \mathbf{M}_{2,i}(11,5) & & \end{bmatrix}_{11x11}$$

And elements of the above mass matrix of are given as follows:

$$\mathbf{P}_{2,i} = \frac{m_2 l_2}{420}\begin{bmatrix} 140 & 0 & 0 & 70 & 0 & 0 \\ 0 & 156 & 22l_2 & 0 & 54 & -13l_2 \\ 0 & 22l_2 & 4l_2^2 & 0 & 13l_2 & -3l_2^2 \\ 70 & 0 & 0 & 140 & 0 & 0 \\ 0 & 54 & 13l_2 & 0 & 156 & -22l_2 \\ 0 & -13l_2 & -3l_2^2 & 0 & -22l_2 & 4l_2^2 \end{bmatrix} \tag{B.10}$$

$$\begin{aligned} \mathbf{M}_{2,i}(1,1) &= m_2\left[l_2\left((L_1+u_{1,tip})^2 + v_{1,tip}^2\right) + 2Al_2^2\left(i-\frac{1}{2}\right) + l_2^3\left(i^2 - i + \frac{1}{3}\right)\right] + \\ &+ m_2 l_2\begin{bmatrix} (A+\frac{l_2}{3}(3i-2)) & B & \frac{Bl_2}{6} & (A+\frac{l_2}{3}(3i-1)) & B & -\frac{Bl_2}{6} \end{bmatrix}\mathbf{q}_{f_{2,i}} + \\ &+ \mathbf{q}_{f_{2,i}}^T \mathbf{P}_{2,i}\mathbf{q}_{f_{2,i}} \end{aligned} \tag{B.11}$$

where

$$A = (L_1 + u_{1,tip})\cos\hat{\theta}_2 + v_{1,tip}\sin\hat{\theta}_2$$

$$B = -(L_1 + u_{1,tip})\sin\hat{\theta}_2 + v_{1,tip}\cos\hat{\theta}_2$$

Similarly

$$\begin{aligned} \mathbf{M}_{2,i}(1,2) &= -m_2 l_2\left[v_{1,tip} + \sin\hat{\theta}_2 l_2\left(i-\frac{1}{2}\right)\right] - \\ &- \frac{m_2 l_2}{2}\begin{bmatrix} \sin\hat{\theta}_2 & \cos\hat{\theta}_2 & \frac{l_2\cos\hat{\theta}_2}{6} & \sin\hat{\theta}_2 & \cos\hat{\theta}_2 & -\frac{l_2\cos\hat{\theta}_2}{6} \end{bmatrix}\mathbf{q}_{f_{2,i}} \end{aligned} \tag{B.12}$$

$$\mathbf{M}_{2,i}(1,3) = \frac{m_2 l_2}{2}\left[\begin{array}{cccccc}\cos\hat{\theta}_2 & -\sin\hat{\theta}_2 & -\frac{l_2\sin\hat{\theta}_2}{6} & \cos\hat{\theta}_2 & -\sin\hat{\theta}_2 & \frac{l_2\sin\hat{\theta}_2}{6}\end{array}\right]\mathbf{q}_{f_{2,i}} + + m_2 l_2(L_1+u_{1,tip}) \quad \text{(B.13)}$$

$$\mathbf{M}_{2,i}(1,4) = m_2 l_2\left[\begin{array}{cccccc}\left(A+\frac{l_2}{3}(3i-2)\right) & B & \frac{Bl_2}{6} & \left(A+\frac{l_2}{3}(3i-1)\right) & B & -\frac{Bl_2}{6}\end{array}\right]\mathbf{q}_{f_{2,i}} + + m_2\left[Al_2^2\left(i-\frac{1}{2}\right)+l_2^3\left(i^2-i+\frac{1}{3}\right)\right]+\mathbf{q}_{f_{2,i}}^T\mathbf{P}_{2,i}\mathbf{q}_{f_{2,i}} \quad \text{(B.14)}$$

$$\mathbf{M}_{2,i}(1,5) = m_2 l_2\left[\begin{array}{cccccc}\left(A+\frac{l_2}{3}(3i-2)\right) & B & \frac{Bl_2}{6} & \left(A+\frac{l_2}{3}(3i-1)\right) & B & -\frac{Bl_2}{6}\end{array}\right]\mathbf{q}_{f_{2,i}} + + m_2\left[Al_2^2\left(i-\frac{1}{2}\right)+l_2^3\left(i^2-i+\frac{1}{3}\right)\right]+\mathbf{q}_{f_{2,i}}^T\mathbf{P}_{2,i}\mathbf{q}_{f_{2,i}} \quad \text{(B.15)}$$

$$\mathbf{M}_{2,i}(1,6) = -\frac{m_2 l_2 B}{2}-\frac{m_2 l_2}{60}\left[\begin{array}{cccccc}0 & 21 & 3l_2 & 0 & 9 & -3l_2\end{array}\right]\mathbf{q}_{f_{2,i}} \quad \text{(B.16)}$$

$$\mathbf{M}_{2,i}(1,7) = \frac{m_2 l_2}{2}\left[A+l_2\left(i-\frac{7}{10}\right)\right]+\frac{m_2 l_2}{20}\left[\begin{array}{cccccc}-13 & 0 & 0 & 3 & 0 & 0\end{array}\right]\mathbf{q}_{f_{2,i}} \quad \text{(B.17)}$$

$$\mathbf{M}_{2,i}(1,8) = \frac{m_2 l_2^2}{12}\left[A+l_2\left(i-\frac{3}{5}\right)\right]+\frac{m_2 l_2^2}{20}\left[\begin{array}{cccccc}1 & 0 & 0 & 4 & 0 & 0\end{array}\right]\mathbf{q}_{f_{2,i}} \quad \text{(B.18)}$$

$$\mathbf{M}_{2,i}(1,9) = -\frac{m_2 l_2 B}{2}-\frac{m_2 l_2}{60}\left[\begin{array}{cccccc}0 & 9 & 2l_2 & 0 & 21 & -3l_2\end{array}\right]\mathbf{q}_{f_{2,i}} \quad \text{(B.19)}$$

$$\mathbf{M}_{2,i}(1,10) = \frac{m_2 l_2}{2}\left[A+l_2\left(i-\frac{3}{10}\right)\right]+\frac{m_2 l_2}{20}\left[\begin{array}{cccccc}17 & 0 & 0 & 7 & 0 & 0\end{array}\right]\mathbf{q}_{f_{2,i}} \quad \text{(B.20)}$$

$$\mathbf{M}_{2,i}(1,11) = -\frac{m_2 l_2^2}{12}\left[A+l_2\left(i-\frac{2}{5}\right)\right]+\frac{m_2 l_2^2}{60}\left[\begin{array}{cccccc}-2 & 0 & 0 & 3 & 0 & 0\end{array}\right]\mathbf{q}_{f_{2,i}} \quad \text{(B.21)}$$

$$\mathbf{M}_{2,i}(2,2) = m_2 l_2 \quad \text{(B.22)}$$

$$\mathbf{M}_{2,i}(2,3) = 0 \quad \text{(B.23)}$$

$$\mathbf{M}_{2,i}(2,4) = -m_2 l_2^2\sin\hat{\theta}_2\left(i-\frac{1}{2}\right) - \frac{m_2 l_2}{2}\left[\begin{array}{cccccc}\sin\hat{\theta}_2 & \cos\hat{\theta}_2 & \frac{l_2\cos\hat{\theta}_2}{6} & \sin\hat{\theta}_2 & \cos\hat{\theta}_2 & -\frac{l_2\cos\hat{\theta}_2}{6}\end{array}\right]\mathbf{q}_{f_{2,i}} \quad \text{(B.24)}$$

$$\mathbf{M}_{2,i}(2,5) = -m_2 l_2^2\sin\hat{\theta}_2\left(i-\frac{1}{2}\right) - \frac{m_2 l_2}{2}\left[\begin{array}{cccccc}\sin\hat{\theta}_2 & \cos\hat{\theta}_2 & \frac{l_2\cos\hat{\theta}_2}{6} & \sin\hat{\theta}_2 & \cos\hat{\theta}_2 & -\frac{l_2\cos\hat{\theta}_2}{6}\end{array}\right]\mathbf{q}_{f_{2,i}} \quad \text{(B.25)}$$

$$\mathbf{M}_{2,i}(2,6) = \frac{m_2 l_2 \cos\hat{\theta}_2}{2} \tag{B.26}$$

$$\mathbf{M}_{2,i}(2,7) = -\frac{m_2 l_2 \sin\hat{\theta}_2}{2} \tag{B.27}$$

$$\mathbf{M}_{2,i}(2,8) = -\frac{m_2 l_2^2 \sin\hat{\theta}_2}{12} \tag{B.28}$$

$$\mathbf{M}_{2,i}(2,9) = \frac{m_2 l_2 \cos\hat{\theta}_2}{2} \tag{B.29}$$

$$\mathbf{M}_{2,i}(2,10) = -\frac{m_2 l_2 \sin\hat{\theta}_2}{2} \tag{B.30}$$

$$\mathbf{M}_{2,i}(2,11) = \frac{m_2 l_2^2 \sin\hat{\theta}_2}{12} \tag{B.31}$$

$$\mathbf{M}_{2,i}(3,3) = m_2 l_2 \tag{B.32}$$

$$\begin{aligned}\mathbf{M}_{2,i}(3,4) &= -\frac{m_2 l_2}{2}\left[\, -\cos\hat{\theta}_2 \quad \sin\hat{\theta}_2 \quad \tfrac{l_2\sin\hat{\theta}_2}{6} \quad -\cos\hat{\theta}_2 \quad \sin\hat{\theta}_2 \quad -\tfrac{l_2\sin\hat{\theta}_2}{6} \,\right]\mathbf{q}_{f_{2,i}} + \\ &+ m_2 l_2^2 \cos\hat{\theta}_2\left(i-\frac{1}{2}\right)\end{aligned} \tag{B.33}$$

$$\begin{aligned}\mathbf{M}_{2,i}(3,5) &= -\frac{m_2 l_2}{2}\left[\, -\cos\hat{\theta}_2 \quad \sin\hat{\theta}_2 \quad \tfrac{l_2\sin\hat{\theta}_2}{6} \quad -\cos\hat{\theta}_2 \quad \sin\hat{\theta}_2 \quad -\tfrac{l_2\sin\hat{\theta}_2}{6} \,\right]\mathbf{q}_{f_{2,i}} + \\ &+ m_2 l_2^2 \cos\hat{\theta}_2\left(i-\frac{1}{2}\right)\end{aligned} \tag{B.34}$$

$$\mathbf{M}_{2,i}(3,6) = \frac{m_2 l_2 \sin\hat{\theta}_2}{2} \tag{B.35}$$

$$\mathbf{M}_{2,i}(3,7) = \frac{m_2 l_2 \cos\hat{\theta}_2}{2} \tag{B.36}$$

$$\mathbf{M}_{2,i}(3,8) = \frac{m_2 l_2^2 \cos\hat{\theta}_2}{12} \tag{B.37}$$

$$\mathbf{M}_{2,i}(3,9) = \frac{m_2 l_2 \sin\hat{\theta}_2}{2} \tag{B.38}$$

$$\mathbf{M}_{2,i}(3,10) = \frac{m_2 l_2 \cos\hat{\theta}_2}{2} \tag{B.39}$$

$$\mathbf{M}_{2,i}(3,11) = -\frac{m_2 l_2^2 \cos\hat{\theta}_2}{12} \tag{B.40}$$

$$\mathbf{M}_{2,i}(4,4) = m_2 l_2^3\left(i^2 - i + \frac{1}{3}\right) +$$

Appendix C

Contribution of Term S_2 in Final Dynamic Equation of Two-Link Flexible Manipulator

From equation 4.48

$$S_2 = \mathbf{q}_{f_2}^T \mathbf{P}_2 \mathbf{q}_{f_2} (\dot{\theta}_2^{\,2} + 2\dot{\theta}_1 \dot{vx}_{n_1+1} + 2\dot{\theta}_1\dot{\theta}_2 + \dot{vx}_{n_1+1}^2 + 2\dot{\theta}_2 \dot{vx}_{n_1+1} + \dot{\theta}_2^{\,2})$$

S_2 can be written in the form:

$$S_2 = S_{2,1} + S_{2,2} + S_{2,3} + S_{2,4} + S_{2,5} + S_{2,6}$$

where

$$\begin{aligned}
S_{2,1} &= \mathbf{q}_{f_2}^T \mathbf{P}_2 \mathbf{q}_{f_2} \dot{\theta}_1^{\,2} \\
S_{2,2} &= \mathbf{q}_{f_2}^T \mathbf{P}_2 \mathbf{q}_{f_2} 2\dot{\theta}_1 \dot{vx}_{n_1+1} \\
S_{2,3} &= \mathbf{q}_{f_2}^T \mathbf{P}_2 \mathbf{q}_{f_2} 2\dot{\theta}_1\dot{\theta}_2 \\
S_{2,4} &= \mathbf{q}_{f_2}^T \mathbf{P}_2 \mathbf{q}_{f_2} \dot{vx}_{n_1+1}^2 \\
S_{2,5} &= \mathbf{q}_{f_2}^T \mathbf{P}_2 \mathbf{q}_{f_2} 2\dot{\theta}_2 \dot{vx}_{n_1+1} \\
S_{2,6} &= \mathbf{q}_T f_2 \mathbf{P}_2 \mathbf{q}_{f_2} \dot{\theta}_2^{\,2})
\end{aligned}$$

$$\begin{aligned}
\frac{1}{2}\left[\frac{d}{dt}\left(\frac{\partial S_{2,1}}{\partial \dot{\mathbf{q}}}\right) - \frac{\partial S_{2,1}}{\partial \mathbf{q}}\right] &= \frac{1}{2}\left[\frac{d}{dt}\left(\frac{\partial}{\partial \dot{\mathbf{q}}}\left(\mathbf{q}_{f_2}^T \mathbf{P}_2 \mathbf{q} f_2 \dot{\theta}_1^2\right)\right) - \frac{\partial}{\partial \mathbf{q}}\left(\mathbf{q}_{f_2}^T \mathbf{P}_2 \mathbf{q} f_2 \dot{\theta}_1^2\right)\right] \\
&= \left[\ \mathbf{q}_{f_2}^T \mathbf{P}_2 \mathbf{q}_{f_2} \ \ 0 \ \ \ldots \ \ 0 \ \ 0 \ \ 0 \ \ \ldots \ \ 0 \ \right]^T \ddot{\theta}_1^2 + \\
&+ \left[\ 2\mathbf{q}_{f_2}^T \mathbf{P}_2 \dot{\mathbf{q}}_{f_2} \ \ 0 \ \ \ldots \ \ 0 \ \ 0 \ \ 0 \ \ \ldots \ \ 0 \ \right]^T \dot{\theta}_1 - \\
&- \left[\ 0 \ \ \ldots \ \ \ldots \ \ 0 \ \ 2\left[\mathbf{P}_2 \mathbf{q}_{f_2}\right]^T \ \right]^T \dot{\theta}_1^2
\end{aligned} \tag{C.1}$$

$$\frac{1}{2}\left[\frac{d}{dt}\left(\frac{\partial S_{2,2}}{\partial \dot{\mathbf{q}}}\right) - \frac{\partial S_{2,2}}{\partial \mathbf{q}}\right] = \frac{1}{2}\left[\frac{d}{dt}\left(\frac{\partial}{\partial \dot{\mathbf{q}}}\left(2\mathbf{q}_{f_2}^T \mathbf{P}_2 \mathbf{q}_{f_2} \dot{\theta}_1 \dot{vx}_{n_1+1}\right) - \frac{\partial}{\partial \mathbf{q}}\left(2\mathbf{q}_{f_2}^T \mathbf{P}_2 \mathbf{q}_{f_2} \dot{\theta}_1 \dot{vx}_{n_1+1}\right)\right]$$

$$
\begin{aligned}
&= \left[\ \mathbf{q}_{f_2}^T\mathbf{P}_2\mathbf{q}_{f_2}\dot{vx}_{n_1+1}\ \ 0\ \ \ldots\ \ \mathbf{q}_{f_2}^T\mathbf{P}_2\mathbf{q}_{f_2}\ddot{\theta}_1\ \ 0\ \ 0\ \ \ldots\ \ 0\ \right]^T + \\
&+ \left[\ 2\mathbf{q}\mathbf{f}_2^T\mathbf{P}_2\dot{\mathbf{q}}_{f_2}\dot{vx}_{n_1+1}\ \ 0\ \ \ldots\ \ 2\mathbf{q}_{f_2}^T\mathbf{P}_2\dot{\mathbf{q}}_{f_2}\dot{\theta}_1\ \ 0\ \ 0\ \ \ldots\ \ 0\ \right]^T - \\
&- \left[\ 0\ \ \ldots\ \ \ldots\ \ 0\ \ 2\left[\mathbf{P}_2\mathbf{q}_{f_2}\right]^T\ \right]^T \dot{\theta}_1\dot{vx}_{n_1+1} \qquad \text{(C.2)}
\end{aligned}
$$

$$
\begin{aligned}
\frac{1}{2}\left[\frac{d}{dt}\left(\frac{\partial S_{2,3}}{\partial\dot{\mathbf{q}}}\right) - \frac{\partial S_{2,3}}{\partial\mathbf{q}}\right] &= \frac{1}{2}\left[\frac{d}{dt}\left(\frac{\partial}{\partial\dot{\mathbf{q}}}\left(2\mathbf{q}_{f_2}^T\mathbf{P}_2\mathbf{q}_{f_2}\dot{\theta}_1\dot{\theta}_2\right) - \frac{\partial}{\partial\mathbf{q}}\left(2\mathbf{q}_{f_2}^T\mathbf{P}_2\mathbf{q}_{f_2}\dot{\theta}_1\dot{\theta}_2\right)\right]\right. \\
&= \left[\ \mathbf{q}_{f_2}^T\mathbf{P}_2\mathbf{q}_{f_2}\ddot{\theta}_2\ \ 0\ \ \ldots\ \ 0\ \ \mathbf{q}_{f_2}^T\mathbf{P}_2\mathbf{q}_{f_2}\ddot{\theta}_1\ \ 0\ \ \ldots\ \ 0\ \right]^T + \\
&+ \left[\ 2\mathbf{q}_{f_2}^T\mathbf{P}_2\dot{\mathbf{q}}_{f_2}\dot{\theta}_2\ \ 0\ \ \ldots\ \ 0\ \ 2\mathbf{q}_{f_2}^T\mathbf{P}_2\dot{\mathbf{q}}_{f_2}\dot{\theta}_1\ \ 0\ \ \ldots\ \ 0\ \right]^T - \\
&- \left[\ 0\ \ \ldots\ \ \ldots\ \ 0\ \ 2\left[\mathbf{P}_2\mathbf{q}_{f_2}\right]^T\ \right]^T \dot{\theta}_1\dot{\theta}_2 \qquad \text{(C.3)}
\end{aligned}
$$

$$
\begin{aligned}
\frac{1}{2}\left[\frac{d}{dt}\left(\frac{\partial S_{2,4}}{\partial\dot{\mathbf{q}}}\right) - \frac{\partial S_{2,4}}{\partial\mathbf{q}}\right] &= \frac{1}{2}\left[\frac{d}{dt}\left(\frac{\partial}{\partial\dot{\mathbf{q}}}\left(\mathbf{q}_{f_2}^T\mathbf{P}_2\mathbf{q}_{f_2}\dot{vx}_{n_1+1}^2\right)\right) - \frac{\partial}{\partial\mathbf{q}}\left(\mathbf{q}_{f_2}^T\mathbf{P}_2\mathbf{q}_{f_2}\dot{vx}_{n_1+1}^2\right)\right] \\
&= \left[\ 0\ \ 0\ \ \ldots\ \ \mathbf{q}_{f_2}^T\mathbf{P}_2\mathbf{q}_{f_2}\ \ 0\ \ 0\ \ \ldots\ \ 0\ \right]^T \ddot{vx}_{n_1+1}^2 + \\
&+ \left[\ 0\ \ 0\ \ \ldots\ \ 2\mathbf{q}_{f_2}^T\mathbf{P}_2\dot{\mathbf{q}}_{f_2}\ \ 0\ \ 0\ \ \ldots\ \ 0\ \right]^T \dot{vx}_{n_1+1} - \\
&- \left[\ 0\ \ \ldots\ \ \ldots\ \ 0\ \ 2\left[\mathbf{P}_2\mathbf{q}_{f_2}\right]^T\ \right]^T \dot{vx}_{n_1+1}^2 \qquad \text{(C.4)}
\end{aligned}
$$

$$
\begin{aligned}
\frac{1}{2}\left[\frac{d}{dt}\left(\frac{\partial S_{2,5}}{\partial\dot{\mathbf{q}}}\right) - \frac{\partial S_{2,5}}{\partial\mathbf{q}}\right] &= \frac{1}{2}\left[\frac{d}{dt}\left(\frac{\partial}{\partial\dot{\mathbf{q}}}\left(2\mathbf{q}_{f_2}^T\mathbf{P}_2\mathbf{q}_{f_2}\dot{vx}_{n_1+1}\dot{\theta}_2\right) - \frac{\partial}{\partial\mathbf{q}}\left(2\mathbf{q}_{f_2}^T\mathbf{P}_2\mathbf{q}_{f_2}\dot{vx}_{n_1+1}\dot{\theta}_2\right)\right]\right. \\
&= \left[\ 0\ \ 0\ \ \ldots\ \ \mathbf{q}_{f_2}^T\mathbf{P}_2\mathbf{q}_{f_2}\ddot{\theta}_2\ \ \mathbf{q}_{f_2}^T\mathbf{P}_2\mathbf{q}_{f_2}\dot{vx}_{n_1+1}\ \ 0\ \ \ldots\ \ 0\ \right]^T + \\
&+ \left[\ 0\ \ 0\ \ \ldots\ \ 2\mathbf{q}_{f_2}^T\mathbf{P}_2\dot{\mathbf{q}}_{f_2}\dot{\theta}_2\ \ 2\mathbf{q}_{f_2}^T\mathbf{P}_2\dot{\mathbf{q}}_{f_2}\dot{vx}_{n_1+1}\ \ 0\ \ \ldots\ \ 0\ \right]^T - \\
&- \left[\ 0\ \ \ldots\ \ \ldots\ \ 0\ \ 2\left[\mathbf{P}_2\mathbf{q}_{f_2}\right]^T\ \right]^T \dot{vx}_{n_1+1}\dot{\theta}_2 \qquad \text{(C.5)}
\end{aligned}
$$

$$
\begin{aligned}
\frac{1}{2}\left[\frac{d}{dt}\left(\frac{\partial S_{2,6}}{\partial\dot{\mathbf{q}}}\right) - \frac{\partial S_{2,6}}{\partial\mathbf{q}}\right] &= \frac{1}{2}\left[\frac{d}{dt}\left(\frac{\partial}{\partial\dot{\mathbf{q}}}\left(\mathbf{q}_{f_2}^T\mathbf{P}_2\mathbf{q}_{f_2}\dot{\theta}_2^2\right)\right) - \frac{\partial}{\partial\mathbf{q}}\left(\mathbf{q}_{f_2}^T\mathbf{P}_2\mathbf{q}_{f_2}\dot{\theta}_2^2\right)\right] \\
&= \left[\ 0\ \ 0\ \ \ldots\ \ 0\ \ \mathbf{q}_{f_2}^T\mathbf{P}_2\mathbf{q}_{f_2}\ \ 0\ \ \ldots\ \ 0\ \right]^T \ddot{\theta}_2^2 + \\
&+ \left[\ 0\ \ 0\ \ \ldots\ \ 0\ \ 2\mathbf{q}_{f_2}^T\mathbf{P}_2\dot{\mathbf{q}}_{f_2}\ \ 0\ \ \ldots\ \ 0\ \right]^T \dot{\theta}_2 - \\
&- \left[\ 0\ \ \ldots\ \ \ldots\ \ 0\ \ 2\left[\mathbf{P}_2\mathbf{q}_{f_2}\right]^T\ \right]^T \dot{\theta}_2^2 \qquad \text{(C.6)}
\end{aligned}
$$